University of Stavanger

Faculty of Science and Technology

MASTER'S THESIS

Study program/ Specialization: **MSc in Petroleum Engineering/Reservoir Engineering**	**Spring semester, 2015** **Open**
Writer: **Victor Chukwudi Anokwuru**	..... (Writer's signature)
Faculty supervisor: **Prof. Hans Kleppe** External supervisor(s): **Prof. Dag Chun Standnes**	
Thesis title: **Simulation of Water Diversion Using ECLIPSE Options**	
Credits (ECTS): 30	
Key words: **-Silicates** **-Simulation** **-ECLIPSE** **-RRF** **-EOR** **-Thief zone** **-Refinement** **-Threshold**	Pages: **155** + enclosure: **4** **Stavanger, 15th June, 2015**

ABSTRACT

A recent large scale inter-well field pilot project on in-depth water diversion using silicates done at Snorre field in the Norwegian continental shelf (NCS) by Statoil ASA in 2013 revealed that even though the operation was successful, there are still several challenges in modeling the process. There are currently no known commercial software that has silicate-specific options that can simulate the physics and chemistry associated to this process. While research is ongoing to develop numerical codes that can simulate the water diversion process using silicates with significant accuracy, it is necessary to test the applicability of available options in commercial software that can give some insight into the process. This thesis uses the polymer option in ECLIPSE 100 to simulate water diversion using silicates. The idea is that since polymer and silicates share slightly similar characteristics with respect to gel formation, it is expected that the polymer option in ECLIPSE should be able to model to some extent the silicate water diversion process. Various 2D refined models were used to check the limits of refinement to obtaining realistic results and also for sensitivity on injection rate and thief zone location. 3D models were used to run sensitivity on important process design parameters such as activation temperature (gel location), injection time, slug size, permeability contrast and residual resistance factor (RRF). The grid size was found to influence the results and the 9x grid refinement gave acceptable results with minimal influence of numerical dispersion. Sensitivity on the injection rate using the 2D model indicated that the injection rate has no impact on the simulation results. However, this is not according to theory. It could be that the system here is not in a sensitive range with respect to the velocity variations. The 3D model sensitivities on design parameters gave expected and insightful results. It was observed that there is a threshold temperature of about 75^{o}C at which the diversion process is most efficient. The sensitivity on the injection time revealed that the process will be more effective when applied earlier than later. Also, sensitivity results on slug size showed that the larger the silicate slug size, the higher incremental recoveries obtained, however, it could also mean lesser efficiency taking into consideration the amount of oil recovered compared to the amount of silicate injected and also the economics. In addition, the sensitivity on permeability contrast confirms literature. There is a threshold of permeability contrast above which the water diversion process becomes increasingly effective and profitable. The new keyword (PLYATEMP) in ECLIPSE was tested and ascertained to function as expected. Based on the results obtained and analysis made, it was concluded that the polymer option in ECLIPSE can be used to model in-depth water diversion with silicate

TABLE OF CONTENTS

ACKNOWLEDGMENT

My profound gratitude goes to God Almighty for sustaining me throughout my master study.

Special thanks to my supervisor in Statoil, Professor Dag Chun Standnes for giving me the required guidance needed to complete this thesis and for much time and resources spent on me.

My sincere appreciation to my beloved parents, Mr. and Mrs. Samuel Anokwuru Nwachukwu who made the sacrifice for my study abroad and for their prayers and blessings. Also, to my siblings and loved ones for their best wishes.

Thanks also to my internal supervisor Professor Hans Kleppe for providing me with software support.

Thanks to my family in Norway, the Redeemed Christian Church of God, Dayspring Parish, Stavanger for standing by me all the way. Special thanks to Pastor Minika for her motherly care, Pastor and Engr. Samuel Aderemi in Schlumberger for the foundational lessons in Petrel, and Pastor Dickson Uyiomendo for the conferences I attended.

I also appreciate the kindness of PhD student, Engr. Yen Adams for his advice and support and Engr. Segun Aiyeru for guiding me in the referencing of this report.

LIST OF TABLES

LIST OF FIGURES

NOMENCLATURE

Abbreviation

CAT	Computerized Axial Tomography
EOR	Enhanced Oil Recovery
FVF	Formation Volume Factor
GOR	Gas-Oil Ratio
IFT	Interfacial Tension
IOR	Improved Oil Recovery
NCS	Norwegian Continental Shelf
NTU	Nephelometric Turbidity Units
OOIP	Original Oil-in-Place
PAM	Polyacrylamide
RF	Resistance Factor, mobility reduction
RRF	Residual Resistance Factor, permeability reduction
SATNUM	Saturation Number
WOR	Water-Oil Ratio
2D	2-Dimensional
3D	3-Dimensional

Symbols

A	Gelation time tuning parameter
a	Exponent
B	Tuning parameter
b	Deposition constant
C_p^a	Adsorbed concentration
$C_p^{a\,max}$	Maximum adsorbed concentration
D	Pore diameter, m
d	Particle diameter = 2R, m
E_a	Activation energy, KJ/mol

H	Hydrogen
K	Dispersion Coefficient
K_{ij}	Total dispersion coefficient
K_{ij}^{num}	Numerical dispersion coefficient
K_{ij}^{phy}	Physical dispersion
k	Permeability, Darcy or md
n	SiO_2:Na_2O molar ratio
O	Oxygen
P	Pressure, bar
q	Flow rate, l/min, m^3/day
R	Pore radius, m or Gas constant, 8.314 $JK^{-1}mol^{-1}$
R_k	Actual resistance factor
r_e	Effective drainage radius, m
r_w	Wellbore radius, m
Si	Silicon
T	Absolute temperature, K or ^oC
t	Turbidity, NTU
t_g	Gelation time, day
μ	Viscosity, cp
φ	Porosity in porous media
α	Silicate dependent exponent, /wt%
β	Acid dependent exponent, /wt% 2M HCl
γ	Calcium dependent exponent, $/ppm^{1/2}$

1.0 INTRODUCTION

Increasing water production from mature oil reservoirs stresses the need for finding methods that will mitigate this problem and improve water flood sweep efficiency and oil recovery. Methods have been suggested to solve the different causes and associated challenges. However, more research is ongoing to develop better means to address this problem and improve recovery.

1.1 Background

The effectiveness of an EOR process has been categorized into two measures: microscopic displacement efficiency and macroscopic displacement efficiency. Microscopic displacement efficiency is a measure of the mobilization or displacement of oil at the pore scale while macroscopic displacement efficiency measures the effectiveness of the injected fluid to contact and mobilize/displace oil at those places in the reservoir where it contacts the oil (Green and Willhite, 1998). Factors affecting microscopic displacement efficiency are interfacial tension (IFT), wettability, capillary pressure and relative permeability. Factors affecting macroscopic efficiency are heterogeneity and anisotropy, relative mobility between the displacing and the displaced fluids, well arrangement or pattern and rock type in which the oil exists (Terry, 2000).

Large mobility ratios (M>1) between the displacing and the displaced fluids results in a phenomenon called “viscous fingering” which reduces the macroscopic sweep efficiency of a water flooding process. For this case, viscous fluids such as polymers are applied to control this phenomenon. For gas injection processes, foam or water are used to control the gas mobility. In addition, fluid displacement in the reservoir will not be uniform if large variations exist in properties such as permeability, porosity or clay content. The presence of micro-fractures or macro-fractures provides a channel for injected fluids to move through thus substantially bypassing residual oil (Terry, 2000). The solution for such cases is to block or plug the high permeable zone with a blocking agent. The plugging is either done near the well bore or deep into the reservoir. Where there is no vertical communication between the zones, near wellbore blocking is applied to reduce injectivity into the high permeable zone or selectively isolate the zones. The more difficult situation is where vertical communication exists between the different zones or layers in the reservoir. For this case, in-depth plugging is applied to divert the injected fluid into the less permeable or unswept zones. *Figure 1* shows the idea behind in-depth water diversion (Skrettingland et al., 2014).

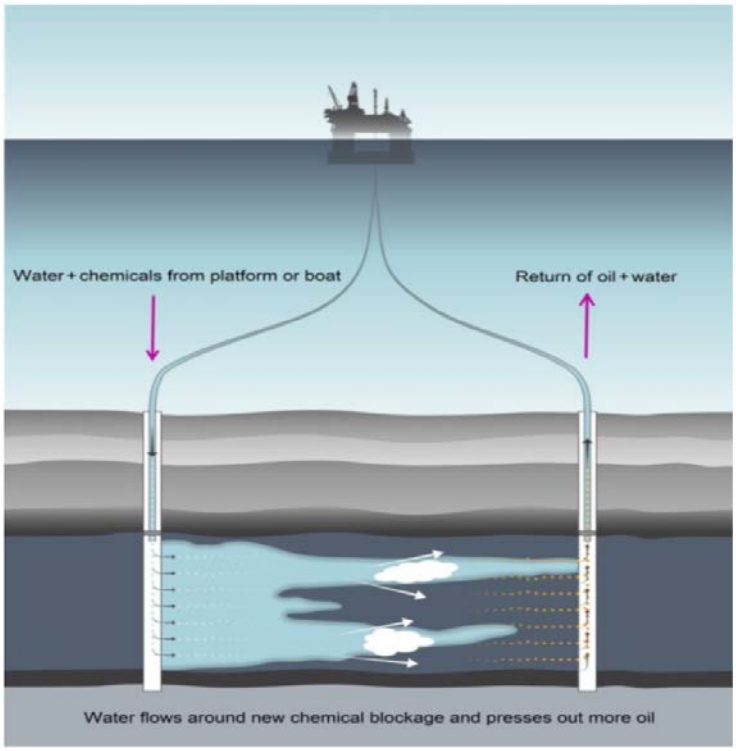

Figure 1: Sketch of idea behind in-depth water diversion (Skrettingland et al., 2014)

Chemical systems such as cements, polymers, silicates and other gels have been applied for near wellbore plugging. In-depth plugging is quite complicated and care need be taken in choosing the type of chemical system to apply.

Alkaline sodium silicate is among the first chemical systems used to control water production in oil reservoirs (Stavland et al., 2011a). As early as 1922, sodium silicate has been suggested for plugging. However, since then, it has only been applied occasionally for near wellbore treatments (Kennedy, 1936, Stavland et al., 2011a). Stavland et al. (2011a) demonstrated that sodium silicate can be used for in-depth water diversion. Silicate have been applied for deeper treatments such as in the Gullfaks field, North Sea (Rolfsvag et al., 1996), in Hungarian oil fields (Lakatos et al., 1999) and on a larger scale in the Snorre oil field (NCS).

Modeling water diversion using silicate could be quite challenging especially because the availability of commercial simulators with silicate-specific options that can simulate the process taking into account the whole physics and chemistry of the process is non-existent or unknown. Notwithstanding, commercial software have been applied to model and predict some behaviors in the process by adjusting certain options. Hansen (2009) did a numerical simulation of sodium silicate injection in the Veslefrikk field (NCS) using the tracer option in ECLIPSE. Hatzignatiou et al. (2014) modeled the core flood experiment on silicate gels done by Stavland

et al. (2011b) using a commercial simulation software (most likely CMG). For this thesis, the polymer option in ECLIPSE is applied.

1.2 Objectives

Generally, the aim of this thesis is to investigate the possibility of using the polymer option in ECLIPSE to simulate the silicate water diversion process.

Emphasis will be placed on the following:

- Determination of the possibility of relying on results obtained from water diversion simulations where numerical dispersion is significant. To achieve this, 2D synthetic models are used to check the impact of grid refinement on:
  - Temperature distribution.
  - Tracer propagation.
  - Polymer (silicate) distribution and diversion.
  - EOR
- The impact of injection design and/or scheme on the oil recovery in more realistic models. This will be achieved by using 3D models to run sensitivities on important design factors such as:
  - Gel activation temperature (Gel location).
  - Slug size.
  - Injection time
  - Permeability contrast.
  - RRF
  - Injection rate (2D model and refinement is used)
  - Location of the thief zone (2D model is used)
- Testing the functionality of the new ECLIPSE (2014) keyword, PLYATEMP for water diversion purposes.

The results will be compared to published results and general expectations on where and to what extent silicate is able to reduce flow of water in affected areas.

2.0 THEORY

Techniques used to recover oil from oilfield reservoirs have been traditionally classified into three stages: The primary, secondary and tertiary stages. The primary recovery stage is the initial phase of oil production and uses the natural energy of the reservoir to drive oil toward production wells. It accounts for about 5-15% of the OOIP (Tzimas et al., 2005). When the reservoir pressure becomes too low to sustain economic production, or when the produced gas-oil ratio becomes high, secondary recovery techniques are applied. Secondary recovery techniques are those used to augment the natural reservoir energy such as water injection, gas injection or other. Typical recovery factor for water flooding is about 30% depending on the fluid and rock properties (Tzimas et al., 2005). After the secondary stage becomes uneconomical, the tertiary stage which involves the use of chemicals, miscible gases, and/or thermal energy to displace additional oil is applied. Because this chronological sequence has not been adhered to, the name 'enhanced oil recovery (EOR)' was used as a replacement for tertiary recovery. Therefore, oil recovery processes are now classified as primary, secondary, and EOR processes (Green and Willhite, 1998). Another term known as 'improved oil recovery (IOR)' which encompasses the secondary and EOR stages have also been used. *Figure 2* gives a schematic flow chart of the different recovery stages and associated techniques.

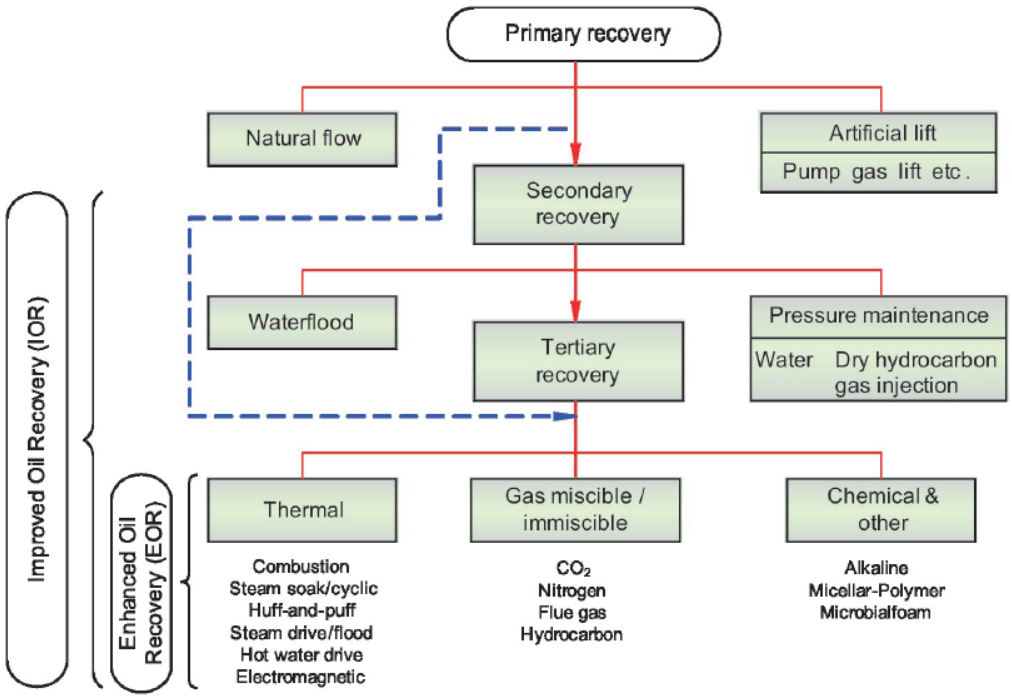

Figure 2: schematic flow chart of the different recovery stages and associated techniques (Secen, 2005)

2.1 Water Production

One of the major challenges confronting the petroleum industry today is the production of large volumes of water during hydrocarbon production from the subsurface. Water often comprises more than 50% of the produced fluids (Grattoni et al., 2001). Produced water is the main source of oil discharge in the North Sea. About 83% of water produced in the North Sea are discharged while just 17% are re-injected (Ramstad, 2013)

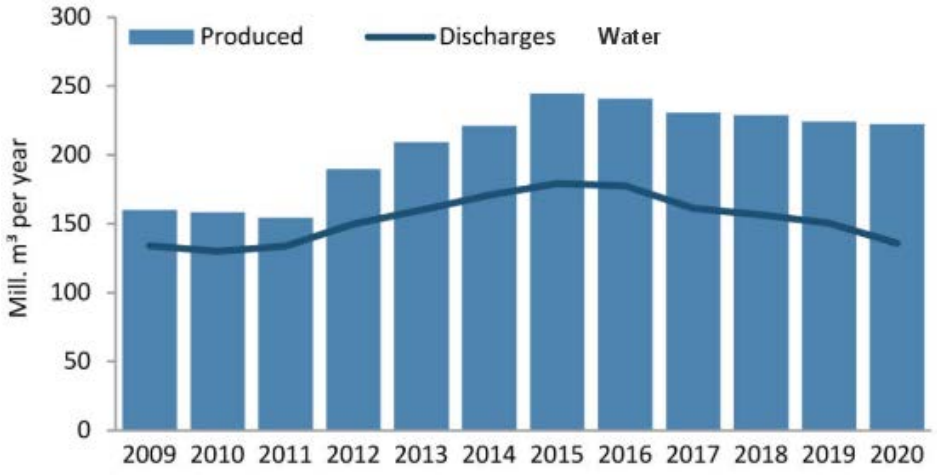

Figure 3: Histogram of water production and discharge in the North Sea (Ramstad, 2013)

Excessive water and gas production cause several issues related to production, such as decreased oil production, increased cost, and environmental problems (Hatzignatiou et al., 2014). *Figure 4* shows some challenges associated to water production.

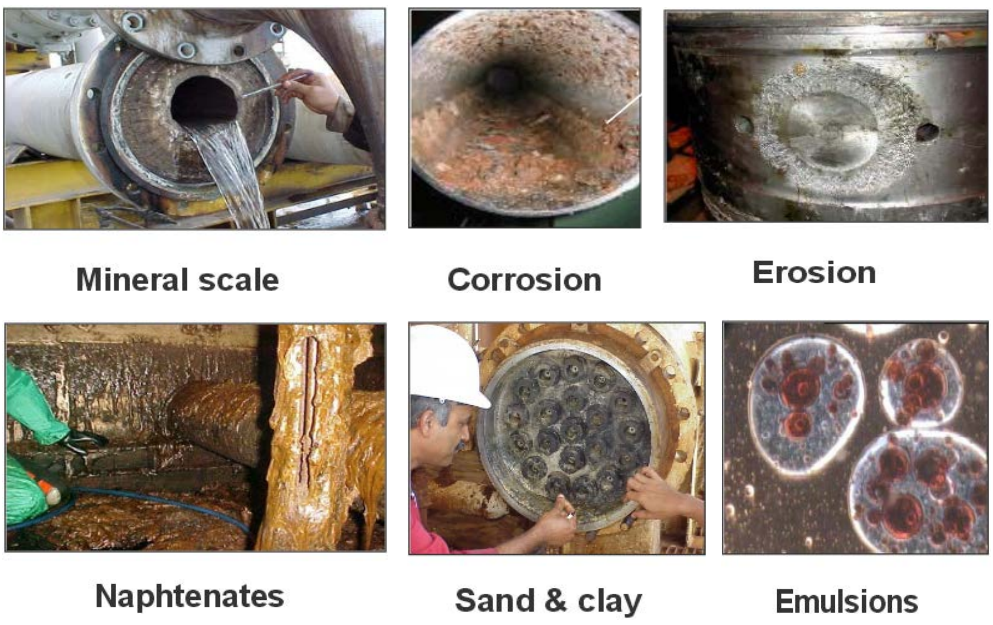

Figure 4: Some challenges related to water production (Ramstad, 2013).

2.2 Causes of Water Production

Identifying the cause behind unwanted water production is the most difficult as well as the most vital part of water control. In order to successfully design a water control program, it is important to properly understand and thoroughly scrutinize the problem (Dahl et al., 1992).

Known causes of unwanted water production include:

2.2.1 Mechanical Related Causes

Casing leaks – Caused by wear, holes from corrosion, excessive pressure or formation deformation (Bedaiwi et al., 2009).

2.2.2 Completion Related Causes

The common completion related causes of water production are:

Channel behind casing – Channels behind casing can be caused by poor casing cement or cement formation bonds. They are most likely to occur immediately after well completion or stimulation (Bedaiwi et al., 2009).

Completion into water or too close to the water zone – Perforation into a zone with a higher water saturation than the irreducible water saturation will result to immediate water production. Impermeable barriers such as shale or anhydrite that separate hydrocarbon-bearing zones from water bearing zones can breakdown close to the wellbore allowing water to migrate through the wellbore. Also, close proximity of the perforations to the water zone can enhance water coning problems (Aminian, 2009).

Fracturing out of zone – Stimulation treatment which may have entered a water zone some distance away from a well, or connected an injector to a producer.

2.2.3 Reservoir Related Causes

Channeling from water flood or natural water drive – Caused by high permeability streaks or thief zones such as fractures/fracture-like features and faults. In unfractured reservoirs, permeability variations among the different layers can cause channeling between the injection and production wells or from an edge water aquifer to the production wells. Deviated and horizontal wells can intersect fractures or faults that are connected to an aquifer thus jeopardizing the well (Aminian, 2009).

Coning – Water coning results from the vertical pressure gradient near the well. In this case, viscous forces due to rapid production from the well will overcome gravity forces and move the aquifer water beneath the oil zone upwards towards the perforations where they are produced. Reduced production rates will only curtail the problem but not cure it. A similar phenomenon is cusping in an inclined water zone up to a vertical well and water cresting in horizontal wells.

Depleted reservoir – A depleted reservoir is prone to water production and very little can be done about it.

Figure 5 shows a schematic of the different causes of unwanted water production.

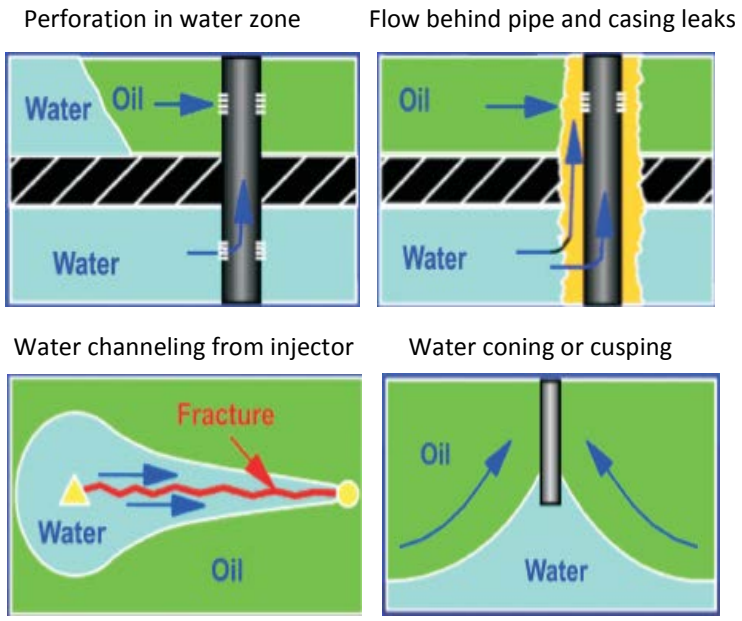

Figure 5: Some Causes of unwanted water production (Bedaiwi et al., 2009)

2.3 Problem Identification Techniques

Appropriate selection of a water control technique depends largely on the identification of the problem causing the water production. Most times, water production problems are not properly diagnosed. In reality, one of the main reasons why water control treatments have not been effective is due to wrong, inadequate or lack of diagnostics (Aminian, 2009).

The first step to identifying the cause of the water production problem is to determine when it started. Water production can occur early in the producing life of a well or later. The use of water/oil or water/gas history plots can provide useful knowledge of when the problem developed. Early water breakthrough in the life of a well is associated to completion problems. Water breakthrough later in the life of a well is associated to mechanical or reservoir causes.

To economically justify a water control treatment, it is important to ascertain whether significant volumes of hydrocarbons are remaining in the vicinity of the well. Reservoirs that are in their final production stage or late waterflood stage are not appropriate candidates for water control treatments (Aminian, 2009).

The next step is to determine whether the problem is caused by channels behind the casing or casing leaks since they are routinely and relatively easy to solve. The most common method for diagnosing casing leaks is mechanical integrity test which involves pressurizing the annulus between the tubing and casing and observing if the pressure builds and holds or not. The most common method for evaluating the cement condition and diagnosing problems related to channels behind casing is by using cement bond logs. Some other different logging methods can also be used such as electrical potential logs, noise logs, temperature surveys, radioactive tracer surveys, borehole televiewers, spinner surveys, electromagnetic inspection, multi-fingered caliper logs, and production logging (Aminian, 2009).

The next step is to determine the flow geometry around the wellbore, whether it is radial or linear. Radial flow is usually associated with flow in unfractured reservoirs while linear flow is associated with channel flow through fractures or high permeability streaks (Aminian, 2009). Seright et al. (2001) proposed a simple and inexpensive method for diagnosing the flow geometry around the wellbore based on injectivity/productivity computations:

$$IF \quad \frac{q}{\Delta P} \gg \frac{\sum kh}{141.2\mu In\left(\frac{r_e}{r_w}\right)} \quad \Rightarrow flow\ is\ linear \tag{1}$$

$$IF \quad \frac{q}{\Delta P} \leq \frac{\sum kh}{141.2\mu In\left(\frac{r_e}{r_w}\right)} \quad \Rightarrow flow\ is\ radial \tag{2}$$

Although the equations may not differentiate between linear and radial flow all the time, yet they can often give an indication of the flow geometry close to the wellbore. Other methods such as pressure transient analyses, pulse tests, core and log analysis, and inter-well tracer studies can determine whether flow is linear. Inter-well tracer test can identify the presence of fractures and whether they are the cause of a channeling problem. They are relatively inexpensive compared to pressure transient analysis (Aminian, 2009).

The next is to determine whether crossflow exist between the different layers in the reservoir. This can be achieved by pressure test between the zones, fluid saturation logs, simulation, seismic etc. (Aminian, 2009).

By doing a series of numerical simulation studies for systematic water control, Chan (1995) demonstrated that it is possible to determine whether a high water cut problem was due to coning or multilayer channeling by using diagnostic plots. According to him, *"log-log plots of the WOR (rather than water cut) vs time were found to be more effective in identifying the production trends and problem mechanisms"*. He reported that this technique has been applied in several fields in California, Texas, Alaska and the Gulf coast to optimize treatments. *Figure 6* shows the WOR log-log plot for water coning and water channeling cases obtained from simulated production result while *Figure 7* shows a real field diagnostic plot from field production history.

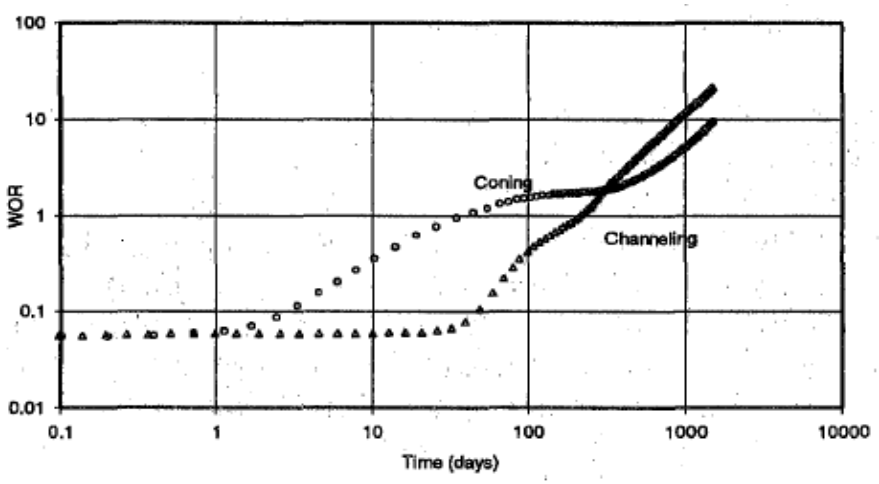

Figure 6: WOR comparison for water coning and water channeling (Chan, 1995)

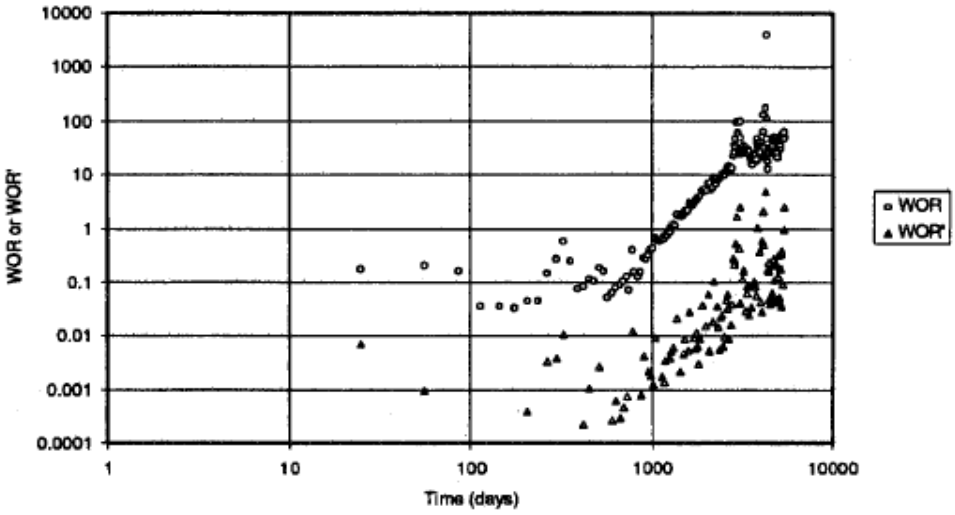

Figure 7: A field example for multilayer channeling (Chan, 1995)

Seright et al. (2001) reported that WOR diagnostic plots can be easily misinterpreted and therefore should not be used in isolation for diagnosing the cause of a water production problem.

2.4 Water Control Techniques

Several methods have been applied or suggested for water control mitigation. They can be categorized into mechanical methods, chemical method s and biological methods.

2.4.1 Mechanical methods

Mechanical methods applied for water control processes include:

- Drilling new wells
- Drilling horizontal and multi-lateral wells
- Liner placement
- Use of downhole separation equipment such as hydro-clones

Generally, mechanical methods require work over rig and are thus expensive (Nasr-El-Din and Taylor, 2005).

2.4.2 Chemical Methods

Compared to mechanical methods, chemical methods are less expensive as their application does not require any rig on the location. Unlike cement plugs, gel forming chemicals such as polymers, monomers and silicates can be used for in-depth plugging. The gel formed acts as a barrier to the flow of injected water for a length of time. The length of time is determined by the characteristics of the gel, reservoir and the movement of water in the treated reservoir (Nasr-El-Din and Taylor, 2005). In addition, chemicals that can cause precipitation in-situ can also be used. Successful chemical treatment in the field is determined by several factors which include: candidate selection, source water identification, proper choice of chemical system and the chemical placement into the target zone. A brief overview of the different chemicals that can be applied is given below.

Polymer Gels

Both organic (biopolymers) and inorganic (polyacrylamides) polymers can be used for water shut-off purposes. Polyacrylamide (PAM) polymers, as a result of their viscosity and their formed gel strength, can plug pores and fissures successfully. Biopolymers which above the critical concentration can form a physical network are not suitable for fracture treatment due to their lower strength but are more suited for pores or fissure plugging (Hatzignatiou et al., 2014). Polymers can be cross-linked with inorganic cross linkers such as Cr^{3+} or Al^{3+}. The cross-linkers can delay gelation time. (Skrettingland et al., 2014). Alternatively, organic cross-linkers can be used to form a stable gel at high temperatures (Nasr-El-Din and Taylor, 2005).

Generally, issues with polymer systems include: control of gelation, adsorption, and deep penetration because of their viscosity (Hatzignatiou et al., 2014). In spite of their commercial availability and the possibility to delay gelation time, the gel placement may pose great challenge. This is primarily due to a requisite critical polymer concentration, which causes the viscosity of the injected gelant to increase and decreases its mobility ratio, with the associated risk of placing a large fraction of the injected gel into the low productive zones (Skrettingland et al., 2014).

Monomer Gels

"Monomer gels are based on the in-situ polymerization of acrylate monomers and can be either cross-linked or not" (Hatzignatiou et al., 2014). Since the injected monomer can have water-like viscosity, their use with thermally controlled activators as discussed by Bergem et al. (1997) can be an alternative to the injection of high viscosity gelant. However, monomer gels are costly and lack environmental friendliness (Hatzignatiou et al., 2014).

Resins

According to Nasr-El-Din and Taylor (2005), phenol-formaldehyde has been applied for high temperature applications by several authors but are generally not environmentally friendly chemicals.

Chemical Precipitation

Plugging in water producing zones can be achieved by the precipitation of inorganic material. Nasr-El-Din et al. (2004) tested water shutoff by mixing two incompatible waters – pit water with high sulphate content and water with high calcium chloride content. Calcium sulphate was observed to precipitate instantly in the process. Field application of in-situ hydrolysis and flocculation of water soluble iron compounds to form gel-like precipitate is presented in Kosztin et al. (2002). The formed precipitate was found to be very stable under the prevailing field condition and no injectivity issues were experienced. Also, remediation in case of failure is said to be simple.

Inorganic Silica Gels

They are mainly colloidal silica gels and sodium silicate gels. *Table 1* shows comparison of colloidal silicate gels and sodium silicate gels gathered by Nasr-El-Din and Taylor (2005) from Iler (1979) and Jurinak and Summers (1991).

Table 1: Comparing colloidal silica and sodium silicate gels (Nasr-El-Din and Taylor, 2005)

Parameter	***Colloidal silica***	***Sodium silicate***
SiO_2 to Na_2O ratio	>50 to 1	< 4 to 1
Gel time at pH 9	1000 days	1000 min
Required SiO_2 concentration	6 to 15 wt.%	5 to 10 wt.%
Silica present as	particles, 4 to 200 nm	Silicate in solution
Gelation mechanism	Particles form a 3-D network	Silica particles form in solution and then create 3-D network
Disadvantages	Particles reduce injectivity into low permeability zones, requires higher silica concentration, more expensive	Weaker Gel

Silicate gels have not enjoyed wide application except for some application in near-wellbore problems. They can be used in water control and near-well applications because of their ability to penetrate deep into the treated zone as a result of their low initial viscosity, good chemical and thermal stability, relative low cost, environmental friendliness, and easy removal in case of failure. The disadvantages of silicate gels are the blocking effect and the gelation mechanisms. Silicate gelation is a function of pH, concentration, temperature and reacting components. There are some challenges in controlling the gelation time because its mechanisms are yet to be fully understood (Hatzignatiou et al., 2014, Lakatos et al., 1999).

Table 2:Gels for use in conformance-improvement treatments (Sydansk and Romero-Zeron, 2011)

- Inorganic based (bulk gels)
  - Silicate gels
  - Aluminum-based gels
- Organic-based polymers
  - Bulk gels
    - Synthetic or biopolymers
      - Acrylamide polymers (most widely used polymer)
      - Xanthan biopolymer
    - Organic crosslinkers
      - Aldehydes
        - Phenol-formaldehyde and derivatives
      - Polyethyleneimine
    - Inorganic crosslinkers
      - Al(III) based
      - Zr(IV) based
      - Cr based
        - Cr(VI) redox
        - Cr(III) with inorganic anions
        - Cr(III) with organic carboxylate complex ions
  - Monomer gels (organic-monomer-based in-situ polymerization)
    - Acrylamide monomer
    - Acrylate monomer
    - Phenolics
  - Lignosulfonate gels
  - Preformed particle gels
    - Swelling organic-polymer "macroparticle" gels
- Mixed silicate and acrylamide-polymer gels
- Microgels
  - Microgels with narrow particle-size distribution
  - CDGs
    - Aluminum-citrate crosslinked
    - Chromic-triacetate crosslinked
  - Delayed "popping"/swelling microgels (Bright Water™)

2.4.3 Microbial Method

Ferris et al. (1992) suggested the use of bacteriogenic mineral plugging as a viable alternative to plug high permeable streaks in order to minimize water production. The procedure involves the use of bacteria to cause the precipitation of calcium carbonate as mineral plugging and cementing agent. The bacterial used will affect the pH of the solution which subsequently will cause precipitation. It was stated from observations of CAT scan and resulting plots that near wellbore plugging may not be a problem with this process and suggested that the reason could be that the pH at this time may not have changed. Plugs produced by this method were said to be stable. They however mentioned that the developed plug is stable to water and solvents but can be destroyed by acids.

3.0 APPLICATION OF SODIUM SILICATE METHOD

3.1 Soluble Silicate Production

Sodium and potassium silicate is produced by the direct fusion of sand (SiO_2) and soda ash (Na_2CO_3) or potash (K_2CO_3) in varying proportions at high temperatures. This results in the formation of glassy materials which are then dissolved in steam to produce liquid silicate also known as water-glass (CEES, 2013).

$$M_2CO_3 + x\,SiO_2 \rightarrow M_2O \cdot xSiO_2 + CO_2 \qquad (M = Na, K) \qquad (3)$$

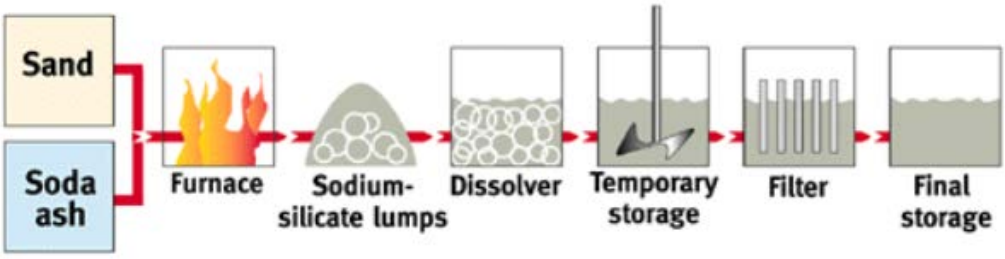

Figure 8: Production process of soluble silicates with high temperature water dissolution (CEES, 2013).

To obtain certain qualities, the silica source (silica sand) can also be dissolved hydrothermally in the respective alkali hydroxide solution (CEES, 2013).

$$2MOH + x\,SiO_2 \rightarrow M_2O \cdot xSiO_2 + H_2O \qquad (M = Na, K) \qquad (4)$$

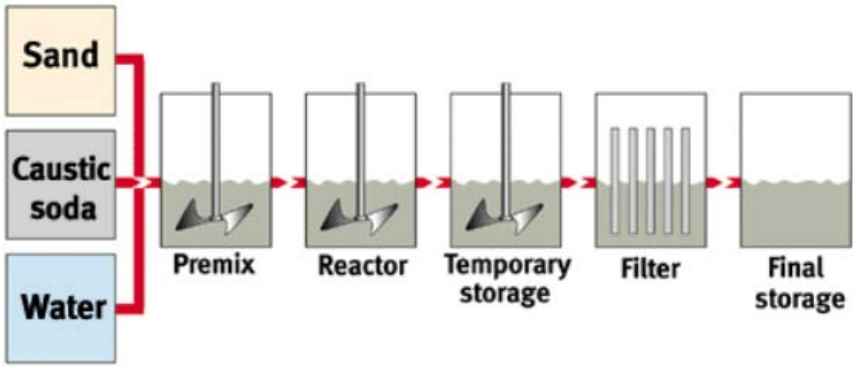

Figure 9: Production process of soluble silicates with alkali hydroxide solution (CEES, 2013).

Sodium silicate is predominantly used for water control applications and can be diluted before it is applied which results in reduced viscosity and deeper penetration into the zone of interest (see *Table 3*). Its dilution is a controlling factor in the determination of the final strength and setting time of the gel plug (PQCorp, NA).

Table 3: Typical properties of Diluted N Sodium Silicate (PQ Corp)

Volume		Density			Viscosity
N®	Water	Lb/gal	Lb/ft³	°Baume	cps
100	0	11.6	86.8	40.8	180
70	30	10.6	79.6	31.5	11
60	40	10.3	77.2	27.9	5.5
50	50	10.0	74.7	24.1	2.5
40	60	9.6	72.3	20.0	2.1
30	70	9.3	69.8	15.6	2.0

3.2 Silicate-Gel Chemistry

The chemistry of silicate is complex and not fully understood. Iler (1979) gave the following equilibria:

$$SiO_2 + 2H_2O = Si(OH)_4$$

$$Si(OH)_4 + OH^- = HSiO_3^- + 2H_2O$$

$$\mathbf{2HSiO_3^- = Si_2O_5^{2-} + H_2O} \quad \textbf{(5)}$$

$$Si_2O_5^{2-} + H_2O = HSi_2O_6^{3-} + H^+$$

$$HSiO_3^- + OH^- = SiO_3^{2-} + H_2O$$

Like polymers, silicate has the ability to polymerize to form gels or plugs with other chemicals. *Figure 10* gives an illustration of the polymerization behavior of polymer. In acidic solution or in the presence of flocculating salts (A in *Figure 10*), the silicate particles aggregate into 3D networks and form gels while in basic solution (B in *Figure 10*), the particles increase in size with decrease in numbers (Iler, 1979)

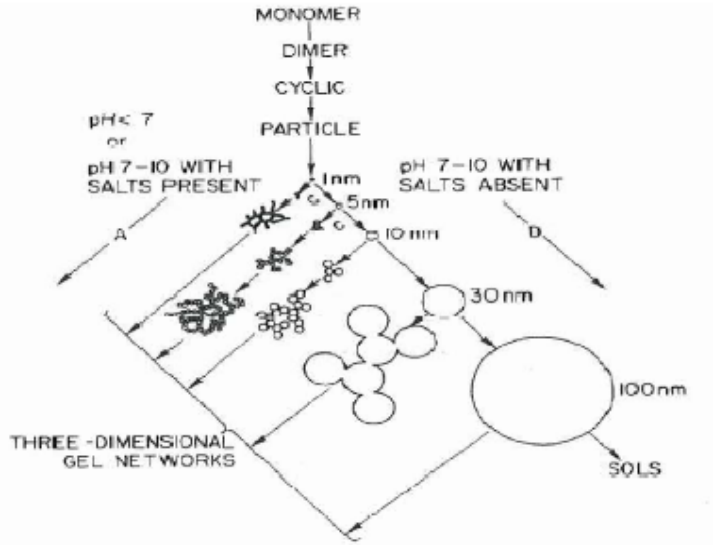

Figure 10: Schematic illustration of polymerization behavior of silica (Iler, 1979).

According to Iler (1979), three stages are recognized in the formation of Silica gels.

- The monomer polymerizes to form particles.
- The particles grow.
- The particles link together into branched chains, then networks, and extends throughout the liquid medium, thickening it until it gels.

The polymerization reaction that causes the silica molecular weight to increase involves the condensation of silanol groups (Iler, 1979):

$$-SiOH + HOSi- = -SiOSi- + H_2O \quad (6)$$

3.3 Silicate Particle Size and Deposition

The silicate particle size plays an important role for it to gel. This is because the solubility of the silicate is dependent on the particle size. Solubility increases with decreasing particle size (Hatzignatiou et al., 2014). *"The higher solubility of the smaller particles is pronounced only when the particle size is smaller than about 5 nm and very pronounced when it is less than 3 nm" (Iler, 1979).* Above pH 7, the dissolution and deposition rate of silicate is high and at ordinary temperatures the particles continue to grow until they are 5-10 nm in diameter, then growth becomes slow afterwards. However at low pH values, the polymerization and depolymerization rate is slower and the particles grow negligibly after they reach a size of 2-4 nm. At higher temperatures and especially above pH 7, they continue to grow to larger sizes (Iler, 1979).

Stavland et al. (2011a) introduced the use of gel codes to quantify gelation time by visual inspection (see *Table 4*).

Table 4: Quantification method for gelation time by visual inspection using gel codes

Gel Code	Description
0	Clear and low viscous fluid
1	Cloudy and low viscous fluid
2	Cloudy and high viscous
3	Rigid Gel

Filtration test of silicate samples was alternatively used to quantify gelation time. Silicate samples under gel code 1 were observed to plug 3 μm filter while samples that have not reached gel code 1 could not plug the filter (Stavland et al., 2011b). Skrettingland et al. (2014) observed

by core flood experiments that the resistance factor, RF increased when filtration of the silicate solution was done with a 5 μm filter but was stable with a filter size of 1.2 μm (see Figure 11)

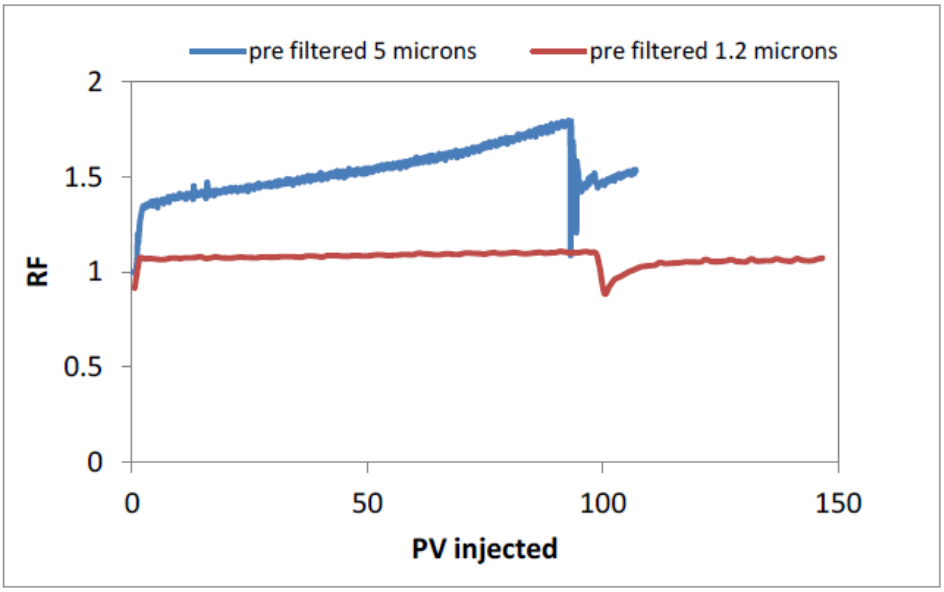

Figure 11: Filter size effect on mobility reduction, RF (Skrettingland et al., 2014)

Another simple and reliable method for quantifying gelation time is by measuring the turbidity of the silicate solution with time. Stavland et al. (2011b) found that the turbidity of the silicate solution increased with time during the process of gelation and that the silicate samples which plugged the 3 µm filter had a turbidity of 170 NTU. A relation between the turbidity and effective particle size was suggested by Stavland et al. (2011b) as follows:

$$d = Bx(t - t_o)^a \quad (7)$$

Where d is particle size, t is turbidity, and a, B and t_o are tuning parameters.

According to Stavland et al. (2011b), increased particle size can be used to model the gelation kinetics of silicate since by reaction, nano-size particles form micro-size particles which in turn react to form macro-size particles (rigid gel).

The deposited silicate particle size can affect permeability reduction. The permeability reduction of the formation is controlled by the ratio between the particle and pore diameter (Stavland et al., 2011b). An equation derived from a capillary tube model that relates the permeability reduction to the pore-particle diameter is given as follows (Stavland et al., 2011b):

$$RRF = (1 - \frac{d}{R})^{-4} \quad (8)$$

Where RRF is the permeability reduction, R is the pore radius, d is the particle size. The equation shows that RRF will increase with increase in particle size. Observation from Figure

12, a plot of permeability reduction vs pore-to-particle diameter by Stavland et al. (2011b) showed that the RRF profile is in qualitative agreement with the formation damage rule of thumb, that is, face plugging if D/d <3, internal plugging if 3< D/d < 7 and no plugging if D/d >7.

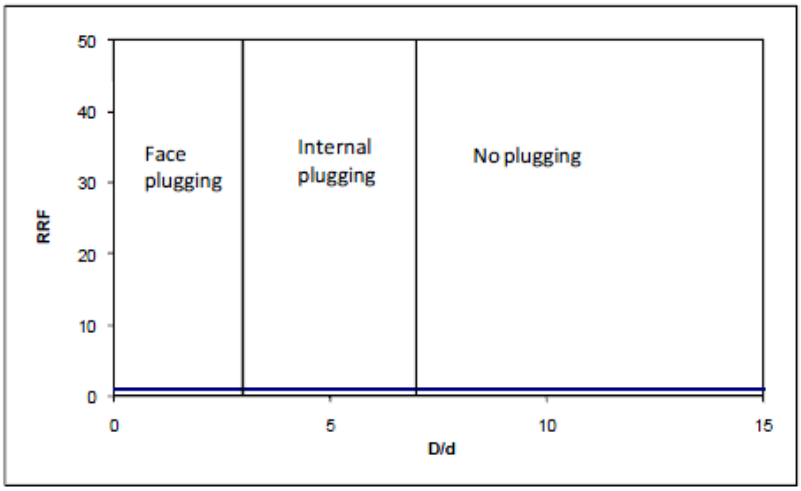

Figure 12: Permeability reduction vs the pore-to-particle diameter (Stavland et al., 2011b)

In addition, Stavland et al. (2011b) also demonstrated experimentally that plugging of aged silicate solution at low injection rates depends on permeability. A 2 Darcy Bentheim core and a 500 mD Berea core plugged at 20 hours and 12 hours respectively at an injection rate of 0.167 ml/min. Similar experiment was done using an unconsolidated sand column of 9 Darcy and 2 Darcy. They observed that the 9 Darcy sand column had in-depth plugging while the 2 Darcy Bentheim core and the 2 Darcy sand column had face plugging approximately at the same time.

The general implication is that the injection velocity, permeability and pore-particle diameter could be critical in determining the plug location.

3.4 Silicate Gelation Kinetics

Bulk gelation experiments were used to model silicate gelation kinetics. The various factors influencing the gelation time were also studied as previously described. A relationship for estimating the silicate gelation time was proposed by Stavland et al. (2011a) with the temperature based on the Arrhenius type thermal energy equation:

$$t_g = A \times e^{\alpha[Si]} \times e^{\beta[HCl]} \times e^{\gamma\sqrt{[Ca^{2+}]}} \times e^{E_a/RT} \qquad (9)$$

Where t_g is the gelation time in days, $[Si]$ is the silicate concentration in wt%, $[HCl]$ is the acid concentration in wt%, $[Ca^{2+}]$ is the concentration of calcium in the make-up water in ppm, E_a is the activation energy, R is the gas constant which is 8.31 $JK^{-1}mol^{-1}$ and T is the absolute

temperature. The constants A, E_a, α, β, and γ are obtained by tuning the model to fit the experimental data. *"This model assumes that the dependency of the silicate-, activator- and make up water salt concentration can be regarded as individual parameters"* (Skrettingland et al., 2012).

Figure 13 shows the result of the matched model and experimental data by Stavland et al. (2011a) with the following values obtained for the constants: $A = 2.1 \times 10^{-8}$, $E_a = 77\ KJmol^{-1}$, $\alpha = -0.6$, $\beta = -0.7$, and $\gamma = 0.1$.

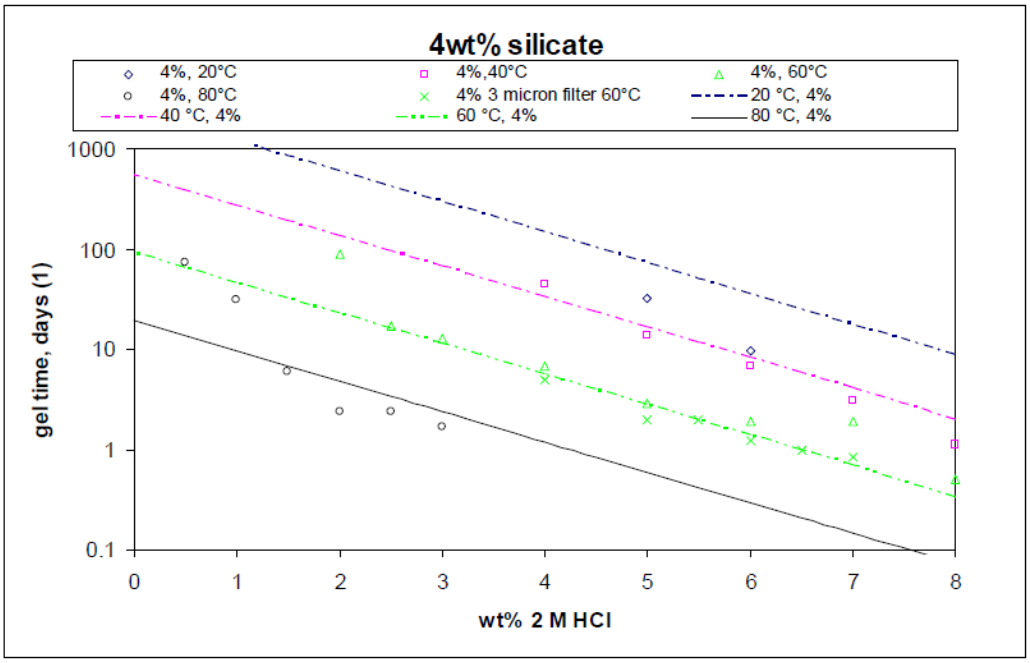

Figure 13: Gelation model matched with experimental data. 4 wt.% silicate (Stavland et al., 2011a)

Figure 13 shows that between 40°C to 60°C, the gelation model gave a good match with the result of the experiment but predicts a longer gelation time at 20°C. Similar experiment conducted by (Skrettingland et al., 2012) shows basically the same gelation kinetic as reported in (Stavland et al., 2011a) with the following constant values obtained by tuning the gelation model using the bulk gelation time: $A = 2.6 \times 10^{-5}$, $E_a = 50.6\ KJmol^{-1}$, $\alpha = -0.6$, $\beta = -0.7$, and $\gamma = 0.11$.

A brief description is given below of the various factors that affect the silicate gelation kinetics.

3.4.1 Effect of pH

The reaction rate of the silicate gel is dependent on pH. The pH of commercially delivered sodium silicate, $(SiO_2)_n$:Na_2O, lies between 11-13 and depends on the SiO_2:Na_2O molar ratio, n. As the molar ratio, n is decreased, the alkalinity and density increases (Skrettingland et al.,

2012). A reduction in the pH of the silicate fluid causes it to gel by a polymerization reaction. Therefore, pH is said to be the controlling parameter for the placement of the silicate gel (Stavland et al., 2011b). The minimum gelation time of the silicate solution have been found to take place just below the neutral pH. *Figure 14* shows the gelation time for the silicate solution at various pH values. Gelation time is maximum at pH of 2, and decreases as the pH is increased from 2 to about 5. Minimum gelation time occurs between pH of 5 and 6. Above pH of 7, the gelation time increases, but at pH of 11, there is no gelation except salt is present due to reduction in charge repulsion (Hatzignatiou et al., 2014)

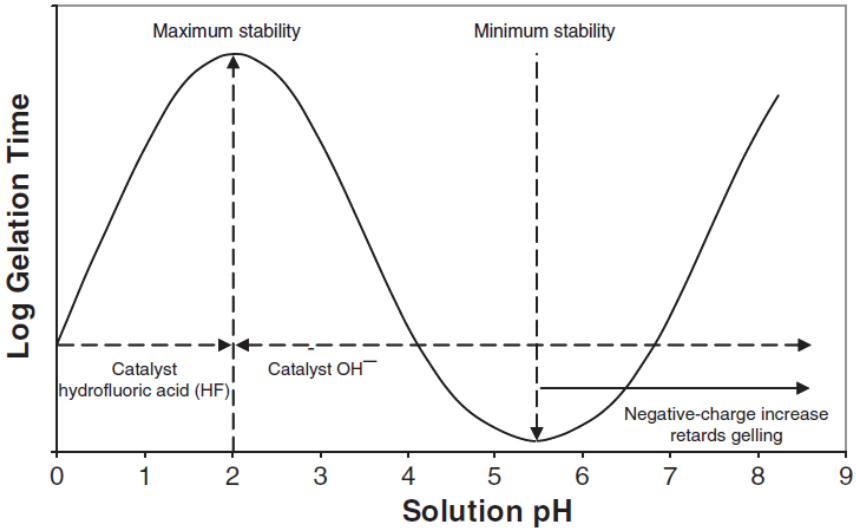

Figure 14: pH effect on silicate gelation time (Iler, 1979, Vinot et al., 1989, Hatzignatiou et al., 2014)

Activators are used to influence gelation by reducing the pH of the silicate solution. Internal or external activators can be used. Internal activators function by decomposition into species that initiate gelation such as acids or ammonium salt while external activators such as calcium and magnesium salts function by precipitation of the silicates during contact or mixture with the silicate solution (Nasr-El-Din and Taylor, 2005). Krumrine and Boyce (1985) gave a good overview of likely gelation agents. Elfrink (1966) suggested the use of urea as an internal activator for silicate gels. The use of a diester was suggested by Vinot et al. (1989). However, the simplest applied method is the addition of acid to the silicate injected (Stavland et al., 2011a). Results from an experimental investigation by Stavland et al. (2011a) as presented in *Figure 15* shows the dependence of gelation time on the pH of the injected silicate solution. From the figure, it can be observed that small changes in the pH have a large effect on the time of gelation.

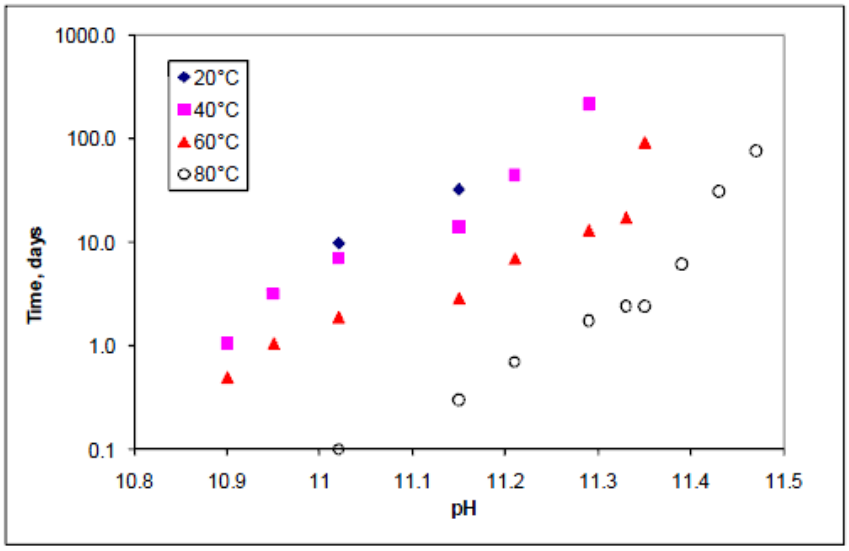

Figure 15: Gelation time, 4 wt.% silicate in distilled water, gel code 1 (Stavland et al., 2011a).

Stavland et al. (2011a) noted that it is difficult to control the gelation time using the pH. This is because of the variation in pH obtained by the different silicate solution samples as seen in Figure 15 which is most likely due to complex reactions. They however suggested that since a plot of the pH against the amount of HCl added gave a linear relationship (see

Figure 16), the gelation time will be more accurately measured using the amount of acid added.

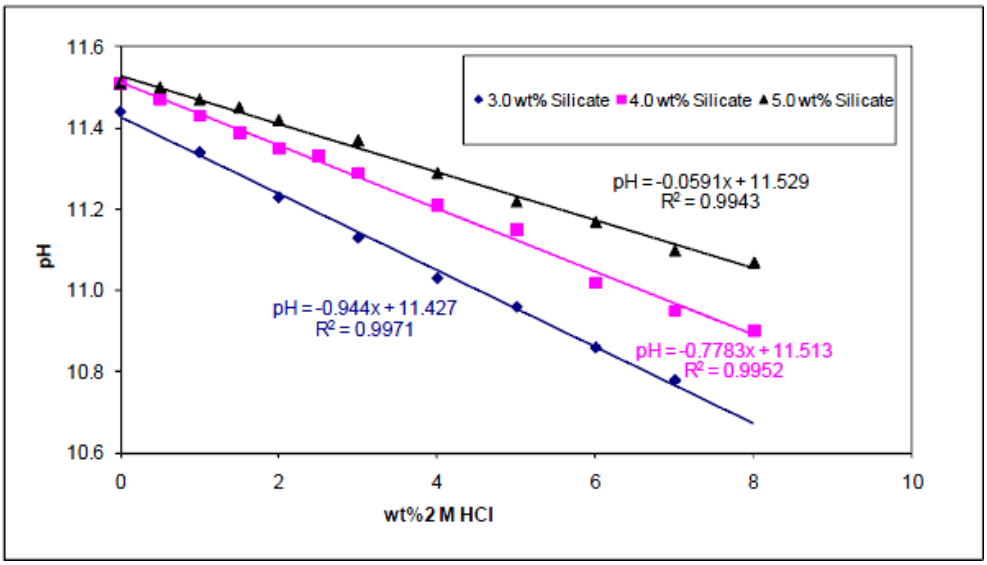

Figure 16: pH versus amount of HCl added (Stavland et al., 2011a).

As reported by Stavland et al. (2011a), if the silicate concentration and the reservoir temperature is constant, the gelation will be controlled by the concentration of the acid added. Experimental result by Skrettingland et al. (2012) presented in Figure 17 show that for all temperatures used, the plugging time decreases as the HCl acid concentration is increased.

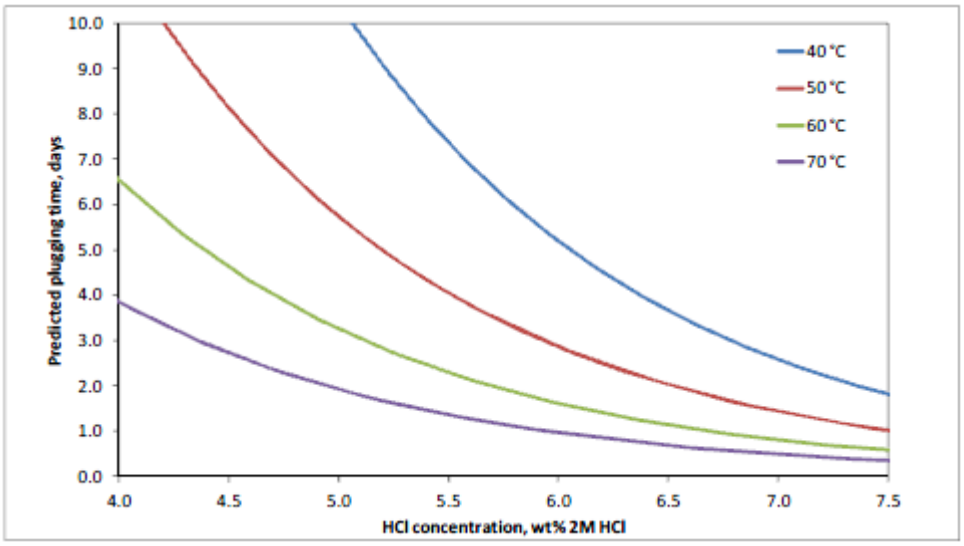

Figure 17: The effect of acid concentration on gelation time for 4 wt.% silicate in tap water (Skrettingland et al., 2012).

3.4.2 Effect of Silicate Concentration

Increase in the sodium silicate concentration decreases gelation time by increasing the pH required for the activation of the gel. *Figure 18* (Nasr-El-Din and Taylor, 2005) shows how the gelation pH varies with the initial silicate concentration. Also, Stavland et al. (2011a) experimentally show that at constant HCl concentration, the gelation time decreases slightly as the silicate concentration is increased.

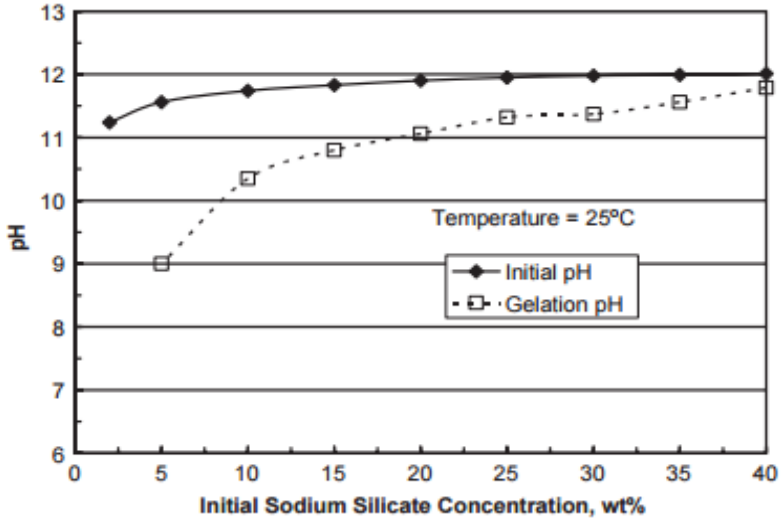

Figure 18: Effect of initial sodium silicate concentration in 15 wt.% HCl on initial and gelation pH (Nasr-El-Din and Taylor, 2005)

3.4.3 Effect of Temperature

Temperature effect on silicate gelation time at constant pH and salinity mimics the Arrhenius equation (Jurinak and Summers, 1991).

$$t_g = Ae^{E_a/RT} \quad (10)$$

Where A is the pre-exponential factor, E_a is the activation energy, R is the gas constant, T is the absolute temperature. As the temperature increases, the rate of polymerization increases, thus decreasing the gelation time. *Figure 19* (Stavland et al., 2011a) shows the effect of temperature on gelation time.

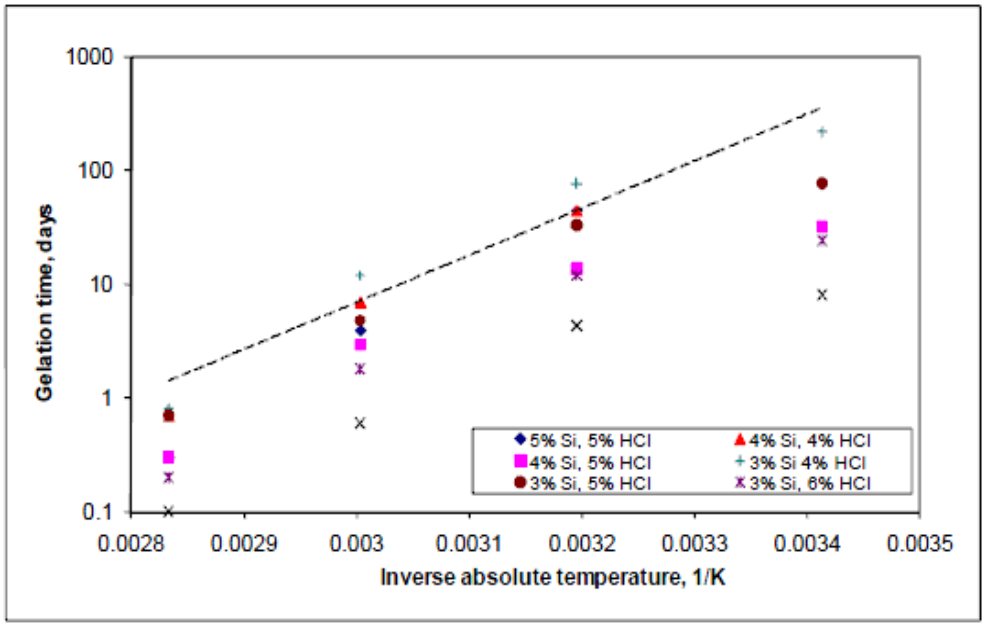

Figure 19: Gelation Time versus Inverse temperature (Stavland et al., 2011a)

3.4.4 Salinity/Cation Exchange

Salt is known to activate gelation. Gelation time is sensitive to brine salinity and decreases when the concentration of NaCl in the makeup water is increased. The calcium concentration in the makeup water also behaves in a similar and more effective manner (Stavland et al., 2011a).

Different salinities between the displacing brine and the displaced is likely to result in cation exchange. When the silicate solution is diluted in distilled water, it takes longer time for gelation to occur than when it is diluted in brine. Stavland et al. (2011a) reported a gelation time that is 1.6 times longer when distilled water is used than when tap water containing 20ppm of Ca^{2+} is used. Experimental results by Stavland et al. (2011a) as illustrated in Figure 20 show how the gelation time is affected by the Ca^{2+} concentration in the makeup water.

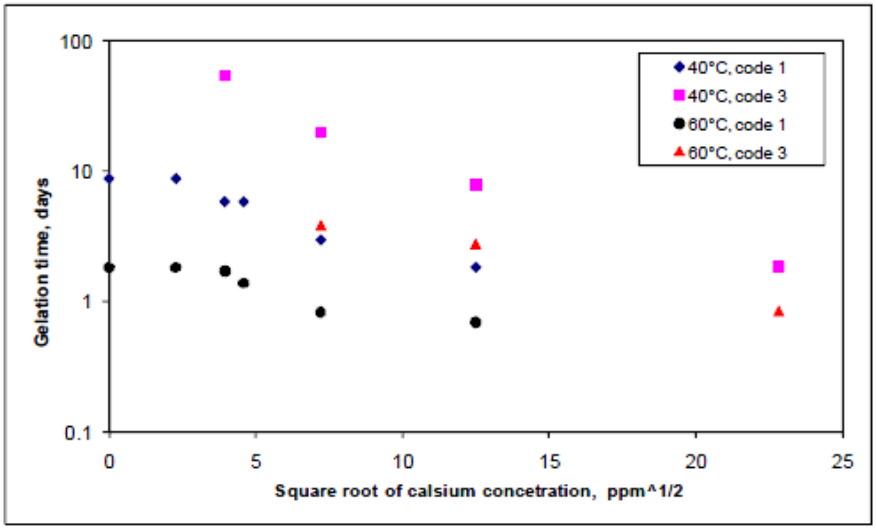

Figure 20: Gelation time versus calcium concentration in the makeup water (Stavland et al., 2011a)

Precipitation occurs when alkaline solutions are mixed with formation water or sea water. This is one of the earlier and main arguments why sodium silicate is not used offshore other than for near-wellbore treatment (Skrettingland et al., 2012). *"Sodium silicate will react with Mg^{2+} and Ca^{2+} and form Mg-Ca-silicate complexes which may precipitate or activate gelation"* (Skrettingland et al., 2014). At pH above 9, $Mg(OH)_2$ will precipitate because of its solubility product $K_{Mg(OH)2} = 1x10^{-11}$ while $Ca(OH)_2$ with solubility product, $K_{Ca(OH)2} = 4x10^{-6}$ is soluble up to a pH of 12 (Skrettingland et al., 2012). (Skrettingland et al., 2014) conducted some experiments to investigate the impact of in-depth mixing of dilute sodium silicate and formation water. Two 2% SiO_2 solution was used to displace formation water made up of 50% sea water in Bentheim cores. It was observed that before the Silicate was injected for both, the differential pressure was constant, but when the silicate was injected, a sharp pressure increase was observed which peaked at the breakthrough of the silicate solution. As the silicate was injected continuously after breakthrough, the RF decreased slowly. After 10 pore volumes of silicate had been injected after breakthrough, KCl brine having a concentration of 5000ppm was injected and the permeability was partially regained due to the dissolution of the precipitates which is an indication of the capacity of KCl brine to exchange the divalent ions. This can be observed in Figure 21 where the mobility reduction was derived from the differential pressure.

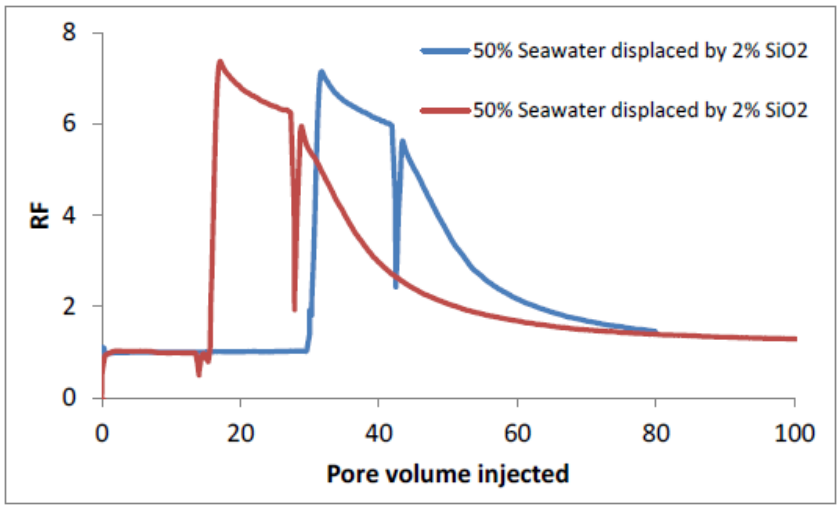

Figure 21: Pressure response during the displacement of formation water (50% sea water) with sodium silicate. Sodium silicate injected at 14 PV and 30 PV for the two tests (Skrettingland et al., 2014).

To prevent near wellbore plugging due to salinity or cation exchange, it is important that the reservoir is pre-flushed before the injection of the silicate solution. Core flood experiments revealed that precipitation will not cause permeability reduction if the relative concentration of the sea water is below 10% (Skrettingland et al., 2012).

Apart from formation brines, reservoir rocks are also known to be made up of certain minerals that contain divalent ions. As a result of this, the pre-flush fluid must not only be able to displace the formation water from the silicate slug as a freshwater pre-flush would do but must also be able to exchange the divalent ions present on the formation rock. This will prevent the silicate slug from forming high magnesium and calcium concentration banks that may result in rapid plugging. KCl or NaCl brine pre-flush can be used to exchange divalent ions on the rock surface. However, KCl brine is preferred because NaCl is known to cause clay swelling (Skrettingland et al., 2014).

The cation exchange capacity, CEC is the controlling parameter for cation exchange. CEC varies with rock material type. Sheng (2010) reported CEC to be strongly dependent on the clay mineral type. He observed the CEC for different rock types to range between 5 to 29 meq/kg rock. CEC can be measured directly on rock samples, or estimated from the mineral composition of rock samples (Skrettingland et al., 2014). Sheng (2010) assumes CEC dependence on rock surface area. Skrettingland et al. (2014) estimated the CEC of a set of reservoir cores from Snorre field with different surface areas computed with the Carman-Kozeny equation for rock surface area:

$$S = 1/4\left(\sqrt{2/\tau}\right).(\varphi/(1-\varphi).(\sqrt{\varphi/k}) \quad (11)$$

Where τ is the tortuosity, φ is porosity and k is permeability. The resulting plot is presented in *Figure 22*. In order to observe how the CEC varied with permeability, Skrettingland et al. (2014) used the same approach and extrapolated to higher permeabilities as shown in *Figure 23*.

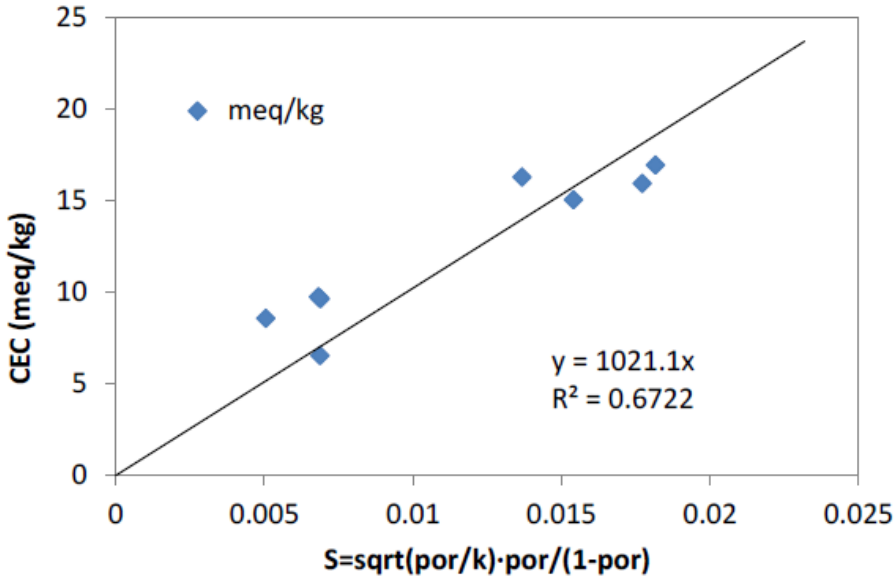

Figure 22: Cation exchange capacity for a set of Snorre reservoir core plugs (Skrettingland et al., 2014).

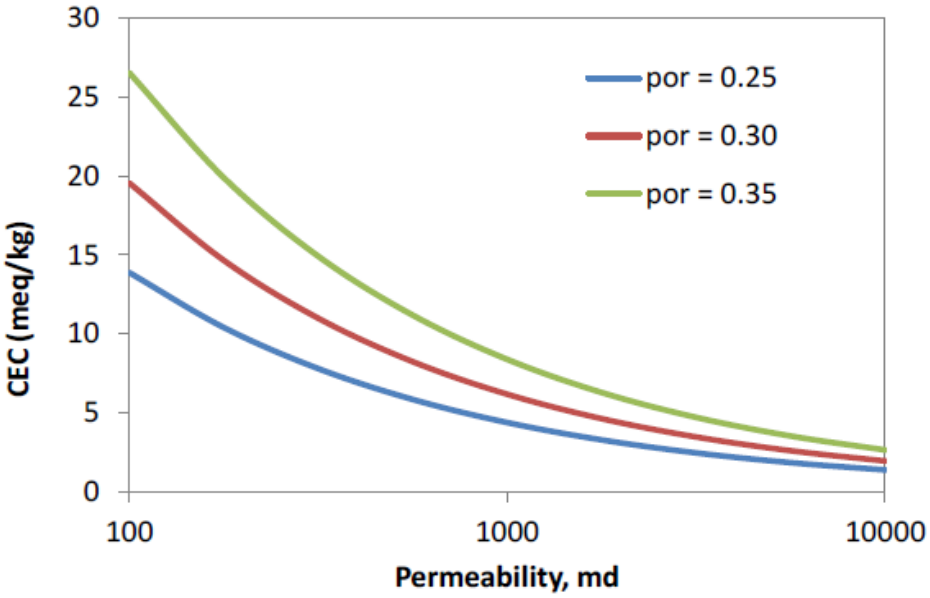

Figure 23: Estimated CEC as a function of reservoir permeability (Skrettingland et al., 2014).

3.5 Silicate Gel Stability and/or Strength

According to Kennedy (1936), *"the effectiveness of a water shutoff treatment depends upon the amount of precipitate that can be formed in the pores, and upon the nature, especially the hardness of the precipitate"*.

Stavland et al. (2011a) observed that the applied pressure gradient influences the gel strength of the silicate gel formed in-situ. Some of the sodium silicate gels are relatively brittle and compared to organic gels they are more easily degraded by high pressure gradients (Skrettingland et al., 2014). The silicate gel formed tends to shrink over time, thus reducing the blocking effect of the gel (Hatzignatiou et al., 2014).

The strength of silicate gels formed in-situ can be improved by adding polymer to the silicate solution (Burns et al., 2008, Lakatos et al., 2011).

3.6 Silicate Treatment Design

Successful chemical treatment is determined by several factors such as candidate selection, source water identification, proper selection of the chemical system, and chemical placement into the target zone (Nasr-El-Din and Taylor, 2005). The chemical treatment design must be considered very important for it to be effective. Factors such as low gel strength, too early gelation, and too small gel size can be avoided if the gelation factors are put into consideration before any application. The impact of these factors should be experimentally investigated and a predictive model or tool developed by numerical simulation using the result obtained to better understand and predict the behavior of the gel. Results from the simulation can then be analyzed and the parameters tuned in order to optimize the gel design (Herbas et al., 2004, Hatzignatiou et al., 2014).

3.6.1 Permeability Contrast

As will be discussed later in the result section of this thesis, one very important factor that determines silicate applicability in an area is the permeability contrast between the high permeable thief zone and the other zones in the reservoir. According to Skrettingland et al. (2014), one of the criteria for choosing an area of application for in-depth water plugging using silicate is that the area must be dominated by a high permeability thief zone which will cause early water breakthrough during water flooding leaving behind mobile oil.

In addition, permeability contrast can have an impact on the mixing of the silicate and the formation water. The relative volume of pre-flush fluid entering the high and low permeable

zones in the formation will be determined by the permeability contrast. The higher the contrast, the higher the volume of pre-flush fluid entering the high permeable zone relative to the low permeable zone. The level of contrast will also determine at what time or location the injected silicate front in the high permeable zone will catch up with the formation water tail in the low permeable zone adjacent to it. If this happens, mixing of the injected silicate and formation water may occur due to the vertical communication or cross flow existing between the zones, resulting in partial plugging. (Skrettingland et al., 2012). This mixing if early is undesirable and hence, steps must be taken to avoid it.

3.6.2 Silicate Slug Size

The silicate slug size is an important design parameter as shown in Skrettingland et al. (2014). A sensitivity study on silicate slug size by Skrettingland et al. (2014) revealed that the 2 months slug size produced the greatest EOR volumes. In addition, the silicate slug size can be optimized to reduce the risk of early precipitation and separation of the gel location in the low and high permeability layers which can cause a reduction in injectivity (Skrettingland et al., 2012).

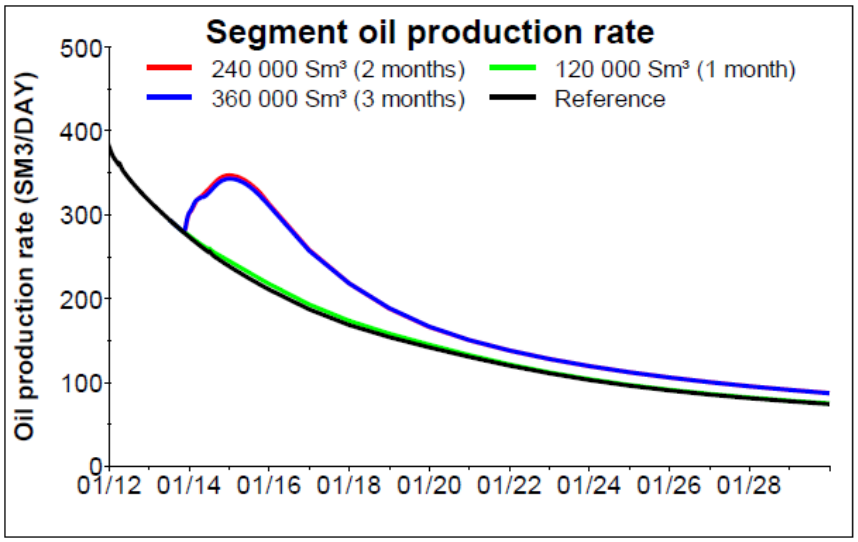

Figure 24: Sensitivity of slug size on EOR volumes (Skrettingland et al., 2014).

3.6.3 Pre-flush slug size/Ion concentration

An important factor that should be considered during the design process is the volume of pre-flush slug that will be required to ensure in-depth placement of the gel far from the injector. Due to dispersion, it is possible for the silicate slug to contact the displaced formation water and therefore cause early plugging. Also, the volume of pre-flush slug can determine the time and location at which the injected silicate front in the high permeable zone will catch up with the displaced formation water in the low permeable zones adjacent to it. Knowledge of the

amount of fluids entering the high and low permeability zones can be used to design the process to delay the mixing (Skrettingland et al., 2012).

In addition, in order to avoid possible early precipitation of the silicate slug due to cation exchange with the rock surface, the pre-flush should be designed such that it not only displaces the formation water but also exchanges the divalent cations. Hence, the size and concentration of ions in the pre-flush is critical for controlling the ion exchange (Skrettingland et al., 2014).

3.7 Numerical Dispersion

Finite difference approximations are used to replace derivatives of fluid flow equations which are most often, non-linear partial differential equations (PDE). The solutions of these approximations introduce an error called *truncation error* which is small for many problems making the solutions to be sufficiently correct for engineering purposes. However, truncation error can be significant for certain types of problems making their solutions inaccurate and unacceptable. Typical examples are miscible and immiscible floods in which the viscous forces are much greater than the capillary forces. The Buckley-Leverett problem in which the capillary pressure is set to zero is the most common example for immiscible floods (Fanchi, 1983)

The 1D convection-dispersion equation below is a relatively simple equation where the impact of truncation error is exhibited.

$$\varphi \frac{ds}{dt} = K \frac{\partial^2 S}{\partial x^2} - v \frac{\partial S}{\partial x} \qquad (12)$$

Where the constant coefficients, $\varphi = porosity$, $K = dispersion\ coefficient$ and $v = velocity$. The solution, S can be either saturation or concentration.

The truncation error introduced by the finite difference solution of equation (12) can cause smearing of an otherwise sharp saturation front as though additional physical dispersion is present. This smearing due to the truncation of Taylor's series is often called *numerical dispersion or numerical diffusion*. Smeared saturation fronts can significantly change calculated quantities which are of interest in reservoir studies. For instance, numerical dispersion can lead to calculated breakthrough times being underestimated. A related case is when gas/oil or water/oil ratios increase prematurely due to calculated earlier breakthrough time of the displacing fluid. (Fanchi, 1983). Numerical grid refinement have been found to reduce the effect of numerical dispersion. However, a balance is usually made because of the effect of grid refinement to simulation runtime.

Apart from the smearing effect, other effects of numerical dispersion on the finite difference solution, especially with respect to multidimensional (2D or 3D) flow problems is the rotation of the principal flow axis and alteration of the magnitude of the dispersion coefficients (Fanchi, 1983). Fanchi (1983) shows that by decreasing the time-step size, the rotation effect in multidimensional studies can be largely minimized.

The general 3D convection-dispersion equation is given as:

$$\varphi \frac{\partial S}{\partial t} = \sum_{i=1}^{3} \left(\sum_{j=1}^{3} K_{ij}^{phy} \frac{\partial^2 S}{\partial x_i \partial x_j} - v_i \frac{\partial S}{\partial x_i} \right) \tag{13}$$

Where $(\partial x_i : i = 1, 2, 3)$ represent the Cartesian coordinates, and the term K_{ij}^{phy} = ijth element of the dispersion tensor.

Truncation error analysis performed by Fanchi (1983) shows that the equation (13) above does not account for the numerical dispersion. To account for the numerical dispersion, the equation was re-written as:

$$\varphi \frac{\partial S}{\partial t} = \sum_{i=1}^{3} \left[\left(\sum_{j=1}^{3} K_{ij} \frac{\partial^2 S}{\partial x_i \partial x_j} \right) - v_i \frac{\partial S}{\partial x_i} \right] \tag{14}$$

Where the total dispersion, is:

$$K_{ij} = K_{ij}^{phy} + K_{ij}^{num} \tag{15}$$

$K_{ij}^{num} = numerical\ dispersion\ resulting\ from\ truncation\ error$. *Table 5* presents values of K_{ij}^{num} for finite difference representations.

Table 5: Summary of multidimensional numerical dispersion results (Fanchi, 1983)

Difference Technique		Numerical Dispersion Tensor (K^{num})
Space	Time	ijth Element
backward-difference	explicit	$\frac{v_i}{2}\left(\Delta x_i - v_i \frac{\Delta t}{\varphi}\right),\ i = j$ $-1/2\, v_i v_j \frac{\Delta t}{\varphi},\ i \neq j$
centered-difference	explicit	$-1/2\, v_i v_j \frac{\Delta t}{\varphi},\ all\ i, j$ $\frac{v_i}{2}\left(\Delta x_i - v_i \frac{\Delta t}{\varphi}\right),\ i = j$
backward-difference	implicit	$1/2\, v_i v_j \frac{\Delta t}{\varphi},\ i \neq j$
centered-difference	implicit	$-1/2\, v_i v_j \frac{\Delta t}{\varphi},\ all\ i, j$

4.0 MODEL SET-UP

For the purpose of this study, 2D and 3D synthetic models are used. The 2D models are used to check the effect of grid refinement on the reliability of the results. The 3D model are used to run important sensitivities on silicate slug size, injection time, gel location and permeability contrast and their effect on recovery.

4.1 Data Files Source

The original data files were obtained from Statoil ASA, Norway. A synthetic model was used to reduce complexity and to save simulation runtime. This implies that apart from the grid block geometry, most of the properties of the reservoir are analogue of the Snorre field. The files were updated and parameters varied for the several simulation runs.

4.2 2D Model Description

4.2.1 Grid Description

The original 2D coarse grid is a simple corner point geometrical grid with a dimensions of 32 x 1 x 17 grid blocks which totals to 544 cells. Depths to gas-oil contact and water-oil contact are 1900 m and 2500 m respectively. The pressure at the gas-oil contact which is also taken as the datum pressure is 270 bar.

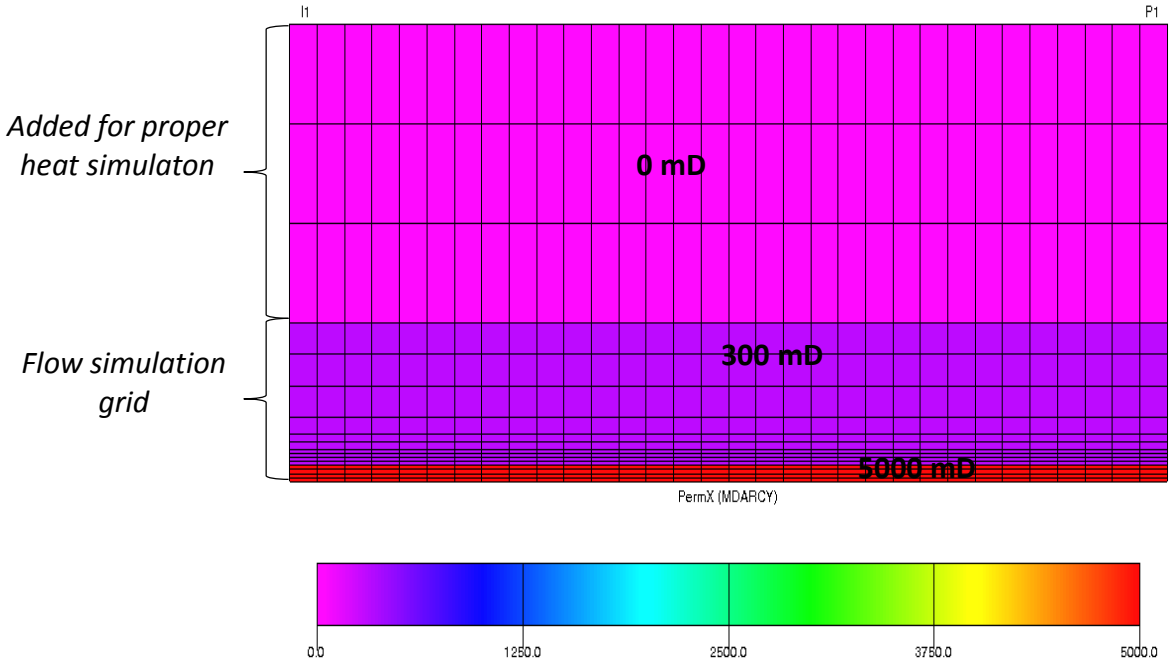

Figure 25: 2D coarse grid.

4.2.2 Well Information

The injection and production wells are located in the first and last blocks of the coarse grid respectively and are connected (perforated) in all layers except layer 1-3 which was mainly added for temperature simulations. A summary of the well information is presented in

Table 6.

Table 6: 2D Model Well Information

Well Name	***Connection Location (X, Y, Z1-Z2)***	***Well Diameter (m)***	***Liquid Rate Target (Sm3/D)***	***BHP Target (Bar)***
Injection "I1"	1, 1, 4-17	0.2	12000	370
Production "P1"	32, 1, 4-17	0.2	125	120

4.2.3 Rock Properties

The fluid phases present in the model are water, oil, gas and dissolved gas. However, no free gas exists in the models since the models are above the bubble point pressure at all times. *Table 7* shows the porosity and permeability for each layer in the grid. The first three large layer blocks from the top were added to act as heat sinks, and is applied for temperature simulations only, that is, to enable heat exchange throughout the reservoir. They were thus made inactive for flow simulations by setting their permeability to zero. This implies that only the last 14 layers of the grid were used for active flow simulations. The rock compressibility is 4.84 x 10^{-5} bar^{-1} at a reference pressure of 277 bars.

Table 7: 2D Model Porosity and Permeability

Layer	***Porosity***	***Permeability***		
		X	***Y***	***Z***
1 - 3	0.05	0	0	0
4 - 13	0.20	300	300	30
14 - 17	0.25	5000	5000	500

4.2.4 Fluid Properties

The densities of the water, oil, and gas phases are 1023.8 kg/m^3, 834.5 kg/m^3, 1.24691 kg/m^3 respectively. The injection water temperature is 30^oC, and the subsurface reservoir temperature vs depth is presented in *Table 8*. Thus, the average reservoir temperature is approximately 98.5^oC. The oil and water viscosity tables are displayed in appendix A2. The model contains

four saturation function tables for different SATNUM regions. The relative permeability values for each SATNUM region, are also displayed in appendix A2. Capillary pressure was assumed to be equal to zero in all cases. The water formation volume factor, FVF, compressibility and viscosity are 1.025 rm^3/sm^3, 0.3895 bar^{-1} and 4.172 x 10^{-4} cp respectively at a reference pressure of 300 bar. The oil and gas FVF as a function of pressure and solution GOR are also displayed in appendix A2.

Table 8: Subsurface reservoir temperature measurements

Depth (m)	Temperature (°C)
1800	90,78
1900	93,36
2300	103,69
2400	106,28

4.3 3D Model Description

4.3.1 Grid Description

The 3D grid is a simple corner point geometrical grid with a dimension of 48 x 48 x 18 grid blocks which is a total of 41472 cells. The total number of active cells for flow and heat simulations is 28800 as shown in *Figure 26*. The number of cells for flow simulations alone is 16000. The 9th layer in the grid is the high permeability thief zone.

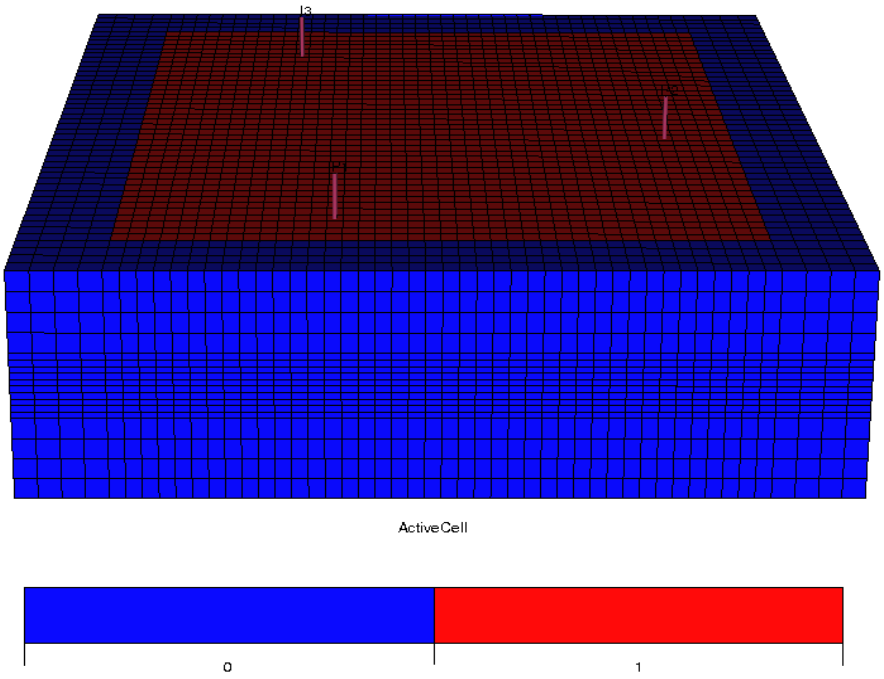

Figure 26: 3D Grid showing total active cells in red for flow and heat simulations

4.3.2 Well Information

Table 9 gives an overview of the well information. There are two production wells and one injection well with wellbore diameter of 0.2 m. The three wells are connected to the reservoir in the 5th to the 14th layer as shown in *Table 9*.

Table 9: 3D Model Well Information

Well Name	Connection Location (X, Y, Z1-Z2)	Wellbore Diameter (m)	Liquid Rate Target (Sm3/D)	BHP (Bar)
Injection "I3"	15, 39, 5-14	0.2	7000	1000
Production "P1"	18, 8, 5-14	0.2	3000	50
Production "P2"	40, 22, 5-14	0.2	3000	50

4.3.3 Rock Properties

As in the 2D models, the fluid phases present in the 3D models are water, oil, gas and dissolved gas. However, no free gas exists in the models since the models are above the bubble point pressure at all times. *Table 10* shows the porosity and permeability for each layer in the grid. The Top four and bottom four larger layer blocks were added to act as heat sinks, and is applied for temperature simulations only, that is, to enable heat exchange throughout the reservoir. The remaining ten middle layer grid blocks are for flow simulations. The Porosity and permeability for each layer are shown in *Table 10*. The rock compressibility is 4.84 x 10^{-5} bar^{-1} at a reference pressure of 277 bars.

Table 10: 3D Model porosity and permeability

Layer	Porosity	Permeability		
		X	Y	Z
1 - 4	0.05	0	0	0
5 - 8	0.20	300	300	30
9	0.25	5000	5000	500
10 - 14	0.20	300	300	30
15 - 18	0.05	0	0	0

4.3.4 Fluid Properties

The 3D model has the same fluid properties as the 2D model presented previously.

4.4 Temperature Options

The temperature option in ECLIPSE is used to model temperature effects in the reservoir, for instance when cold water is injected into a hot reservoir. The main effect of changes in temperature around the injection wells is to modify the fluid viscosities. Also, additional stresses are induced within the reservoir by changes in reservoir temperature which may result to the modification of the rock properties. The temperature option in ECLIPSE 100 works by solving an energy conservation equation at the end of each converged timestep which updates the grid block temperatures. The new calculated temperatures are then used for calculating the water and oil viscosities for the subsequent timestep (ECLIPSE, 2014).

It is important to note that the temperature option in ECLIPSE 100 is treated like a tracer. The rock specific heat is entered as a volume specific heat while the fluid specific heat is entered as mass specific heat (ECLIPSE, 2014). The input parameters for the temperature option are shown in *Table 11*.

Table 11: Temperature Model Data

Temperature Model Parameters		
Injected Water Temperature	30	^{o}C
Rock Thermal Conductivity	270	kJ/m day ^{o}C
Specific Heat Capacity of Rock	2.35E+03	kJ/Rm^{3} ^{o}C
Specific Heat Capacity of Gas	2.1	kJ/kg ^{o}C
Specific Heat Capacity of Oil	2.1	kJ/kg ^{o}C
Specific Heat Capacity of Water	3.9	kJ/kg ^{o}C

ECLIPSE does not take into account the heat losses to and from outside the reservoir model. In the case where the heat losses are likely to be significant, large blocks can be added to the reservoir model to act as heat sinks as shown in the 2D and 3D models. The cells of the added blocks should be made active by assigning non-zero porosities (pore volume > zero) and setting their permeability to zero. This allows for heat exchange between the reservoir and the added blocks but prevents flow simulations between them (ECLIPSE, 2014)

4.5 Polymer Options

The reason polymer option has a potential ability to be used to model water diversion with silicate is the numerical feature of the polymer option (not related to any observation). Mainly, the polymer option can model adsorption as a function of temperature and hence permeability

reduction in affected areas. Since this corresponds more or less to the way silicate is expected to behave; it is a potential model for simulating silicate.

4.5.1 Modeling Permeability Reduction

A very important factor that determines the success of a water diversion process with silicates is the relative permeability reduction to water, k_{rw} obtained after the gel has formed. The term associated to the permeability reduction is the residual resistance factor (RRF) as stated severally in the theory. To compute the rock permeability reduction in ECLIPSE, the RRF is specified under the PLYROCK keyword in the polymer option. The actual resistance factor is then calculated from:

$$R_k = 1.0 + (RRF - 1.0)\frac{C_p^a}{C_p^{a\,max}} \qquad (16)$$

Where C_p^a is the adsorbed concentration in a given block and $C_p^{a\,max}$ is the maximum adsorbed concentration depending on the rock type and specified under the PLYROCK keyword.

The dependence of RRF on temperature can also be specified under the PLYTRRF keyword as shown in appendix A1.

Skrettingland et al. (2012) presented an analytical and simulation plot of injectivity index for different RRF's for both crossflow and non-crossflow cases (see *Figure 27*)

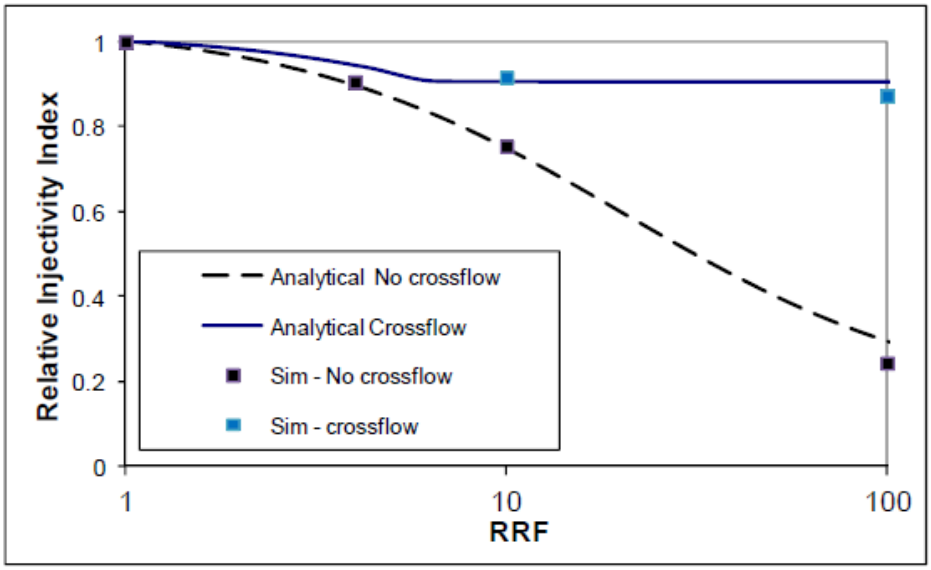

Figure 27: Injectivity index for crossflow and non-crossflow cases between layers (Skrettingland et al., 2012).

Table 12 shows the important data values used in the polymer option of the model.

Table 12: Silicate Model Data

Polymer(Silicate) Model Parameters		
Concentration	40	Kg/sm^3
Level of Mixing with Injection Fluid	2.35E+03	$kJ/Rm^3\,^oC$
Gel Activation Temperature	70	^oC
Maximum Adsorption Concentration	0.0000050	Kg/kg rock
RRF Multiplier at Gelation Temperature	10000	------

4.5.2 Polymer Injection Schedule

The silicate injection was done in slugs. Initial water flood was carried out in the reservoir for 10 years and 6 months from 1 January, 2000 to 1 July 2010 after which the polymer (silicate) slug was injected within the space of 2 months from 1 July, 2010 to 1 September, 2010. (See appendix A2).

4.6 Tracer Options/Injection Schedule

The maximum number of tracers in each of the stock tank phases is input in the RUNSPEC section. In this thesis, two passive tracers, TR1 and TR2 were used in the 2D models and both exist in the water phase. The tracers are non-partitioning. The tracers were injected in slugs for a period of one day. This is normally done in the schedule section of the Eclipse data file using the keyword WTRACER. Tracer TR1 was injected one month after the start of the water injection (from February 1, 2000 to February 2, 2000) while tracer TR2 was injected 11 months after the injection of the silicate slug (from June 1, 2011 to June 2, 2011).

4.7 Grid Refinement

The grid was refined laterally by a factor of three in the x-direction only as follows: 1x, 3x, 9x, 27x, 81x**.** The 1x represents the original coarse grid from which the other refinements were obtained. *Figure 28* illustrates how the refinement was done. *Figure 29* also shows how the well location was obtained for each of the other refinements. All other properties of the grid remained the same for all the grid refinements.

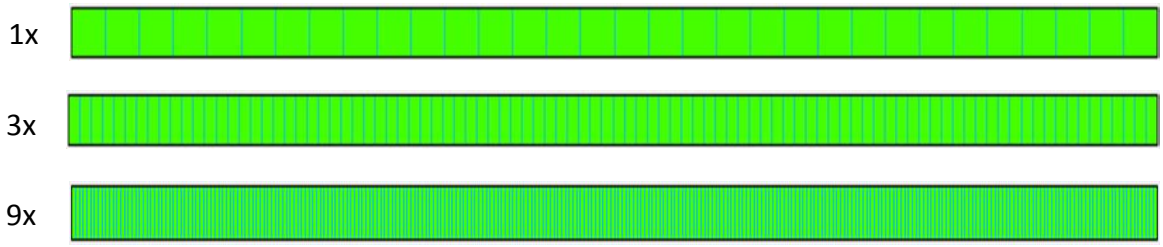

Figure 28: An illustration of the lateral refinement applied to the grid in x-direction only

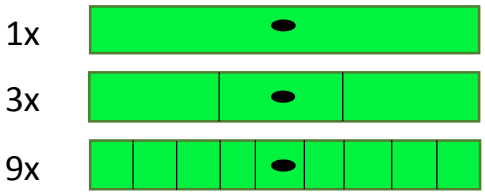

Figure 29: An enlarged block view showing the block location of the wells in x-direction for each grid size refinement

4.8 Keyword Functionality Description

4.8.1 The PLYATEMP keyword

The PLYATEMP keyword is used to associate the polymer adsorption to temperature, that is, to set adsorption dependence on temperature. Multiple adsorption tables are used to give the adsorption data at various temperatures in increasing order of magnitude. The adsorption data for intermediate temperatures are then computed by interpolation between the tables. Adsorption data for temperatures outside the range of temperatures given in the tables is defined using the adsorption values for the maximum and minimum temperature as appropriate. That is, temperatures below the minimum temperature value in the table will have same adsorption values as that of the minimum temperature in the table while temperatures above the maximum temperature value in the table will have same adsorption values as the maximum temperature. Each temperature value under the PLYATEMP keyword has its own adsorption table specified by the PLYADS keyword. The number of tables under the PLYADS keyword depends on the number of saturation number (SATNUM) regions used (ECLIPSE, 2014). In this model, four (4) SATNUM regions were used. The absence of the PLYATEMP keyword in the polymer option of the model does not imply that there will be no adsorption. Since level of adsorption has been recognized to depend on temperature, it is therefore realistic to have a keyword such as this to model that effect. Moreover, since silicate systems does not adsorb as much as polymer systems, this keyword gives the flexibility to make the required adjustment.

The values used under the PLYATEMP keyword for the functionality test can be found in the appendix.

4.8.2 The PLYTRRF keyword

PLYTRRF keyword is used to set the dependence of the residual resistance factor (RRF) on temperature. It is used when the temperature option in Eclipse is specified. The RRF shows the extent to which the water permeability in the reservoir has been reduced by the polymer (silicate). This keyword provides flexibility in the ability to set the gel activation at any desired temperature. High values can be used to obtain partial or complete blocking of a zone in the reservoir when modeling for water diversion purposes such as this.

Values used under the PLYTRRF keyword can be found in Appendix A1.

5.0 RESULT/DISCUSSION

5.1 Grid Refinement Results

The following simulation cases shown in *Table 13* were used to model the effect of grid refinement on the temperature profile, tracer propagation and polymer (silicate) propagation.

It should be recalled that two tracer slugs, TR1 and TR2 were injected. TR1 was injected before the injection of the silicate slug, precisely one month after production commenced while TR2 was injected in about 11 months after the injection of the silicate slug.

Table 13: 2D Simulation cases for grid refinement effects

Case No.	*Model options used*
C0 (Base Case)	Temperature, Polymer (Silicate) and Tracer options
C1	Tracer options only
C2	Temperature options only
C3	Polymer (silicate) options only

5.1.1 Impact on Tracer Propagation

From the tracer results shown below, the following observations can be deduced:

- Generally, grid refinement has more effect on TR1 than TR2 as observed in the respective plots.
- The tracer concentration is much lower for C0 than for C1. This is in agreement with report in (Skrettingland et al., 2014).
- Since TR1 was injected at the same time and conditions for both cases C0 and C1, it is expected that they have similar result, however, this is not the case as shown in Figure 30 and Figure 32. TR1 in case C0 seems to be more smeared than TR1 in case C1 as observed by their different peak concentrations and spread of the leading and trailing edges. This can be attributed to the temperature effect on the viscosities of the reservoir fluids in C0 since C1 has no temperature option.
- In cases C0 and C1, the smearing of tracer TR1 injected before the silicate injection was less compared to tracer TR2. This effect is most likely attributed to the amount of the tracer soluble phase (water in this case) present in the reservoir (especially in the high flow channels) at the times they were both injected. The more water phase in the reservoir when the tracer is injected, the more the smearing effect. This is consistent

with the statement in ECLIPSE (2014) that *" the smearing of tracer interfaces tends to be most apparent in single phase regions"*.

- The peak of the tracer concentration or production rate which gives an idea of the relative arrival times of the tracers at a certain block or producer is higher in TR1 than in TR2 for both cases, C0 and C1. This is because the velocity of travel of the tracer which is proportional to the amount of the tracer soluble phase (water) in which it can only travel is higher in TR1 than in TR2.
- The presence of the polymer (silicate) phase and its plugging in C0 also affected the TR2 production concentrations and speed.
- For the tracer result, the 27x refinement seems to be more representative.

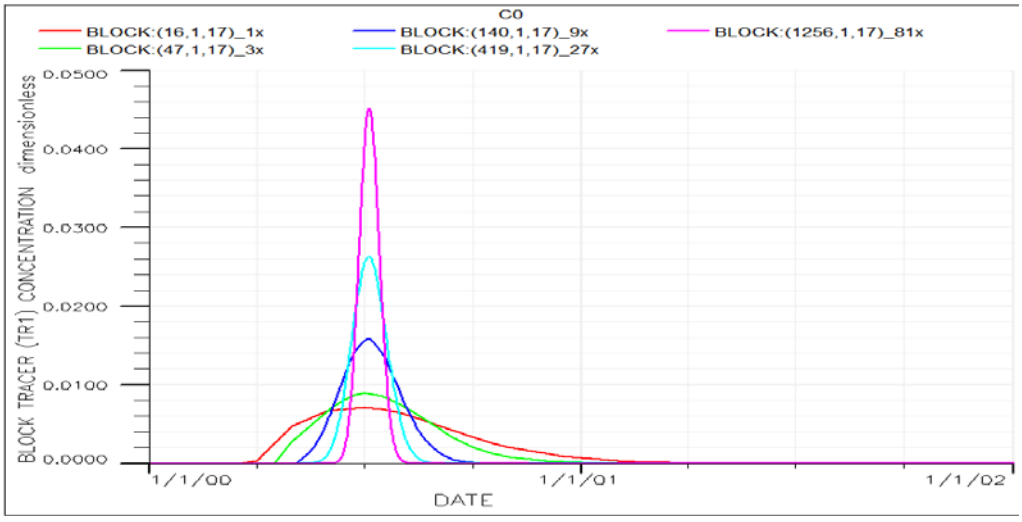

Figure 30: Tracer TR1 concentration in a center block in the thief zone for different refinements in case C0 (Magnified)

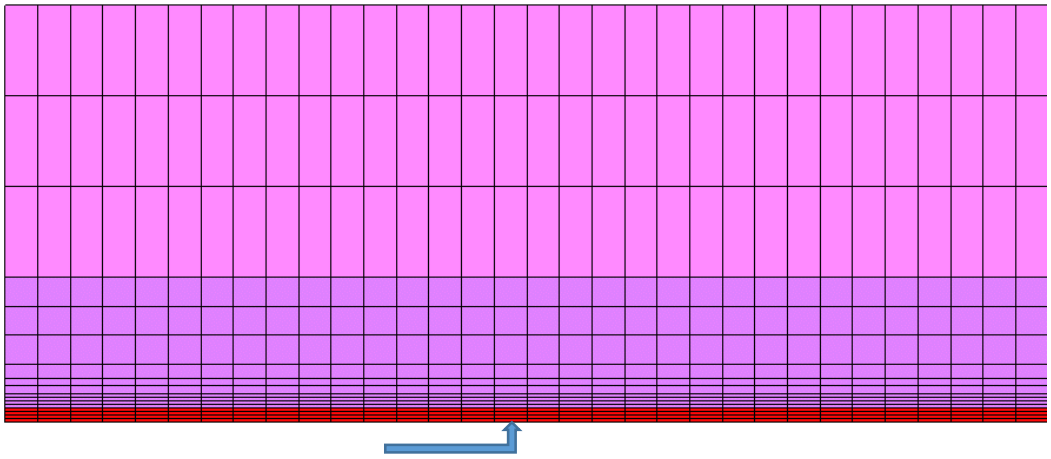

Figure 31: schematic of center block location (arrow) in the last layer.

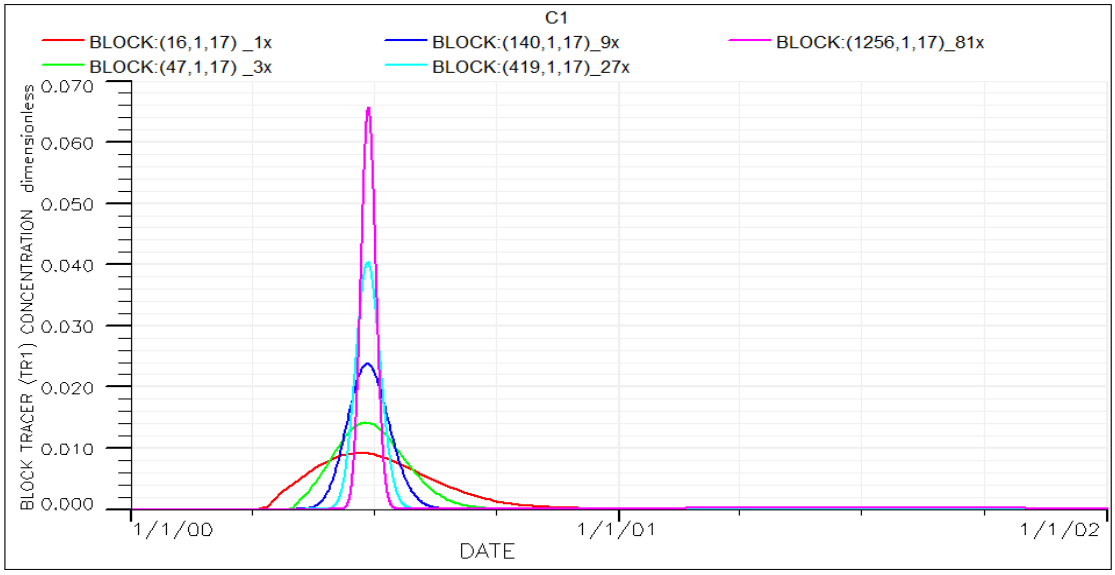

Figure 32: Tracer TR1 concentration in a center block in the thief zone for different refinements in case C1 (Magnified)

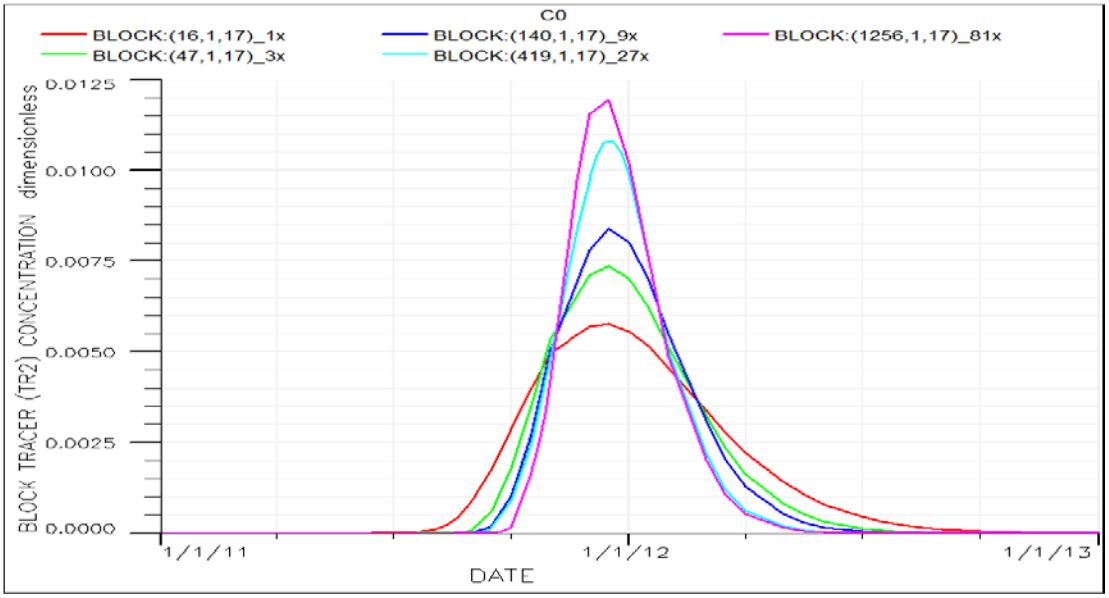

Figure 33: Tracer TR2 concentration in a center block in the thief zone for different refinements in case C0 (Magnified)

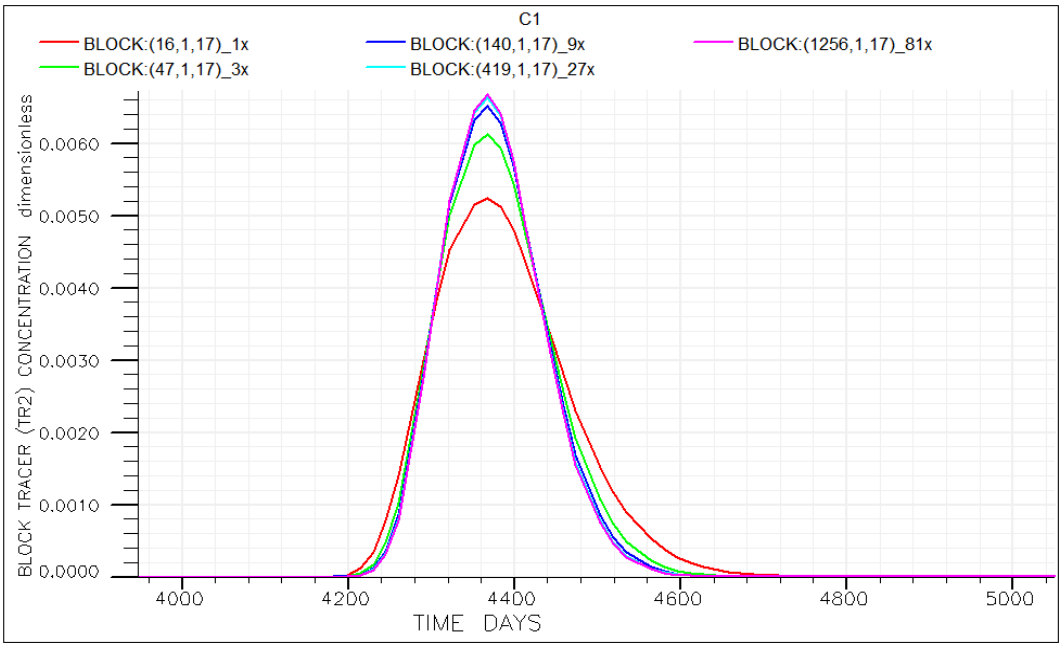

Figure 34: Tracer TR2 concentration in a center block in the thief zone for different refinements in case C1

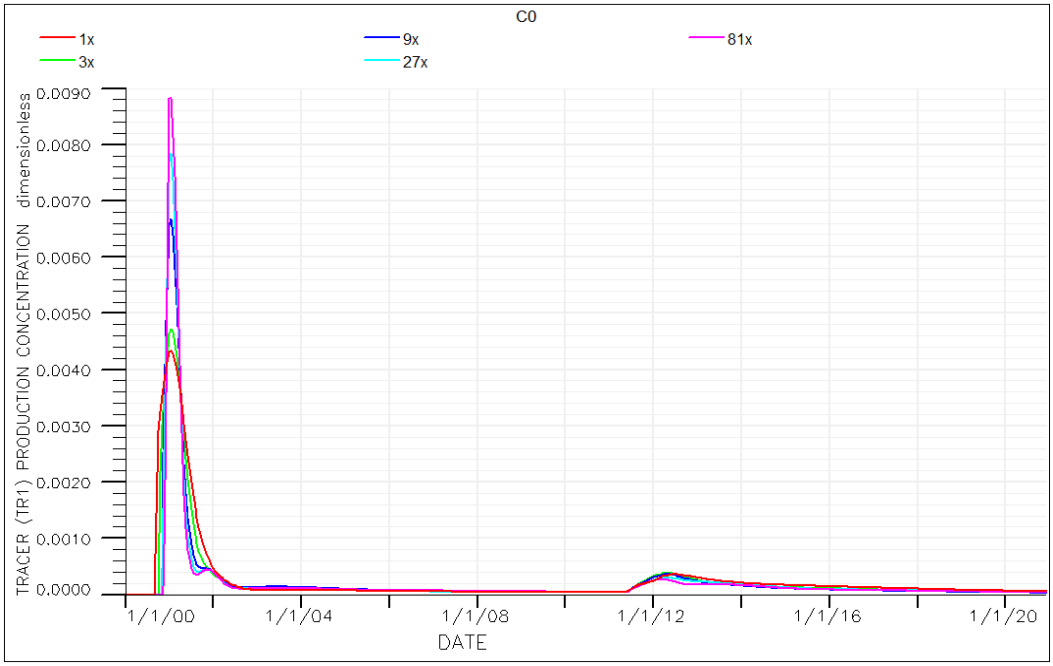

Figure 35: Tracer (TR1) production concentration for different refinements in case C0

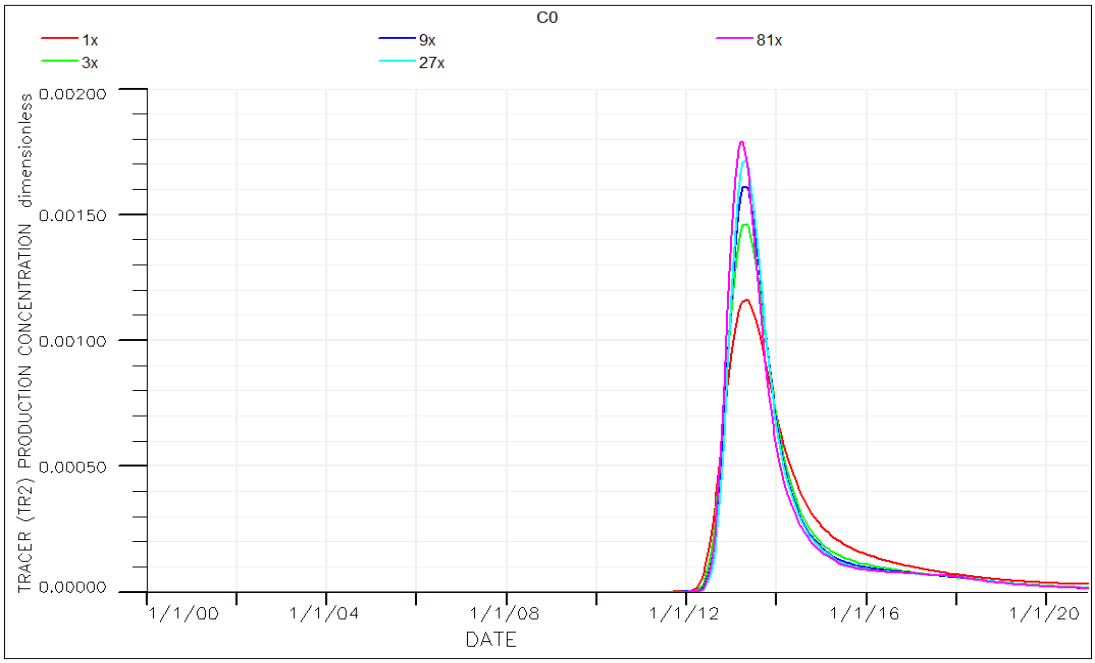

Figure 36: Tracer (TR2) production concentration for different refinements in case C0

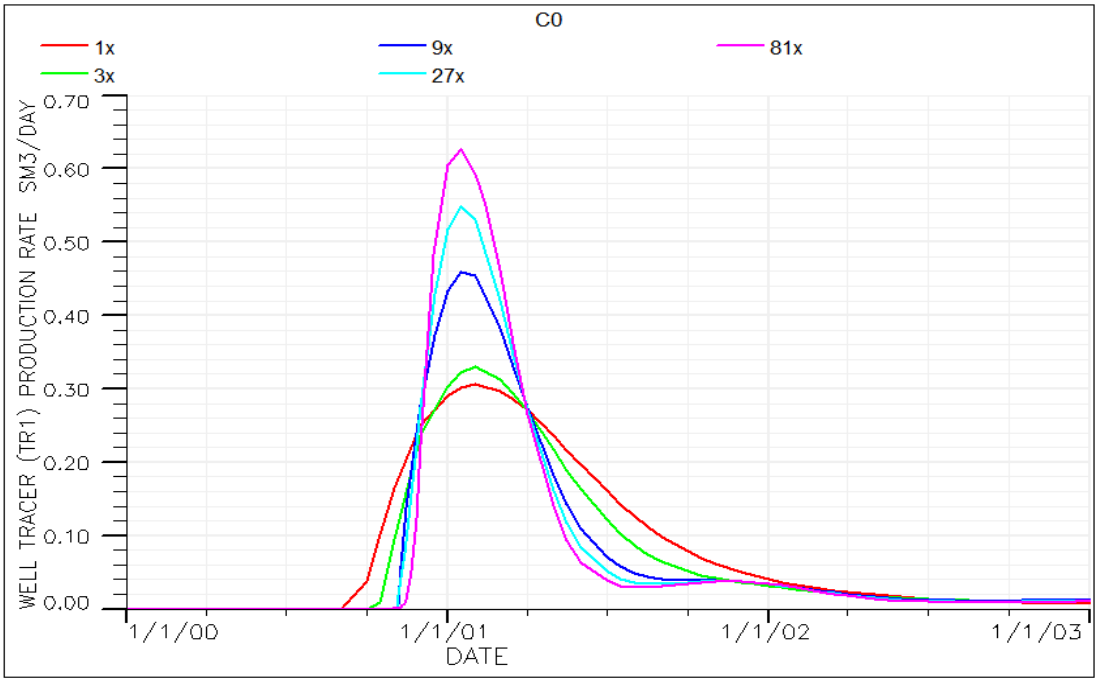

Figure 37: Well tracer TR1 production rate for different refinements in case C0 (Magnified)

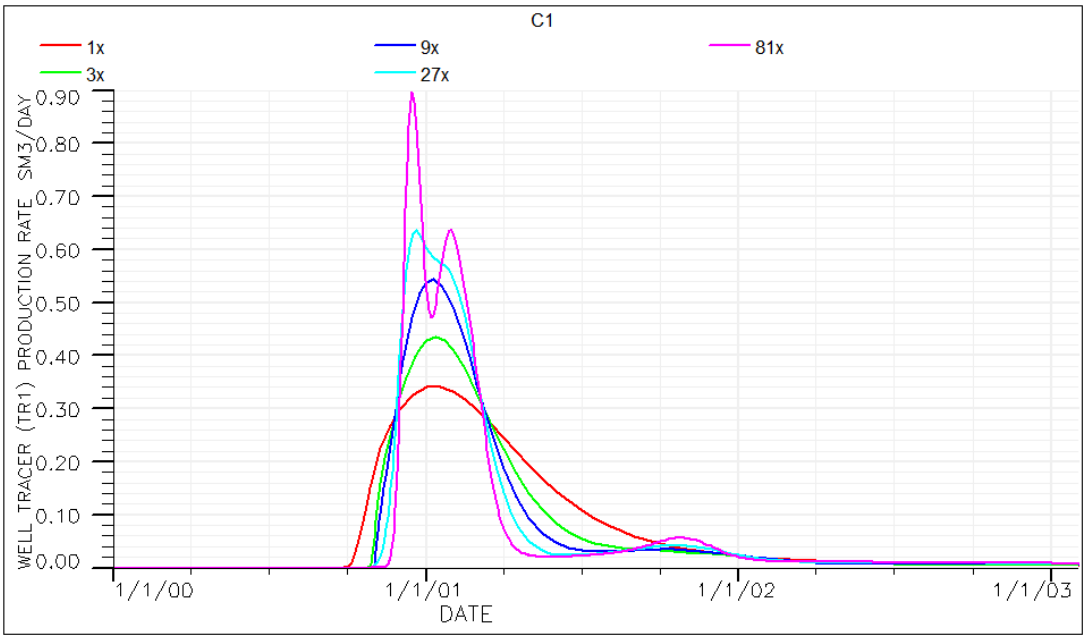

Figure 38: Well tracer TR1 production rate for different refinements in case C1 (Magnified).

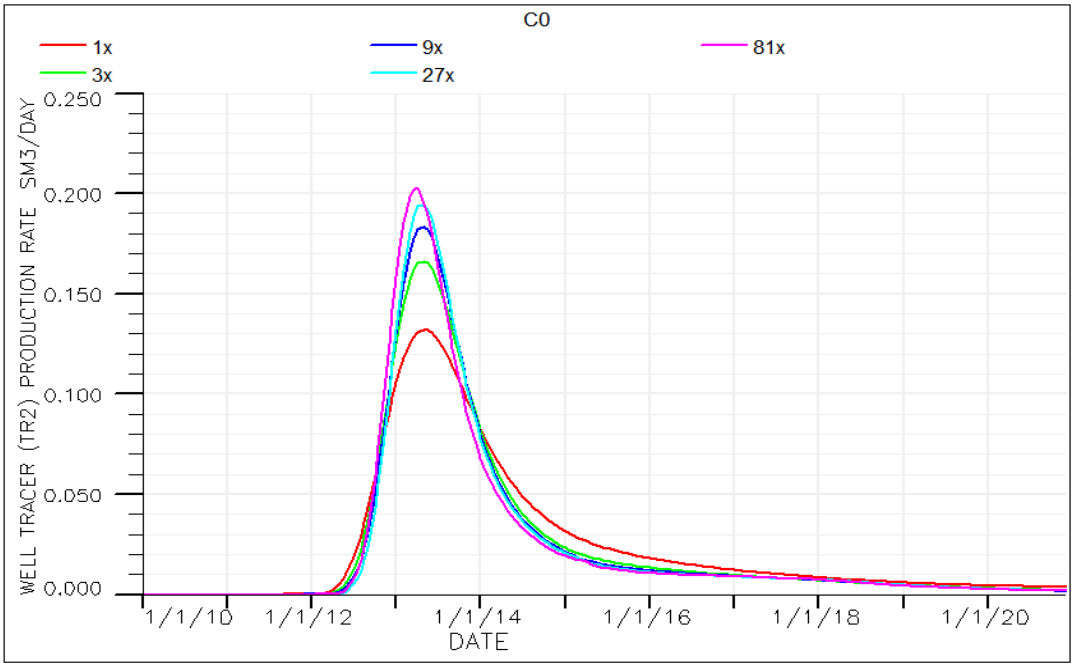

Figure 39: Well tracer TR2 production rate for different refinements in case C0 (Magnified)

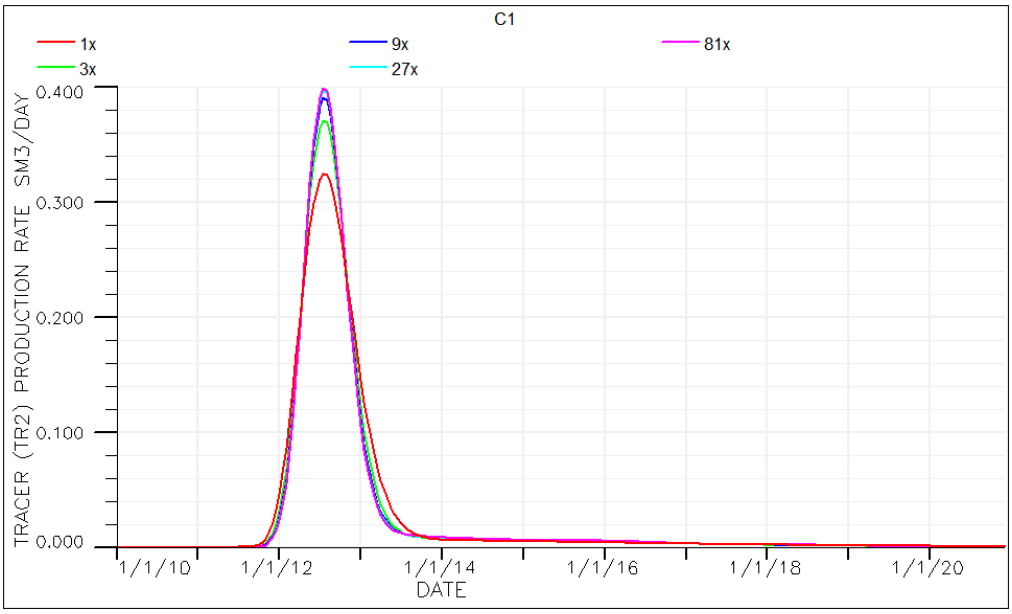

Figure 40: Well tracer TR2 production rate for different refinements in case C1 (Magnified).

5.1.2 Impact on Temperature profile

The impact of grid size on the temperature propagation can be observed in *Figure 41* which is a plot of the temperature history in the center block of the last layer in the thief zone for different refinements in case C0. A plot of the temperature history in the center block of the last layer in the thief zone (*Figure 43*) for different refinements in case C2 showed similar trend. The 9x grid refinement gives minimal numerical dispersion results.

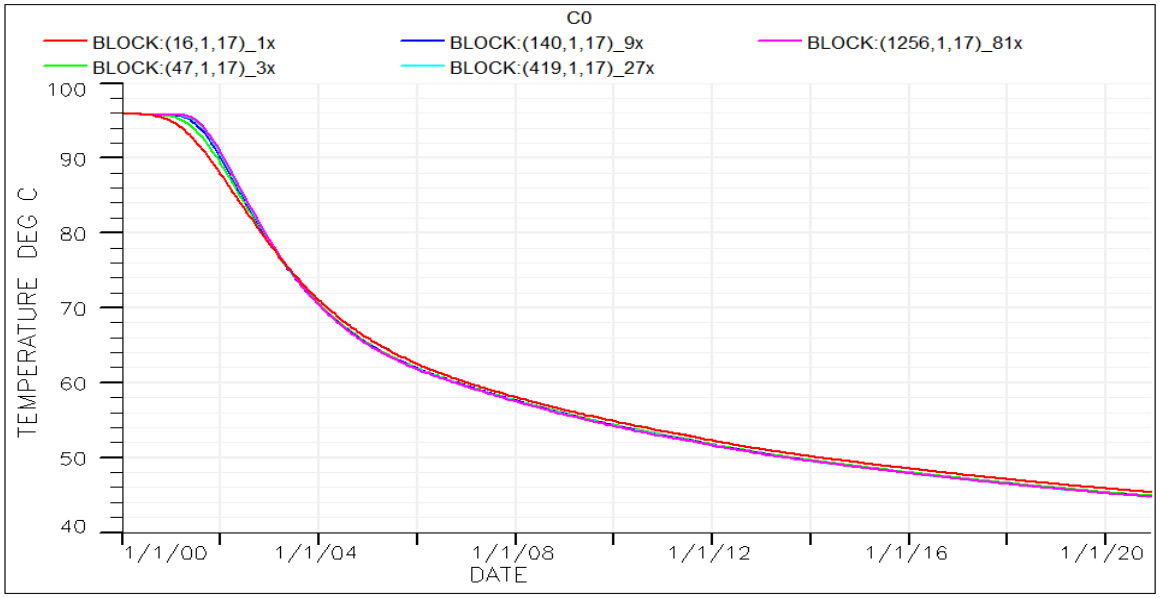

Figure 41: Temperature history for a center block in the thief zone for different refinements in case C0

A close observation of the magnified view (*Figure 42*) of *Figure 41* shows that the time of propagation of the temperature in the block for early times between the 9x grid refinement and

the coarse grid was as high as 5 months and decreased gradually. However, the effect close to or at the activation temperature of the gel is of more significance. This is because, if the time of propagation of the temperature between the coarse grid and a more representative grid refinement (e.g. the 9x grid refinement) is significant, this will impact the interpretation of the time of formation and location of the gel. *Figure 42* shows approximately one and a half months between them as shown by the arrow. The same temperature profile was observed for the grid block where the gelling occurred. As seen in *Figure 42*, the fine grid model will produce a gel earlier than the coarse grid. This implies that the coarse grid will overestimate the gelation time and location.

From the *Figure 42*, it can also be interpreted that the coarse and fine grids will likely show a gel formation at the same time if a temperature of about 75^{o}C is used as the activation temperature. This is because their temperature curves cross at that temperature.

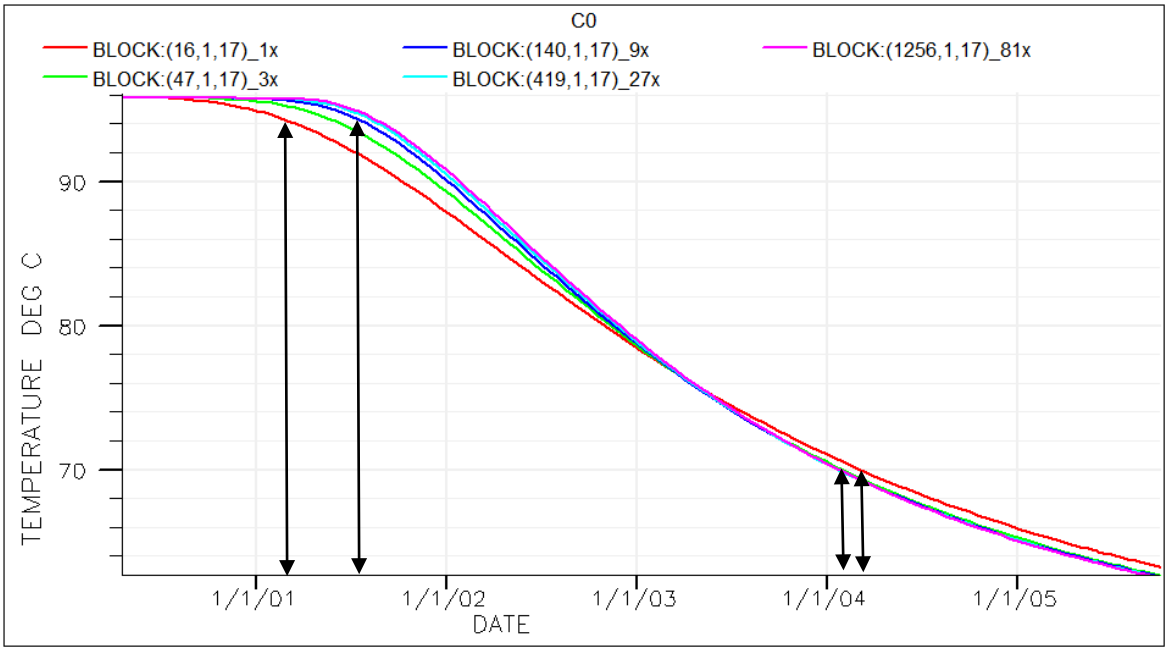

Figure 42: Magnification of figure 36.

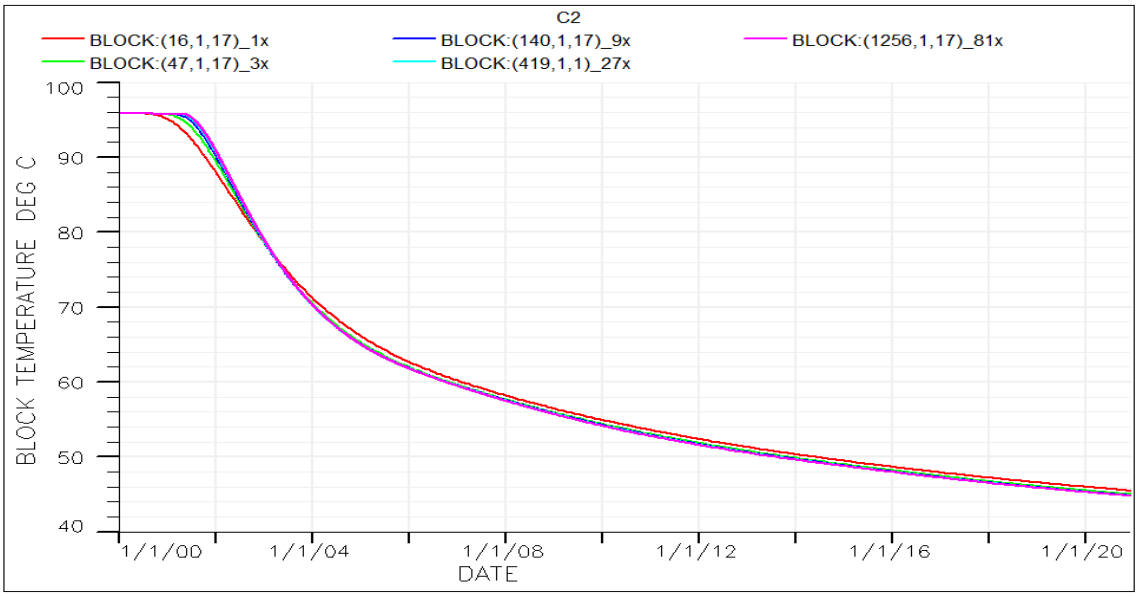

Figure 43: Temperature history for a center block in the thief zone for different refinements in case C2.

5.1.3 Impact on Silicate Propagation

A comparison of cases C0 and C3 as presented in *Figure 44* and *Figure 45* show that refinement indeed has an impact on the simulation results for the water diversion process. Comparing the cumulative silicate production plot for the coarse grid (1x) with that of the fine grid in *Figure 44* shows that much dispersion is obtained using the coarse grid. The 9x grid refinement results can be accepted to give minimal dispersion effect as there is no significant difference in its silicate propagation results compared to the 27x and 81x grid refinement results. Approximately 40,000kg difference in cumulative silicate production between the coarse grid and the fine grids which is about 12% of the total silicate injected (approx. 324,000 kg). This is quite substantial.

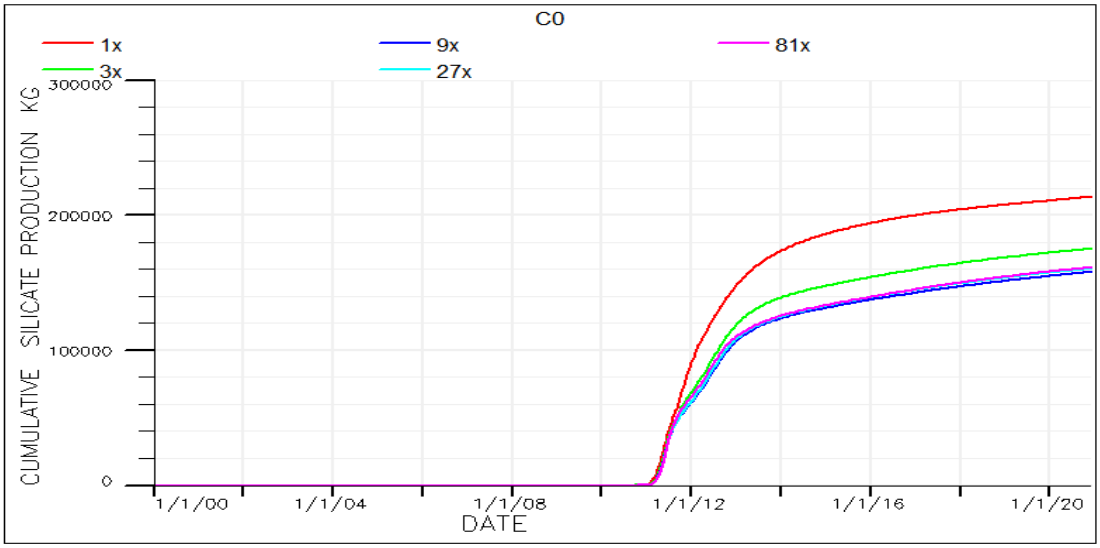

Figure 44: Cumulative silicate production for different refinements in case C0

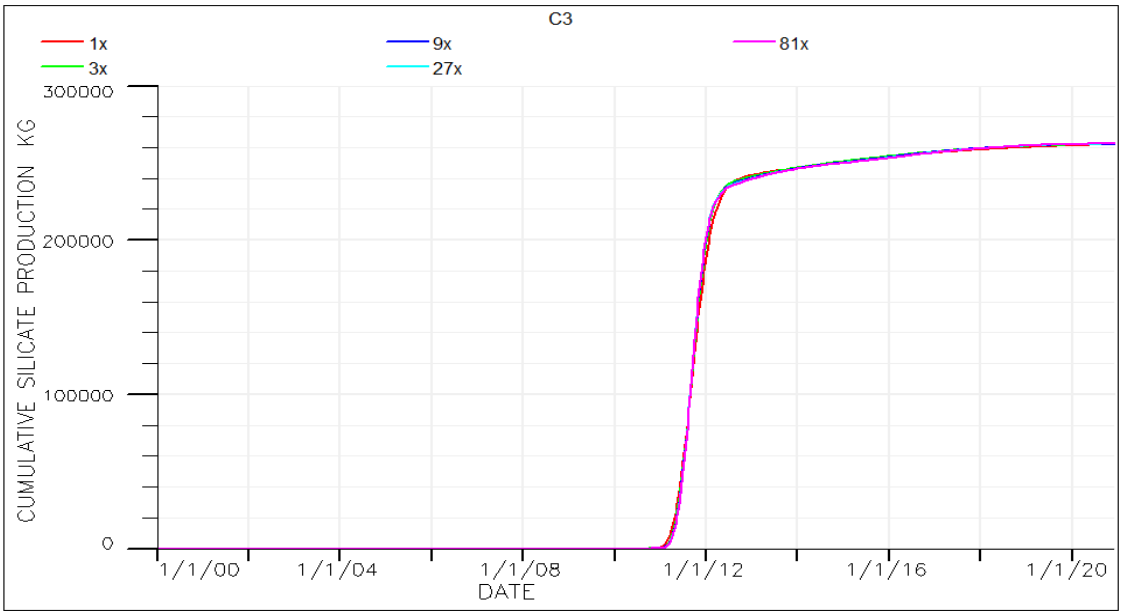

Figure 45: Cumulative silicate production for different refinements in case C3

The silicate production rate plots, the silicate concentration plots and injection rate plot presented in the following figures all show that the 9x grid refinement model will give acceptable results in terms of impact of numerical dispersion on the spreading of the silicate and hence the location when it gels.

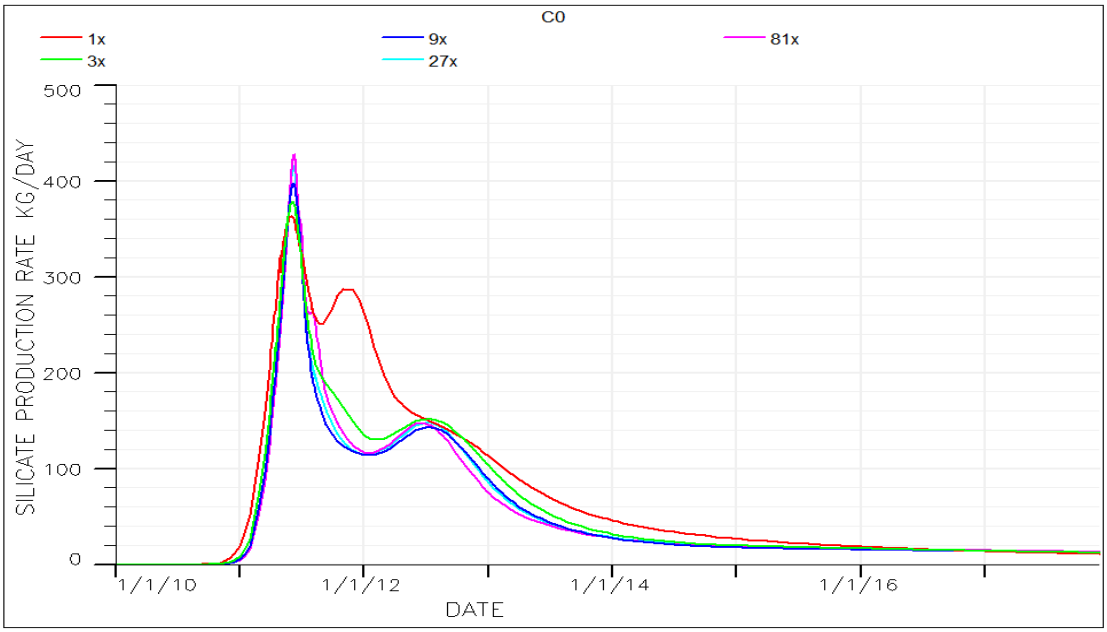

Figure 46: Silicate production rate for different refinements in case C0

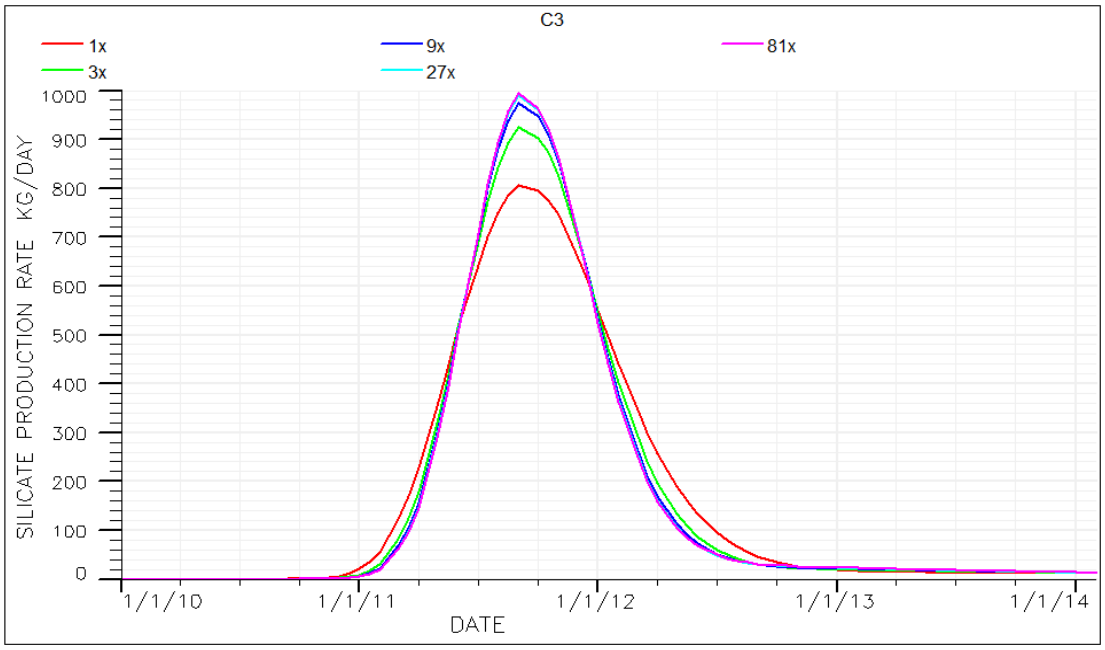

Figure 47: Silicate production rate for different refinements in case C3

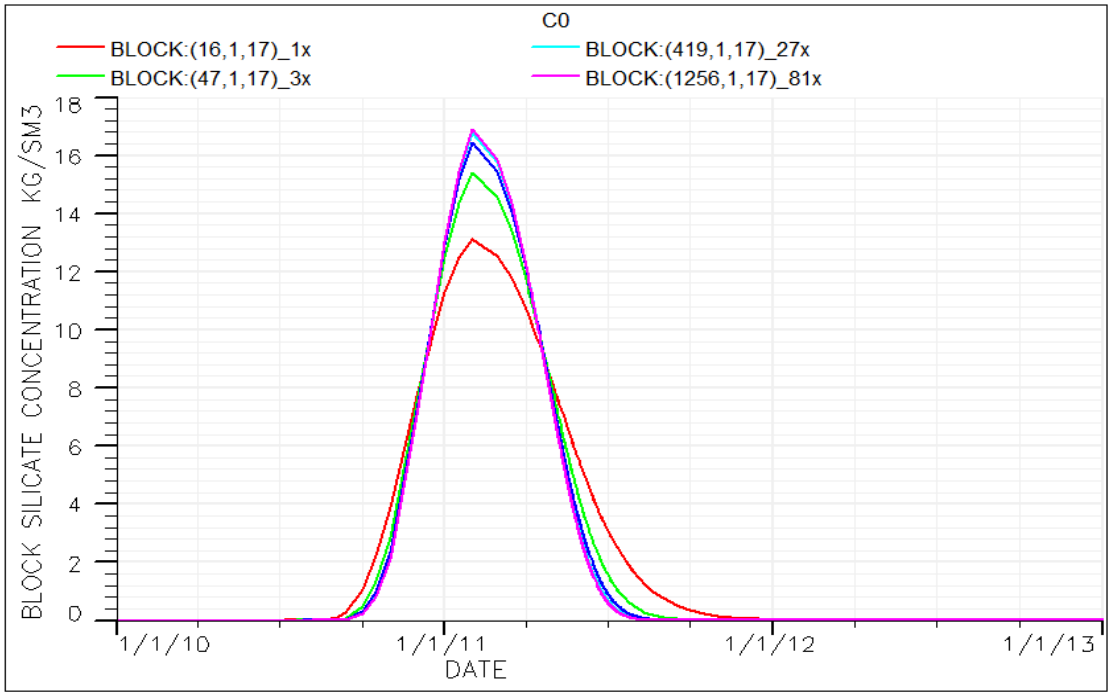

Figure 48: Silicate concentration in a mid-block in the thief zone for different refinements in case C0

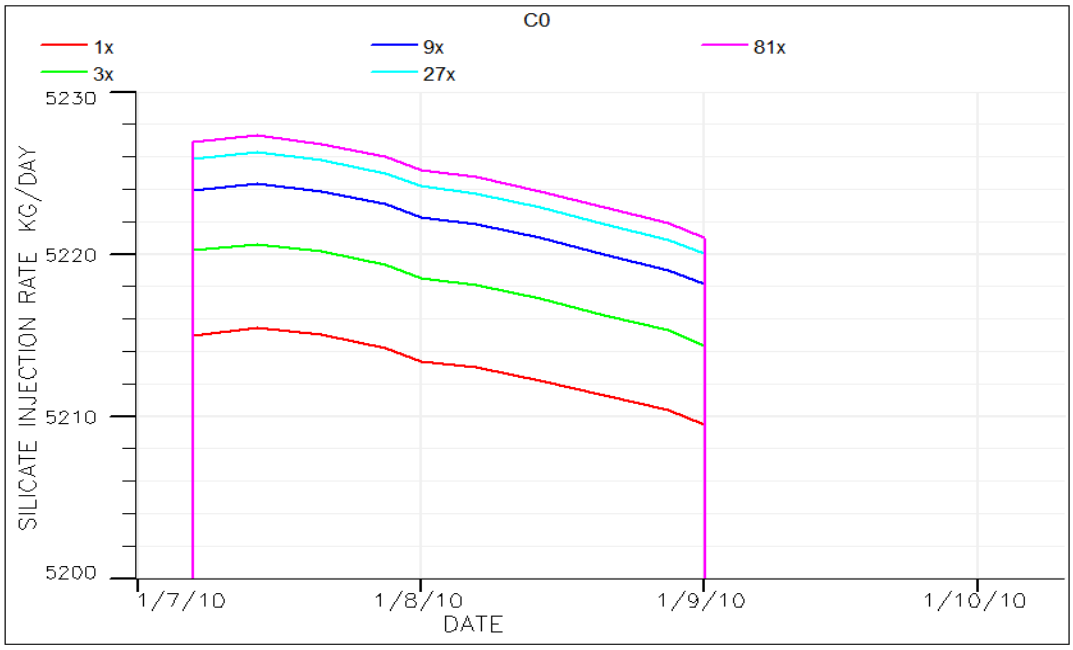

Figure 49: Silicate injection rate for the different grid refinements

5.1.4 Impact on EOR

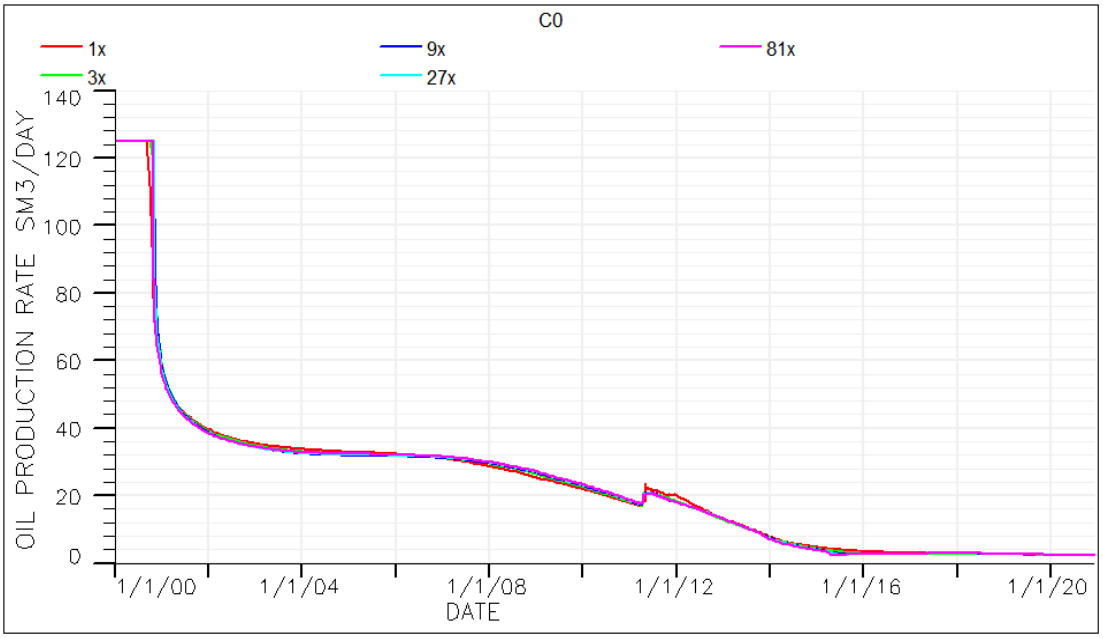

Figure 50: Oil production rate history for the different refinements in C0.

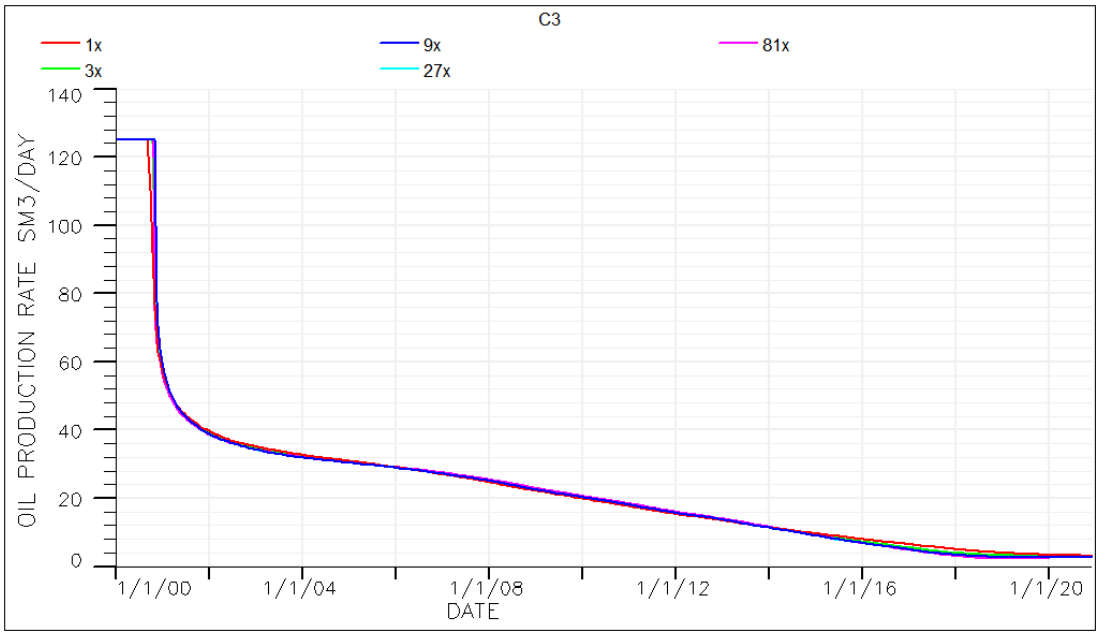

Figure 51: Oil production rate history for the different refinements in C3.

Generally, as observed in the plots and discussed, grid refinements may or may not have significant impact on temperature distribution and EOR. Significant impact of grid refinement on the tracer and silicate results are observed. For the silicate results, the 9x fine grid was observed to reduce the numerical dispersion appreciably.

5.2 2D Model Sensitivity Results

5.2.1 Injection Rate

It should be recalled it was stated previously that the sensitivity on injection rate was done with the 2D model. *Table 14* shows the different case of injection rate used. The 27x refined grid was first used for the sensitivity.

Table 14: Cases for Injection Rate Sensitivity

Case No.	*Rate (Sm^3/Day)*
R0 (Base Case)	12000
R1	1200
R2	6000
R3	60000
R4	120000

Based on the range of injection rates used as outlined in the cases above, there is no observable difference in the results obtained with the different injection rates using the 27x refined 2D

model. The same result was obtained for the silicate propagation, tracer propagation, temperature profile and oil recovery in all cases (see *Figure 52 - Figure 56*).

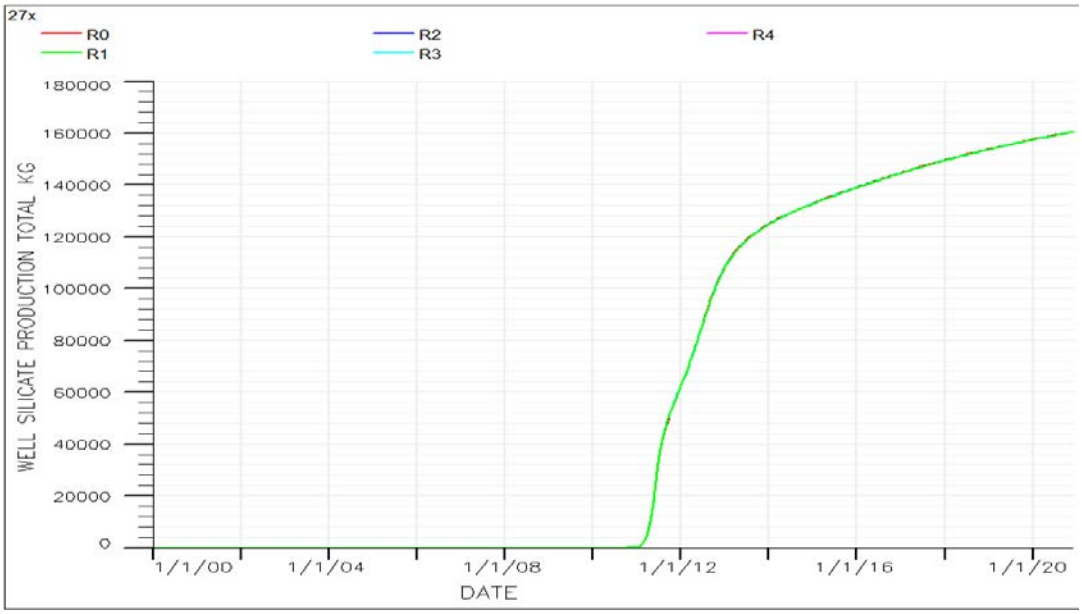

Figure 52: Combined plot of Cumulative silicate production for the different cases of injection rate (using the 27x grid refined 2D model).

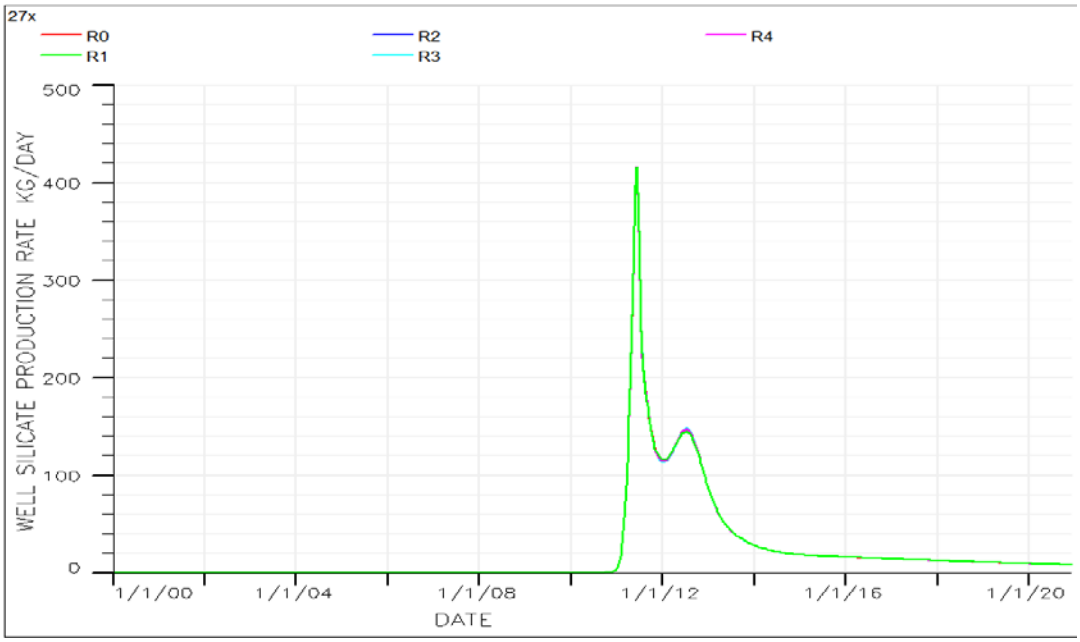

Figure 53: Combined plot of the silicate production rate for the different cases of injection rate (using the 27x refined 2D model).

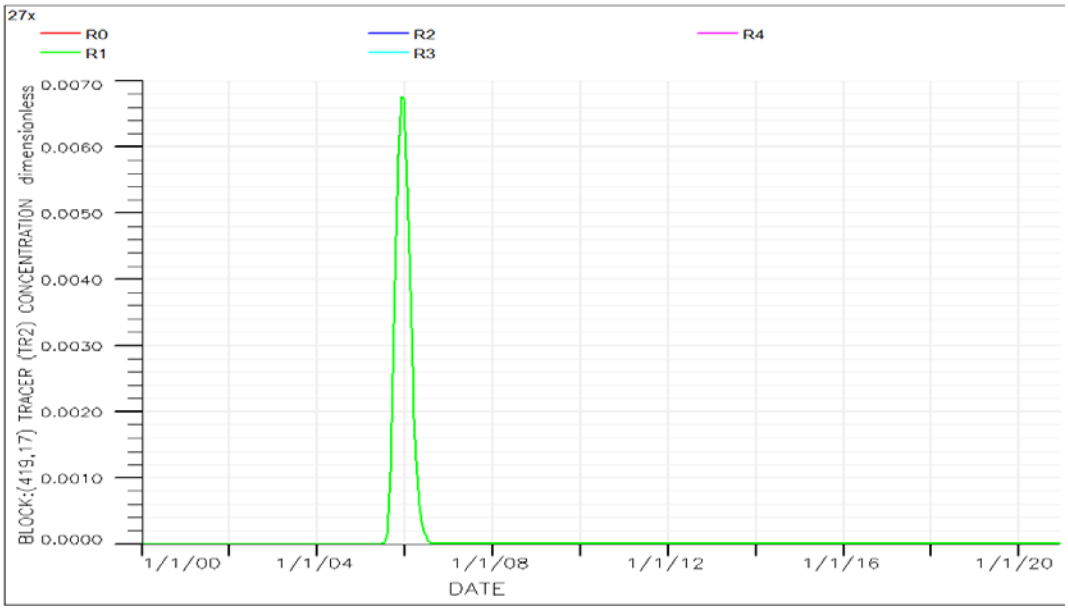

Figure 54: Combined plot of the tracer TR2 concentration in a block located in the thief zone for the different cases of injection rate (using the 27x grid refined 2D model).

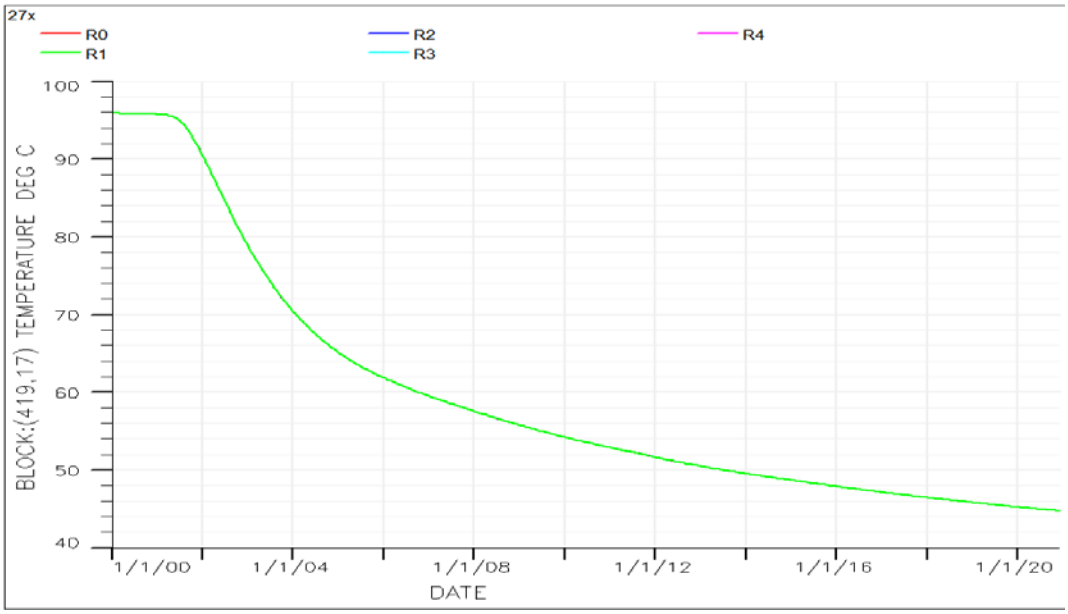

Figure 55: Combined plot of the temperature in a block located in the thief zone for the different cases of injection rate (using the 27x grid refined 2D model.

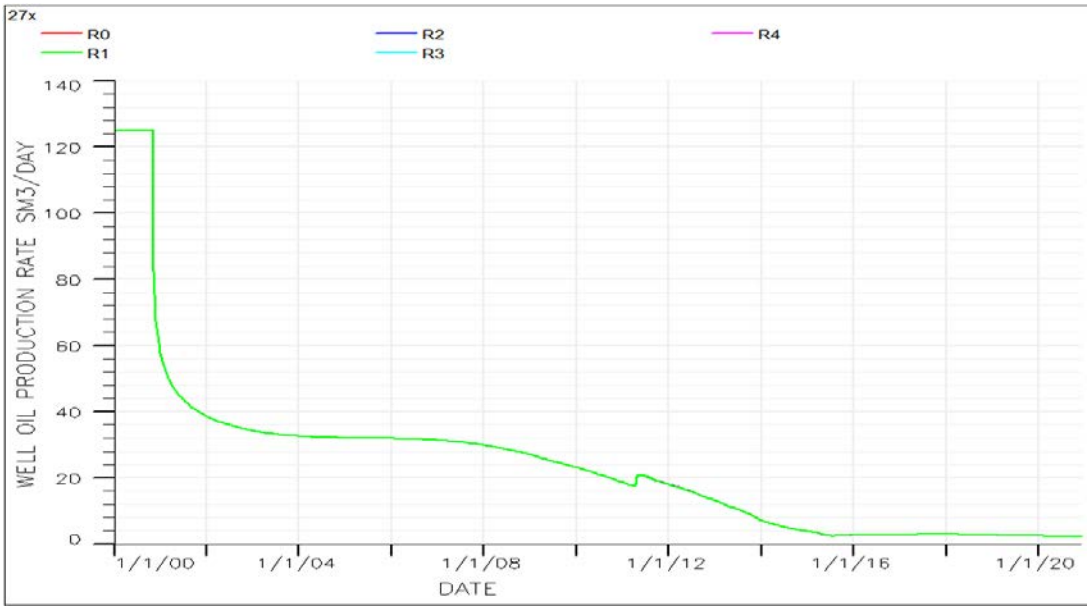

Figure 56: Combined plot of the oil production rate for the different cases of injection rate (using the 27x grid refined 2D model).

In order to confirm the results obtained using the 27x grid refined 2D model, the same sensitivity using the same cases of injection rate was run using the 2D coarse grid model. Surprisingly, similar results were obtained. There was no observable difference in the results with respect to the different cases of injection rates used as shown in *Figure 57 - Figure 61*.

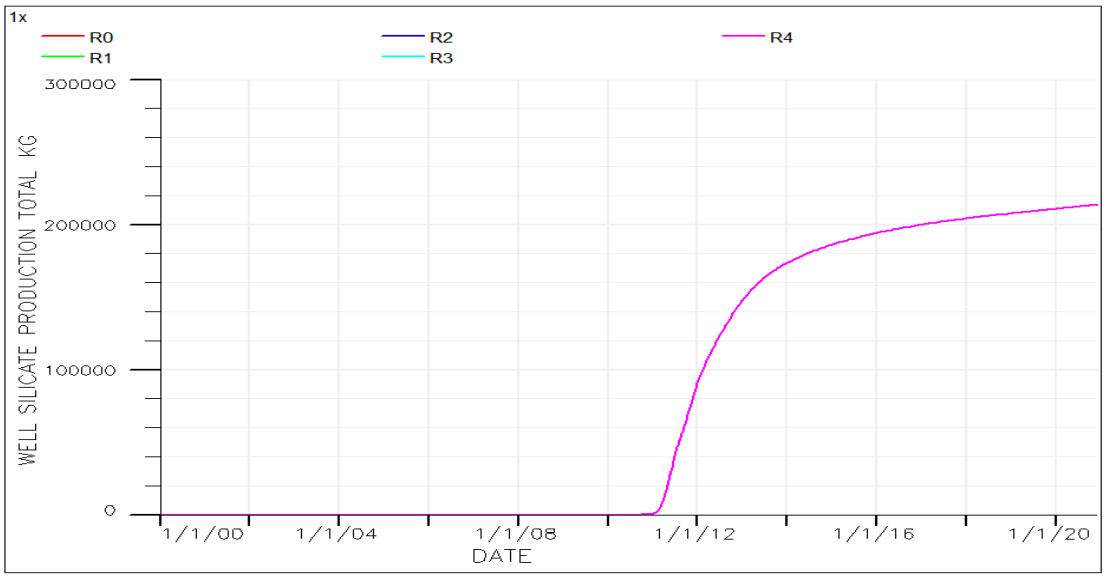

Figure 57: Combined plot of Cumulative silicate production for the different cases of injection rate (using the 2D coarse grid model).

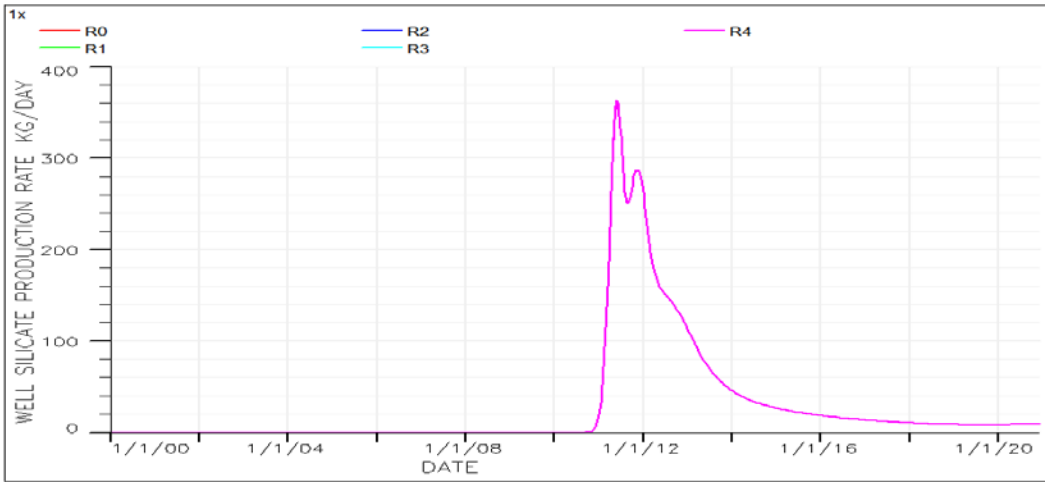

Figure 58: Combined plot of the silicate production rate for the different cases of injection rate (using the 2D coarse grid model).

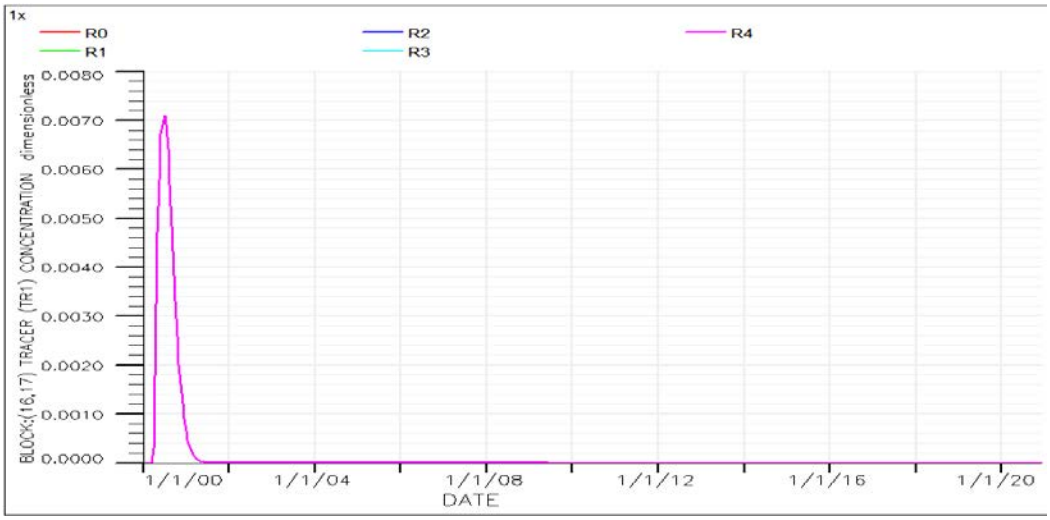

Figure 59: Combined plot of the tracer TR1 concentration in a block located in the thief zone for the different cases of injection rate (using the 2D coarse grid model).

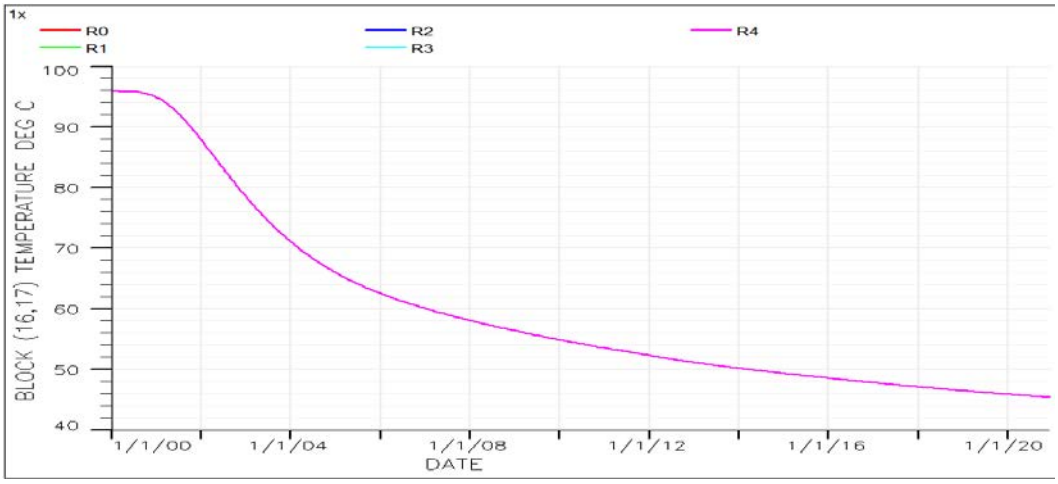

Figure 60: Combined plot of the temperature in a block located in the thief zone for the different cases of injection rate (using the 2D coarse grid model).

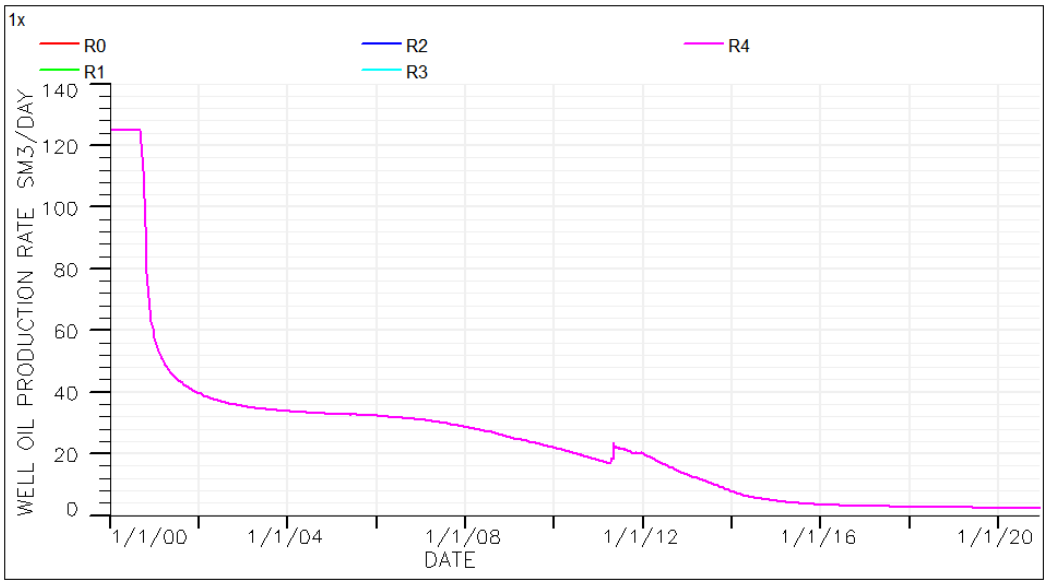

Figure 61: Combined plot of the oil production rate for the different cases of injection rate (using the 2D coarse grid model).

Therefore, given the range of injection rates used, it can be concluded that injection rate has no effect on the simulation results. This however, does not agree with literature as presented previously in section 3.3. It could be that the system here is not in a sensitive range with respect to velocity variations.

5.2.2 Location of the Thief Zone

To conduct a sensitivity analysis on the effect of the location of the thief zone, the thief zone was changed. This was done by a simple change in permeability of the layers or zones concerned. Two cases were considered (*Table 15*): The base case where the thief zone is located in the bottom of the reseroir and a case where the thief zone is located in the top zone of the reservoir, that is in the 4th layer in the grid (recall that the first three layers in the grid were added for temperature modeling and hence is not part of the reservoir). *Table 16* gives the new reservoir properties (porosity and permeability) for the case Z2. The choice of using just one layer for case Z2 was guided by observing the thickness of the layers. The thicness of the four bottom layers used as the thief zone in the base case is approximate to that of the 4th layer used in case Z2. Also since the thief zone for case Z1 is located in the bottom of the reservoir where water will be diverted only in the layers above it, the 4th layer was also chosen so that the injected water will only be diverted into the layers below it. This is to aid for comparison.

The 27x refined 2D grid model was used for the sensitivity.

Table 15: cases used for the sensitivity on thief zone location

Case No.	*Thief zone Location*
Z1 (Base Case)	14-17
Z2	4

Table 16: Properties of the reservoir for case Z2

Layer	Porosity (fraction)	Permeability (mD)		
		X	Y	Z
1 - 3	0.05	0	0	0
4	0.25	5000	5000	5000
5-17	0.20	300	300	300

The following show the results obtained for the sensitivity runs:

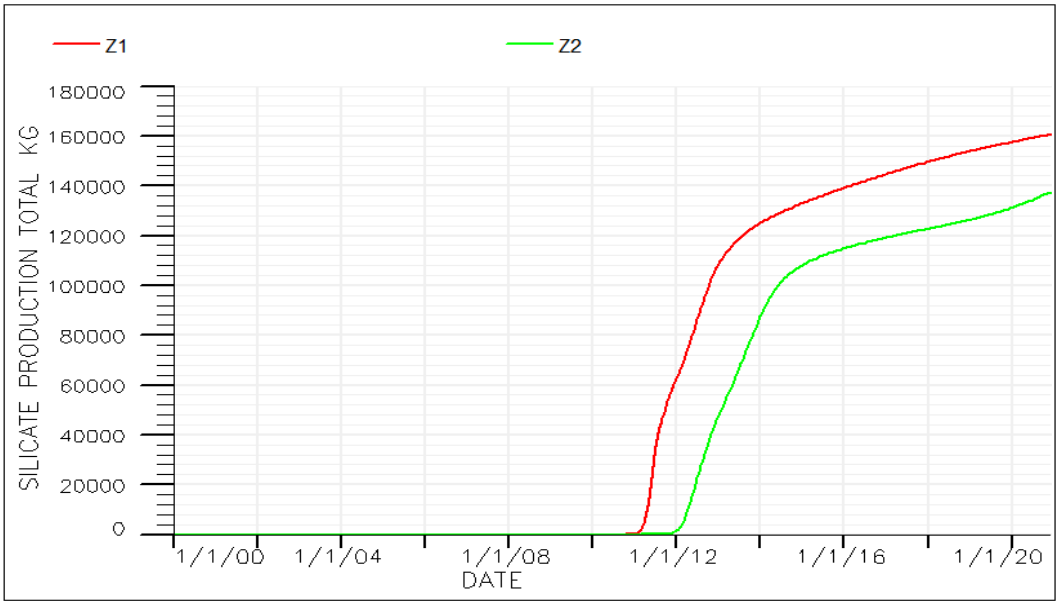

Figure 62: Combined plot of the cumulative silicate produced for the two cases of thief zone location

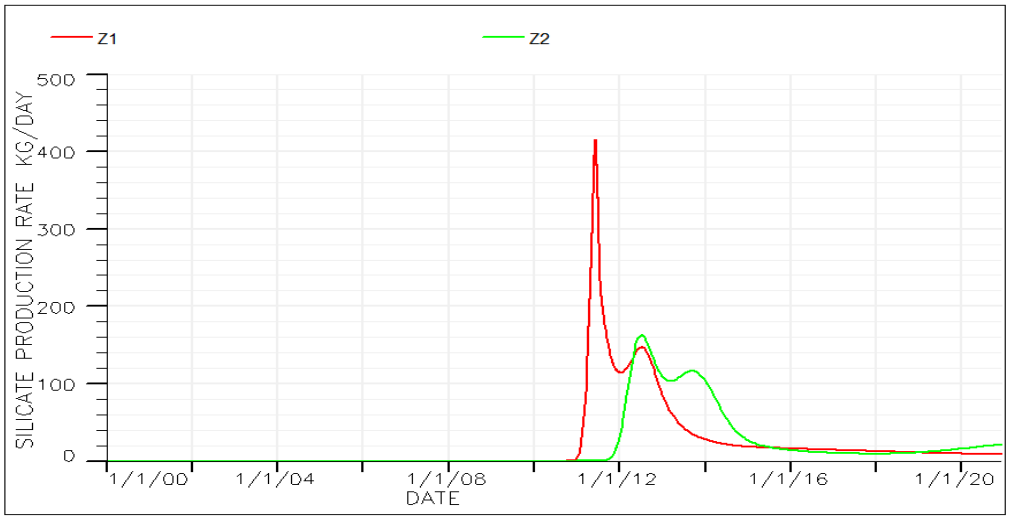

Figure 63: Combined plot of the silicate production rate for the two cases of thief zone location.

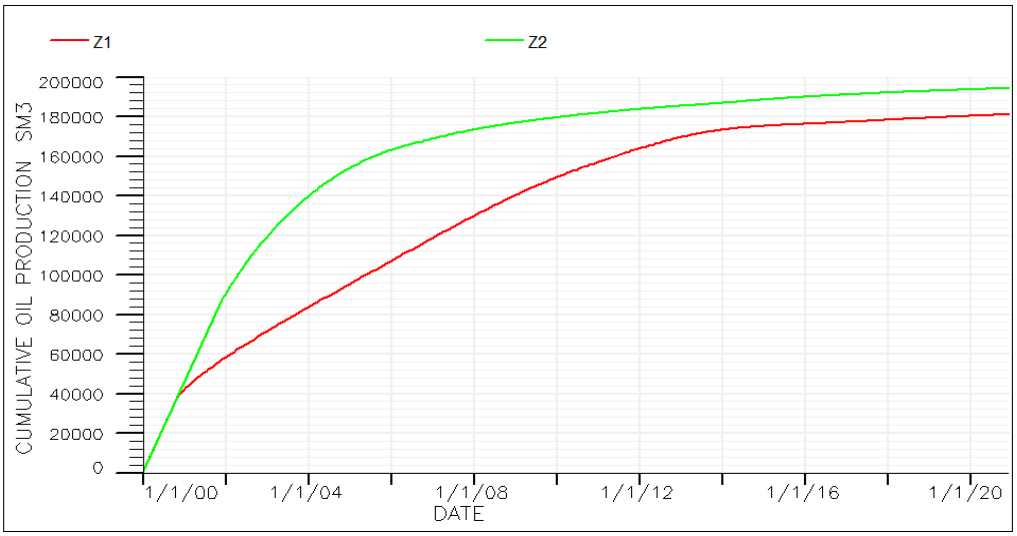

Figure 64: Combined plot of the cumulative oil produced for the two cases of thief zone location.

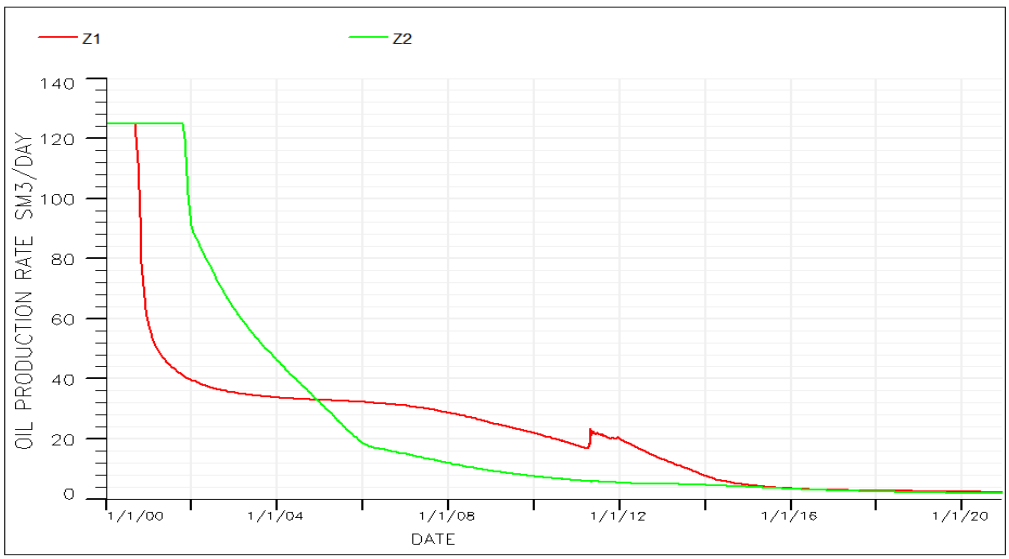

Figure 65: Combined plot of the oil production rate for the two cases of thief zone location.

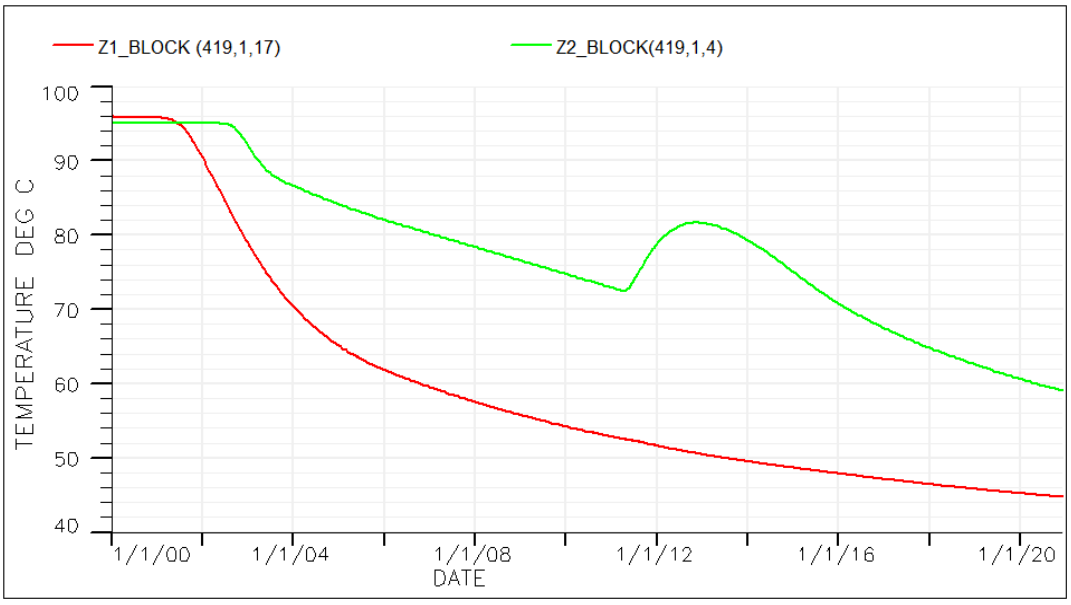

Figure 66: Temperature in a block close to the producer for the two thief zones.

The effect of location can be observed from the results. The silicate production totals and rates for the two cases displayed in *Figure 62* and *Figure 63* respectively show that more silicate is produced when the thief zone is located lower in the reservoir than when it is located higher in the reservoir.

The visualization of the gelling in the two cases presented in *Figure 67* show that the gelling was earlier when the thief zone is above than when it is beneath in the reservoir. One of the causes could be because of the faster heat exchange in case 2 due to heat exchange from above and beneath the thief zone. This is not the case for the thief zone located in the bottom layer of the reservoir in case Z1 since the heat exchange only comes from above the thief zone.

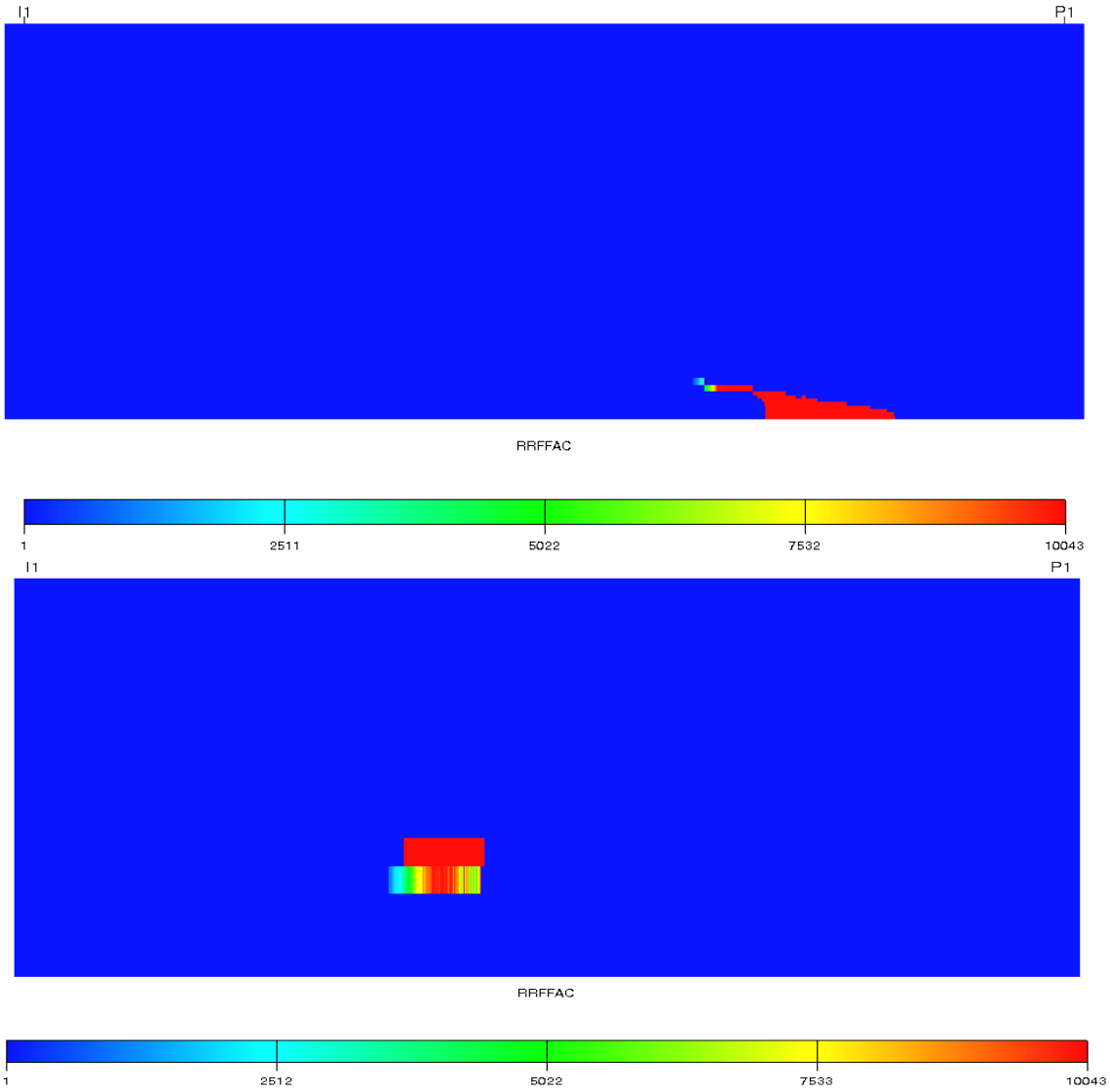

Figure 67: Visualization of gel location for the two cases of thief zone location.

5.3 3D Model Sensitivity Results

As previously stated, the 3D model was used to conduct sensitivities on specific design parameters which include, the gel location (by varying activation temperature), injection slug size, injection time and permeability contrast between the thief zone and the reservoir.

5.3.1 Activation Temperature

To run sensitivity on the gel location, the activation temperature for the permeability reduction was varied as shown in *Table 17*. The recovery obtained at each of these temperatures was compared with the no silicate injection case (the base case) to obtain the incremental oil for each case. Location, L1 to L4 as seen in the *Table 17* represent different locations of the gel plug due to the activation temperature from the injector to the producer.

Table 17: Cases used for the sensitivity on activation temperature

Case No.	*Gel Activation Temp. (^oC)*
L0 (Base Case)	No Silicate Injected
L1	60
L2	70
L3	80
L4	90
L5	100

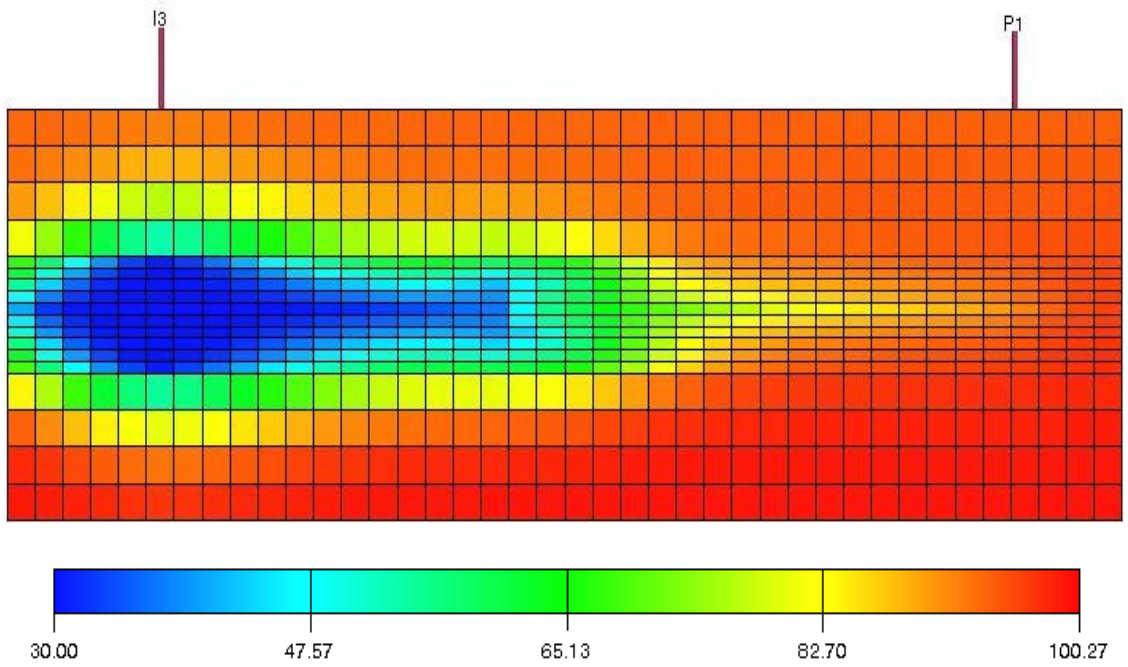

Figure 68: Cross section of the Temperature propagation in the reservoir due to cold fluid injection

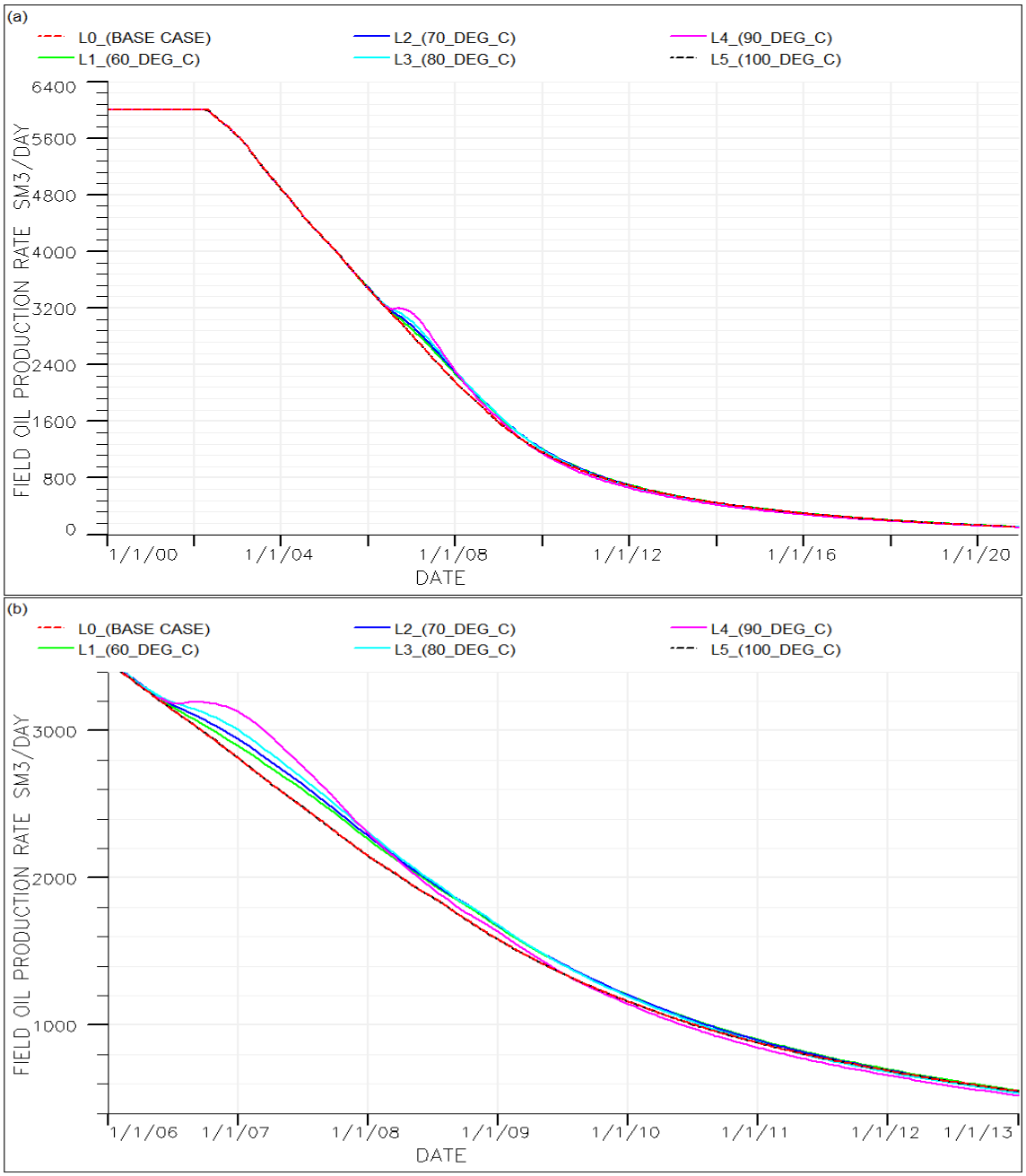

Figure 69: (a) Comparing field oil production rate at different activation temperature, (b) Magnified view of diversion effect in (a)

Figure 69 shows the field oil production rate for the different activation temperatures and/or gel location. Similar plots were observed for the two different wells. From the figure, it seems that the diversion effect increases with the activation temperature (or gel location from the injector) initially. Case L4 which had an activation temperature of 90^{o}C and located closer to the producer had the highest oil production rate initially but after a while its rate decreased below the production rate of the other cases. *Table 18* which gives the summary of the total oil produced for the different cases shows that there is a threshold temperature or location above which there

is a decrease in the oil recovery. A plot of incremental oil versus the gel activation temperature in *Figure 70* shows that the threshold temperature at which there is a maximum EOR effect is about 75°C. Above this temperature, the EOR effect decreases. *Figure 71* shows a visualization of the gelling and location due to the different activation temperatures. It can be seen that as the activation temperature increases, the gel location moves closer to the producer. At the same time because of the effect of dispersion with time, the RRF values gradually begins to decrease at a certain temperature meaning partial plugging as can be observed in the color change.

Table 18: Comparing the field EOR effect of the different activation temperatures

Case No.	*Gel Activation Temp.(°C)*	*Total Silicate Injected (kg)*	*Total Oil Produced (Sm^3)*	*Incremental Oil (sm^3)*
L0	No Silicate	0	16 327 208	0
L1	60	17 360 000	16 464 810	137 603
L2	70	17 360 000	16 473 182	145 975
L3	80	17 360 000	16 468 133	140 925
L4	90	17 360 000	16 410 814	83 607
L5	100	17 360 000	16 322 458	-4 750

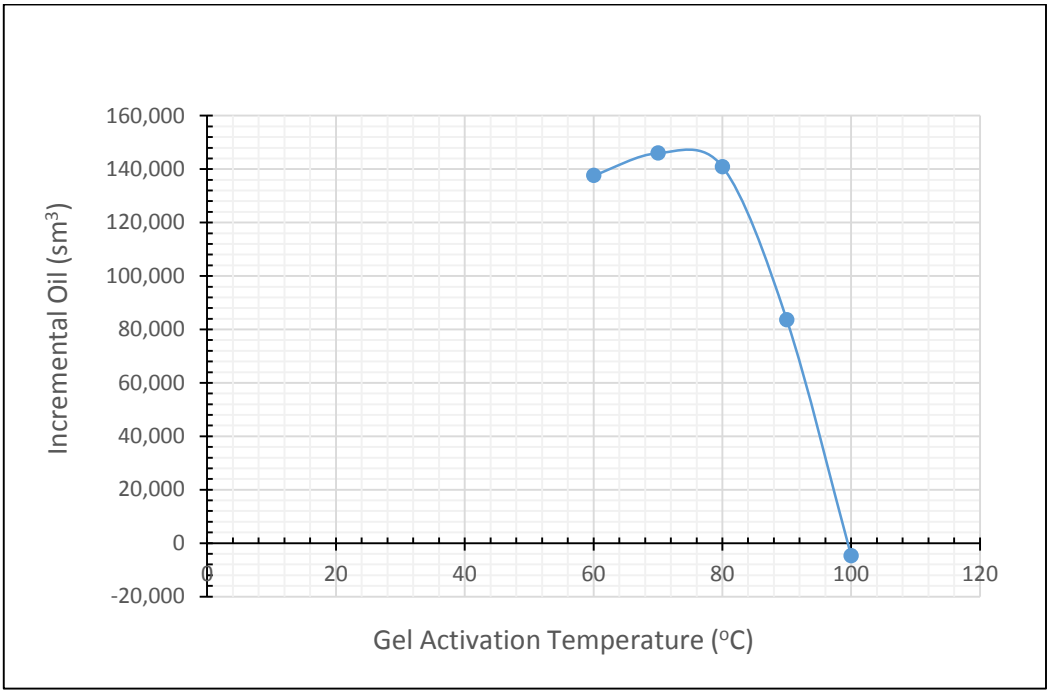

Figure 70: Incremental oil versus gel activation temperature

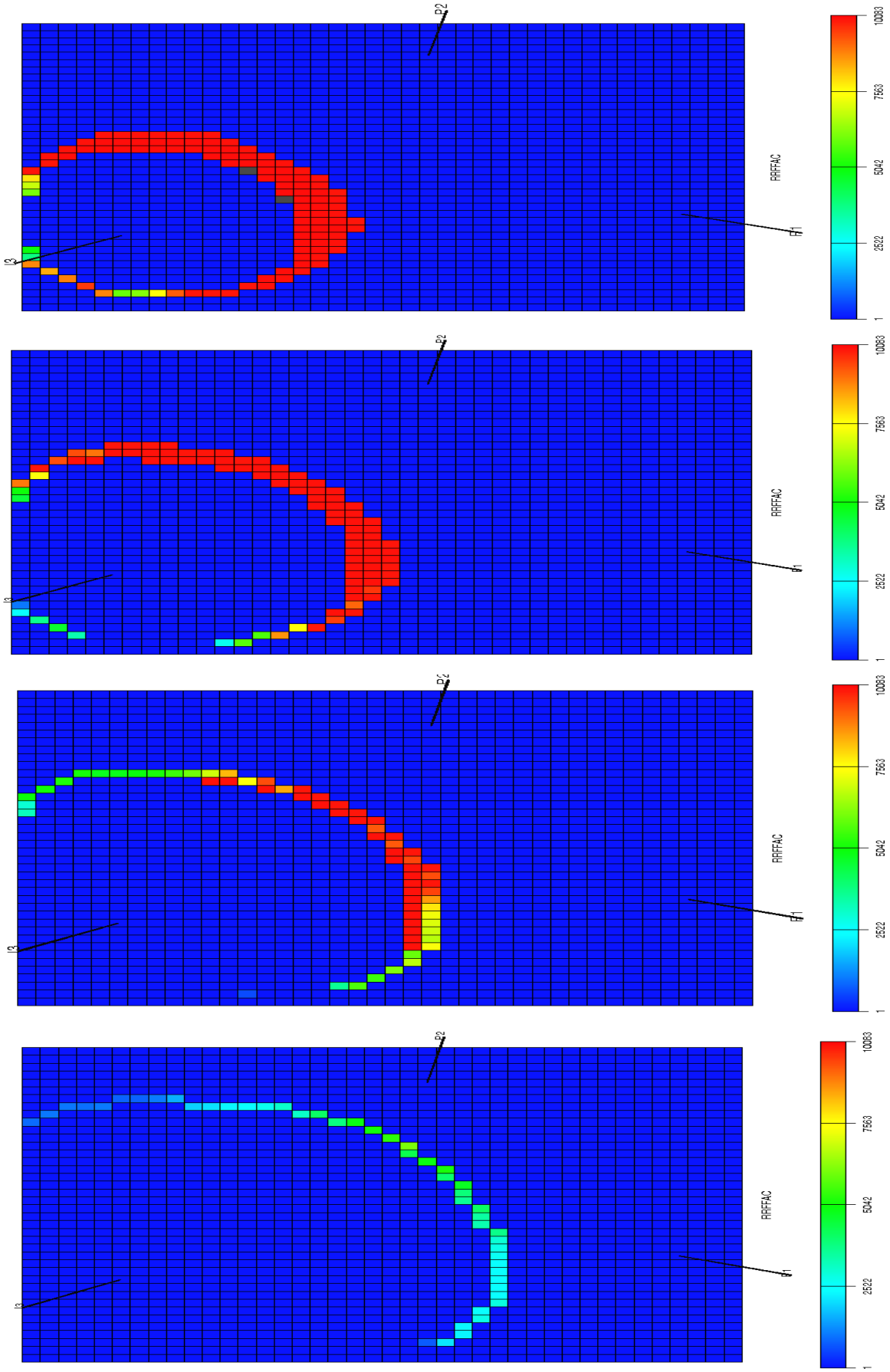

Figure 71: Visualization of gelling for the cases L1 (uppermost) to L4 (Lowermost)

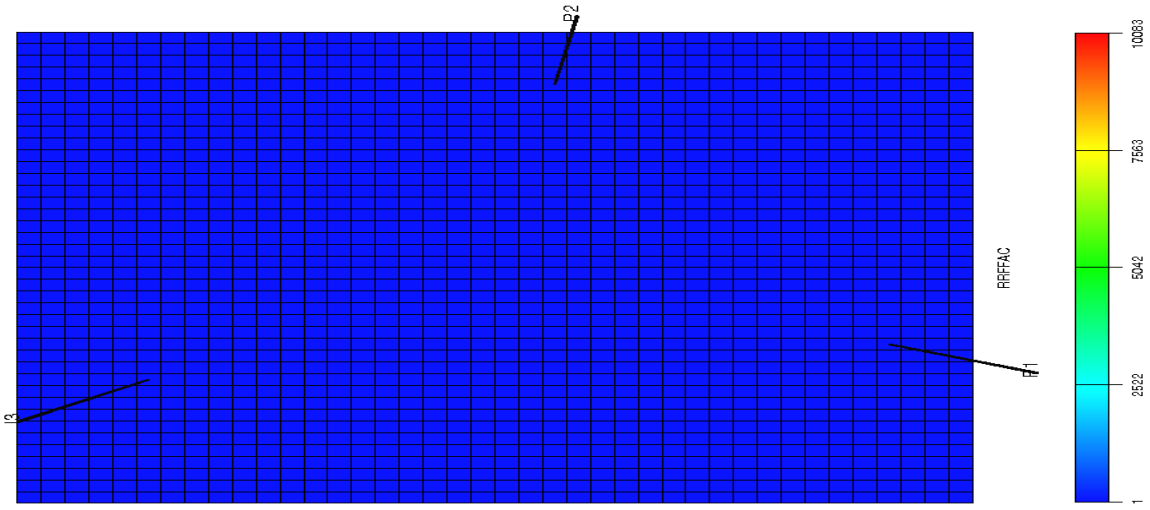

Figure 72: RRF visualization for case L5

Figure 72 shows that there is no gelling of the silicate in the reservoir at a temperature above the reservoir temperature. This confirms the authenticity of the numerical computations.

5.3.2 Injection Time

To ascertain the importance of injection time during the silicate water diversion process, a sensitivity study was done using various injection times. The *Table 19* below shows the various cases used to run the sensitivity on the injection timing. Each of the cases- T1, T2 and T3 were compared with the no silicate case (Base Case T0) to obtain the incremental oil recovery. The incremental oil between the different cases or injection times was compared.

Table 19: Cases for injection time sensitivity

Case No.	*Silicate Injection Time (Year)*
T (Base Case)	No silicate injected
T1	2005
T2	2007
T3	2010

Plots of the oil production rate with time for the different cases as presented in *Figure 73* show that greater EOR effect is obtained at earlier injection times. Injecting too late such as in the T3 case (2010) could result to smaller incremental oil recovery.

Table 20 shows a comparison of the incremental oil recovered for the different cases. The incremental oil recovery plotted against the case times in *Figure 74* show that the efficiency of the process is reduced as the injection time is delayed.

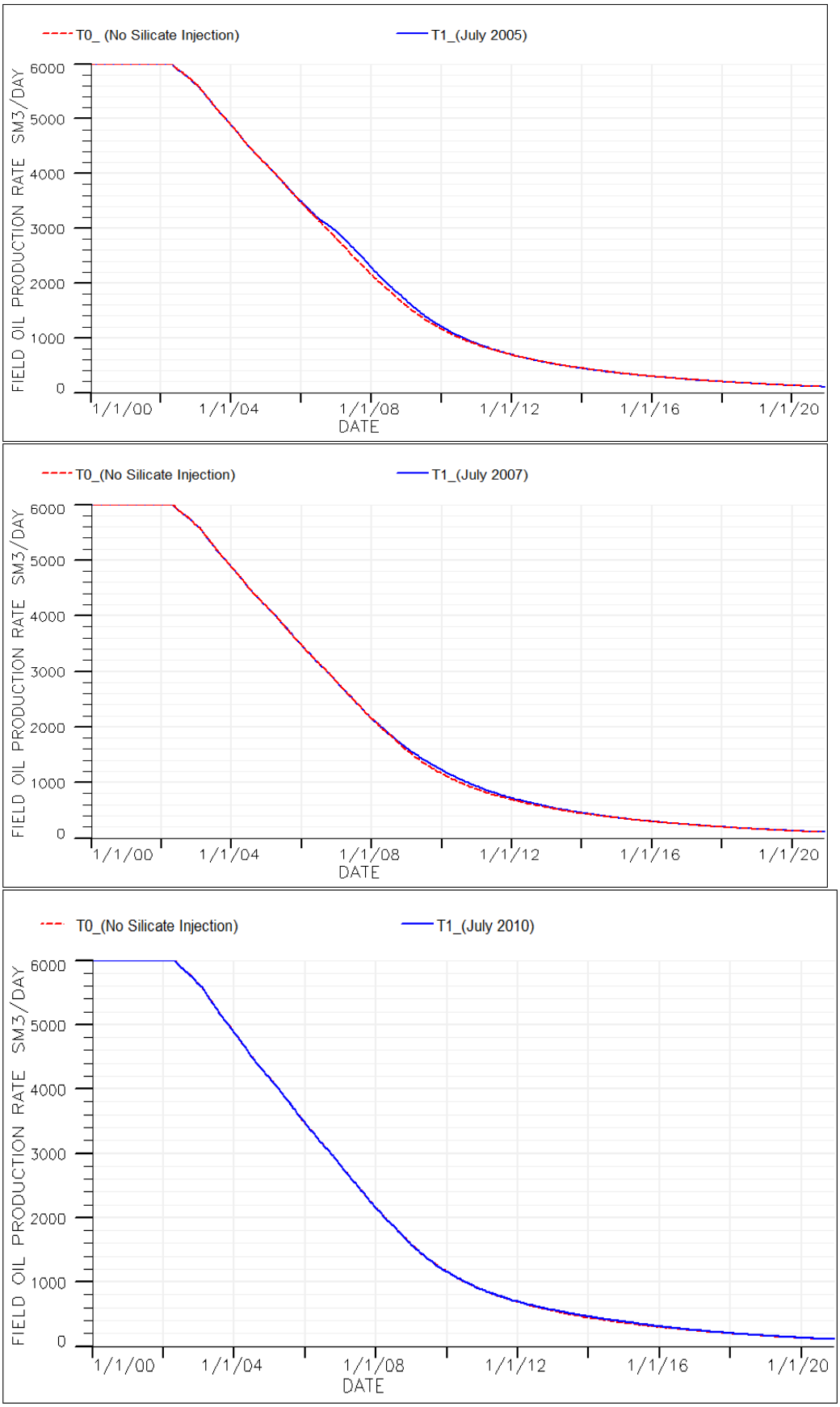

Figure 73: Field oil production rate for the different cases of injection time

Table 20: Comparing field EOR effect and efficiency factor of the different silicate injection time

Case No.	*Silicate Injection Start time (Year)*	*Total Injected Silicate mass (kg)*	*Total Oil Produced (Sm^3)*	*Incremental Oil Produced (sm^3)*
T0	Non	0	16327207,5	0,0
T1	2005	17360000	16473182	145974,5
T2	2007	17360000	16409071	81863,5
T3	2010	17360000	16351230,5	24023,0

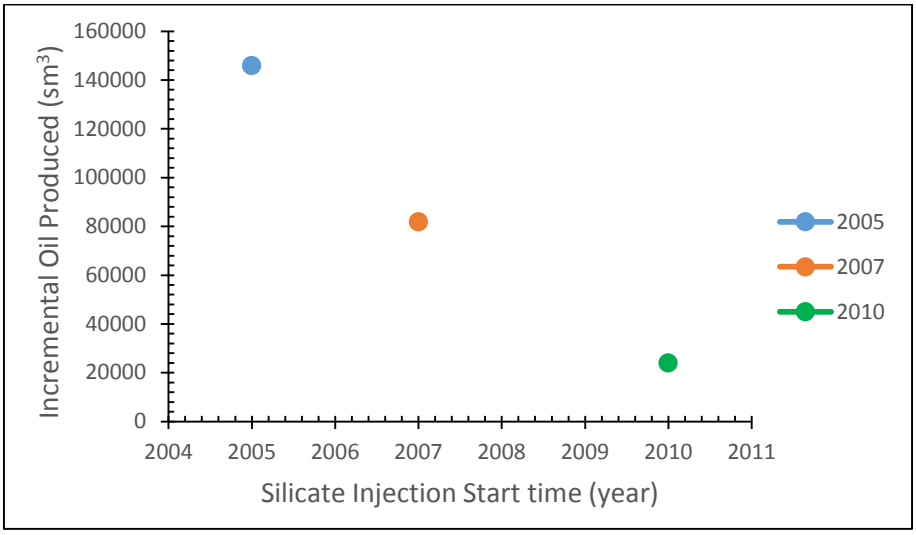

Figure 74: Incremental oil versus silicate injection time

Hence, it can be concluded that the injection start time of silicate is key to a successful implementation of the silicate water diversion process.

5.3.3 Silicate Slug Size Injected

The sensitivity on the slug size of the injected silicate was done by varying the injection period as shown in *Table 21* below.

Table 21: Cases used for sensitivity on silicate slug Size

Case No.	*Injection Period (Months)*
S0 (Base Case)	No Silicate Injected
S1	1,5
S2	2
S3	3
S4	4
S5	6

A plot of the field water cut versus time in *Figure 75* for the different cases of injected slug size shows that the EOR effect increases with the injected slug size. This is further established by a plot of the incremental oil versus the silicate slug size injected as shown in *Figure 78*. However, this does not say anything about the efficiency. By comparing the incremental oil recovery and the chemical efficiency of the different cases as presented in *Table 22*, it can be observed that the efficiency of injecting a larger slug size can be lower than the efficiency of injecting a smaller slug size. A plot of the chemical efficiency factor versus the silicate slug size injected per swept pore volume in *Figure 79* shows that case S2 (2 months injection) with a slug size of 17,360,000 kg had a higher efficiency than the other cases with higher slug size.

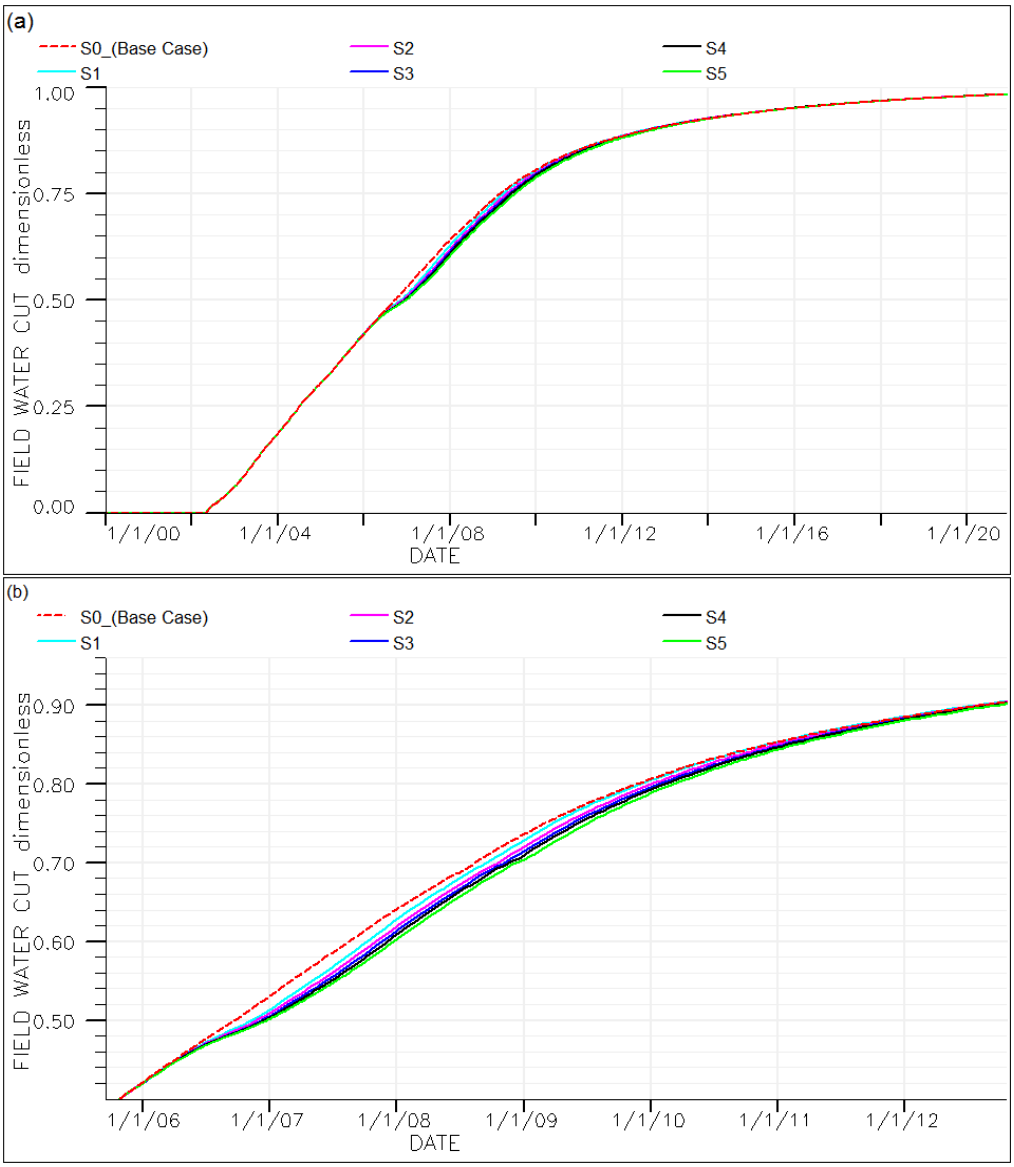

Figure 75: (a)Field water-cut for the different cases of silicate slug size injected, (b) Magnified view of the EOR effect in (a).

The swept pore volume was obtained from the visualization statistics as shown below:

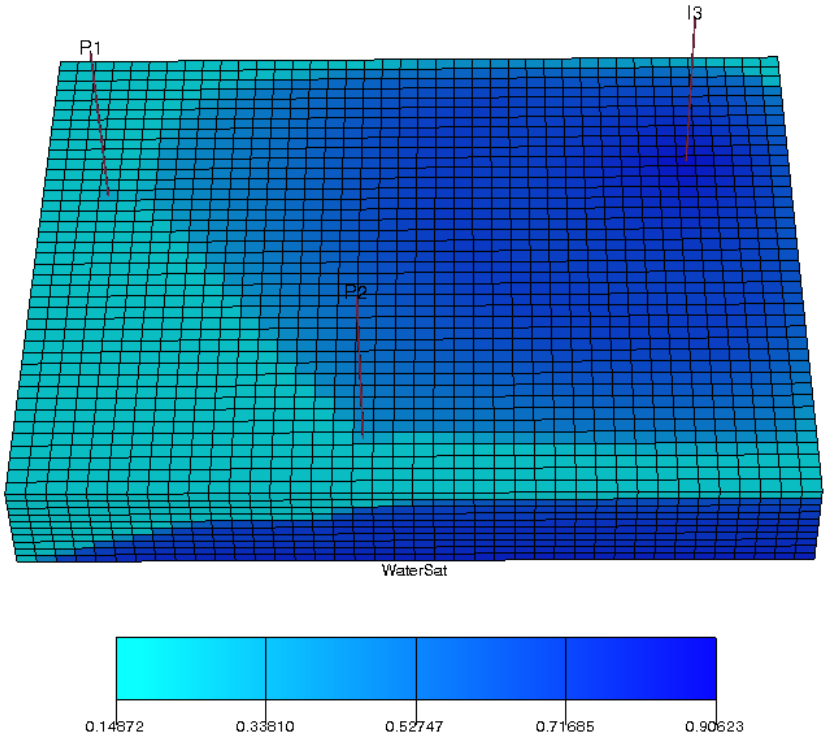

Figure 76: Visualization of the swept fraction of the active cells in the grid

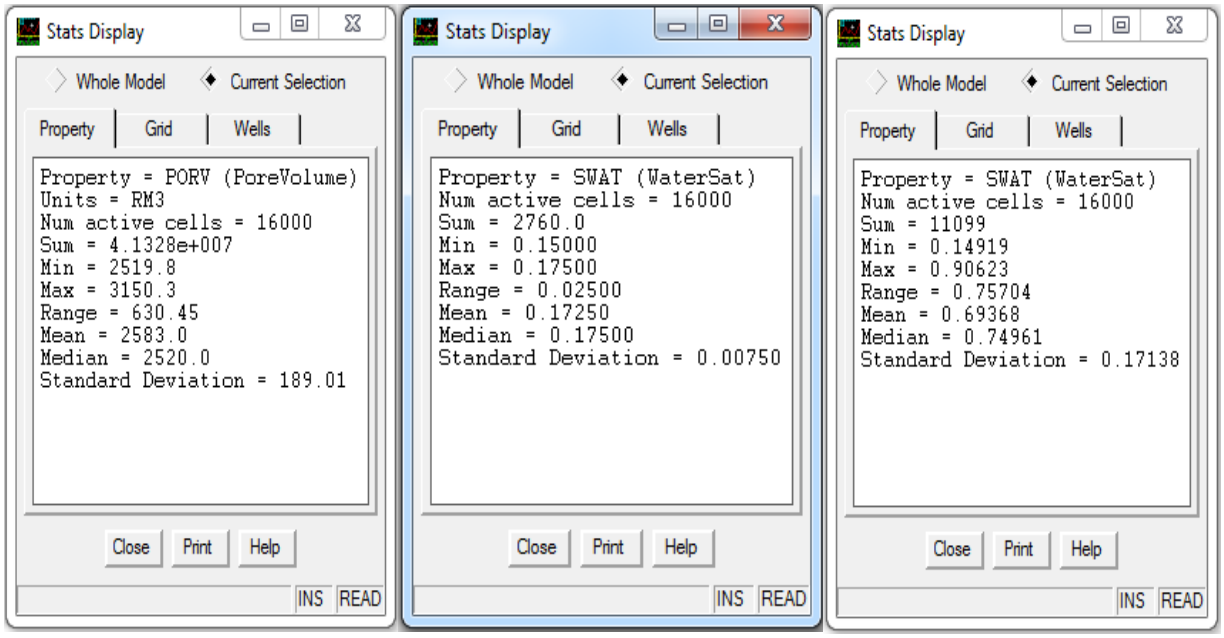

Figure 77: Statistics of the total pore volume in the active cells and the water saturation in the active cells at end of simulation

From *Figure 77*, the total pore volume of the active cells is equal to 41.328 MRm^3. The average water saturation in the active cells at the end of simulation is 0.69368. The average initial water saturation in the cells before injection is 0.1725. Therefore, the swept pore volume is approximately calculated as:

$$Swept\ PV = Avg.S_w\ after\ simulation - Avg.initial\ S_w) \times total\ PV\ of\ active\ cells$$

$$= (0.69368 - 0.1725) \times 41328000$$

$$= 21539327\ Rm^3$$

Table 18: Comparing field EOR effect and efficiency factor of the different silicate slug size injected

Silicate Injection Period (months)	*Silicate Slug Size Injected (kg)*	*Total Oil Produced (Sm^3)*	*Incremental Oil produced (Sm^3)*	*Silicate Slug Injected/Swept Pore Vol. (kg/sm^3)*	Chemical Efficiency Factor (Incr.oil/mass inj.) (m^3/kg)
0	0	16 327 208	0	0,000	0,0000
1,5	12 600 000	16 402 044	74 837	0,585	0,0059
2	17 360 000	16 473 182	145 975	0,806	0,0084
3	25 760 000	16 530 722	203 514	1,196	0,0079
4	34 440 000	16 567 847	240 639	1,599	0,0070
6	51 520 000	16 627 352	300 145	2,392	0,0058

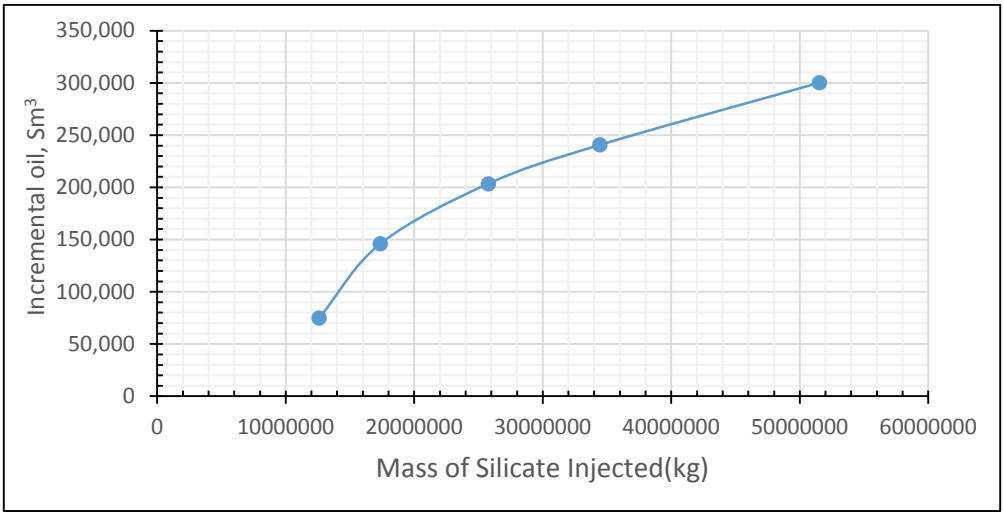

Figure 78: Incremental oil versus silicate slug size injected

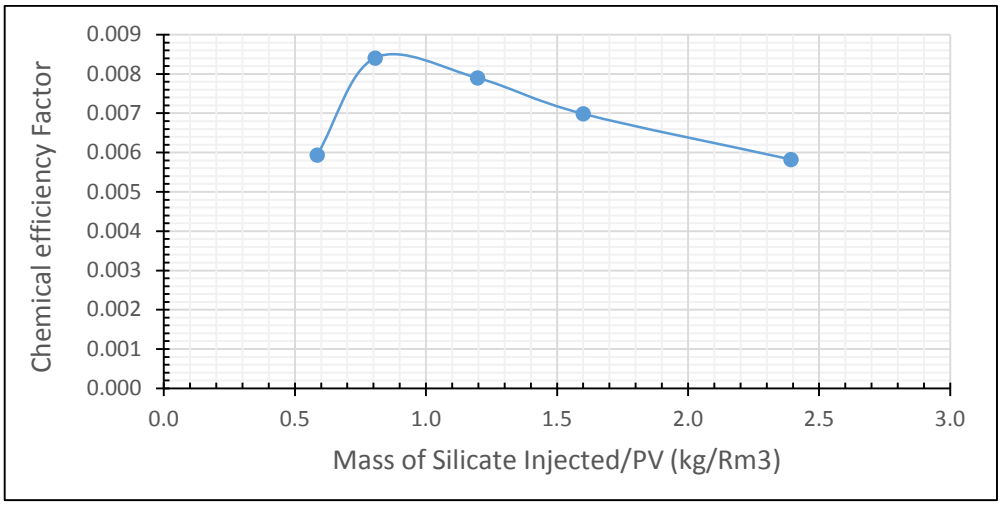

Figure 79: chemical efficiency factor versus injected slug size per pore volume

Figure 79 can be used to estimate the mass of silicate to be used in any injector – producer well pair as it is normalized with respect to reservoir volume. For example, If PV is 30 MRm^3, then the estimated mass of silicate required for maximum efficiency is: 0.9 kg/Rm^3 * 30 MRm^3 = 27 MRm^3.

5.3.4 Permeability Contrast

For the sensitivity run on permeability contrast, the reservoir permeability (that is, the permeability of other layers) was kept constant while the permeability of the thief zone was varied as shown in *Table 22*. Each ratio was compared with its own base case (no silicate injection case) to obtain their respective incremental oil recovery. The incremental oil recoveries of the different permeability contrast were compared and plotted in *Figure 80*.

Table 22: Cases for sensitivity on permeability contrast

Case No.	*Reservoir Perm.*	*Thief zone Perm*	*Permeability ratio*
P1	300	500	1.67
P2	300	1000	3.33
P3	300	2000	6.67
P4	300	3500	11.67
P5	300	5000	16.67
P6	300	10000	33.33
P7	300	20000	66.67

The simulation results for cases P3, P5 and P6 presented in *Figure 80* show that the diversion effect increases as the permeability contrast increases. *Table 23* shows the EOR effect for the different cases of permeability contrast. The incremental oil recovery is plotted against the permeability contrast in *Figure 81* and shows that the greater the permeability contrast between the thief zone and the rest of the reservoir, the more efficient and viable the silicate water diversion process will be. The negative values in the table also shows that implementing this process in a reservoir with not very suitable contrast could amount to severe losses as the plugging could occur in the lower permeable zones where it is not wanted and thus reduce the efficiency of the process.

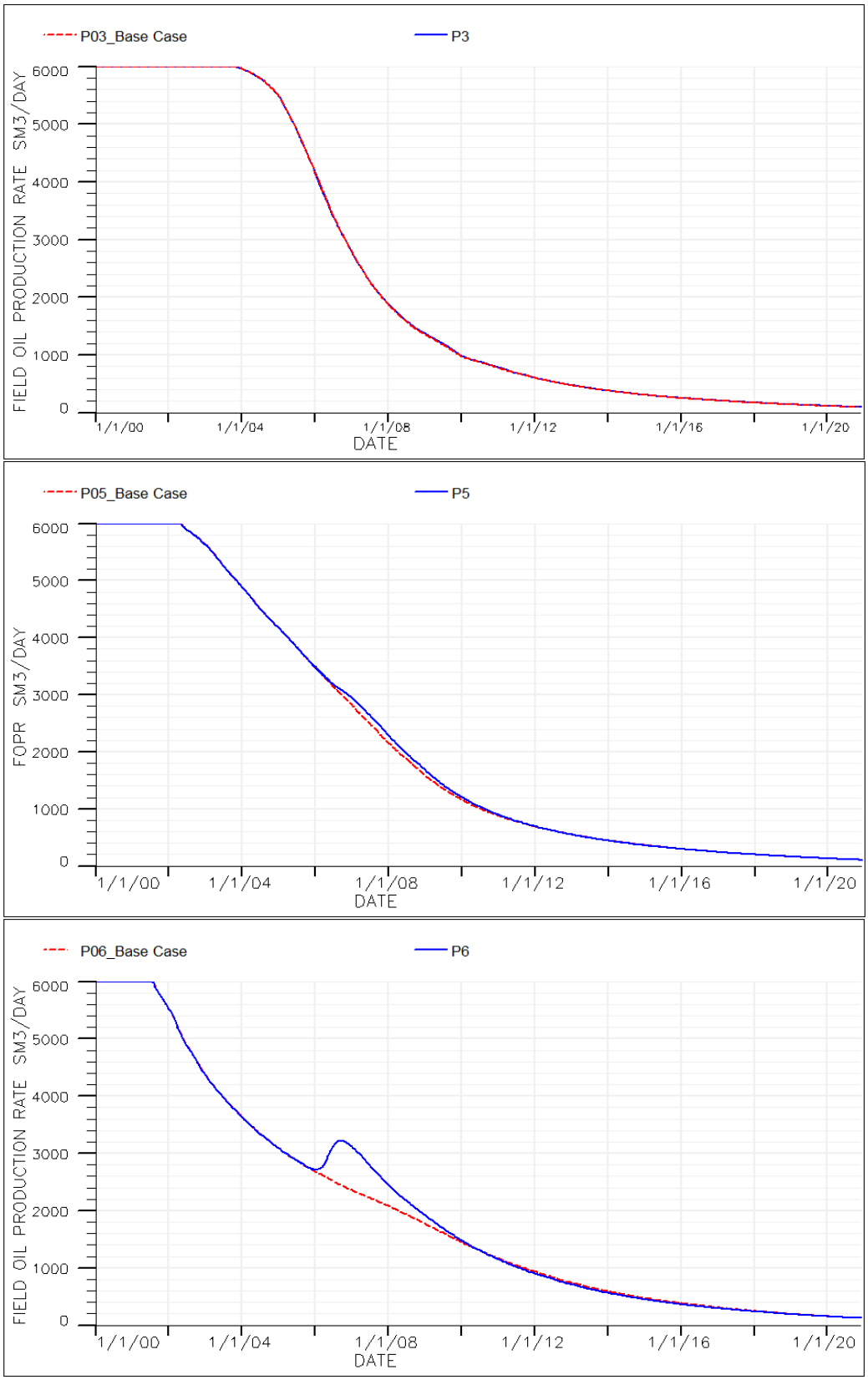

Figure 80: Field oil production rate history for different permeability contrast

Table 23: Comparing field EOR effect of the different cases of permeability contrast

Permeability Contrast ratio	*Total Silicate Injected (kg)*	*Total Oil Produced with silicate (Sm^3)*	*Total Oil Produced without silicate (Sm^3)*	*Incremental Oil (sm^3)*
1,67	17 360 000	17 460 130	17 464 724	-4 594
3,33	17 360 000	17 414 416	17 417 130	-2 714
6,67	17 360 000	17 151 250	17 133 342	17 908
11,67	17 360 000	16 803 966	16 723 460	80 506
16,67	17 360 000	16 473 182	16 327 207	145 975
33,33	17 360 000	15 453 915	15 008 375	445 540
66,67	17 360 000	14 122 430	12 713 735	1 408 695

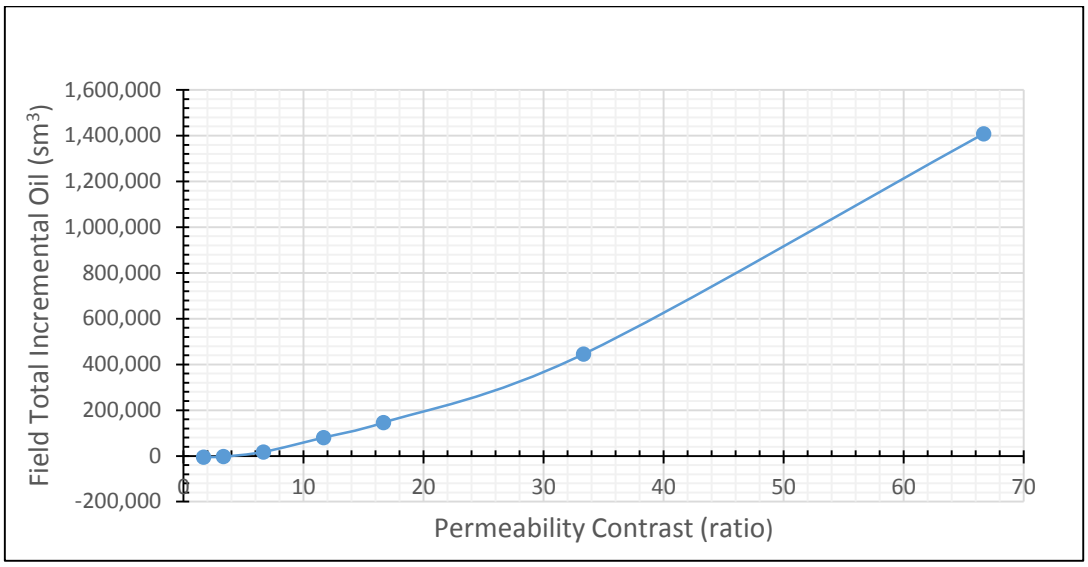

Figure 81: Field Incremental oil versus permeability contrast

These data indicate that the contrast should be maybe more than 10 in order to get significant incremental oil when using deep diversion as an EOR method as compared to polymer flooding for example

5.3.5 Residual Resistance Factor (RRF)

The cases for the sensitivity run on the RRF are shown in *Table 24* below.

Table 24: Cases for RRF sensitivity

Case No.	*RRF*
RRF0 (Base Case)	1 (No silicate injection)
RRF1	10
RRF2	100
RRF3	1000
RRF4	10000

Figure 82 shows the combined plot of the water cut obtained for the different RRF values. The higher the RRF value, the lower the water cut, which implies an improvement in the EOR effect. In addition, the EOR effect for RRF1 and RRF2 are almost same. This is similar to the RRF sensitivity result of Skrettingland et al. (2012) shown in *Figure 27*, where the RRF values of 10 and 100 for the crossflow case in both analytical and simulation models gave almost the same injectivity index.

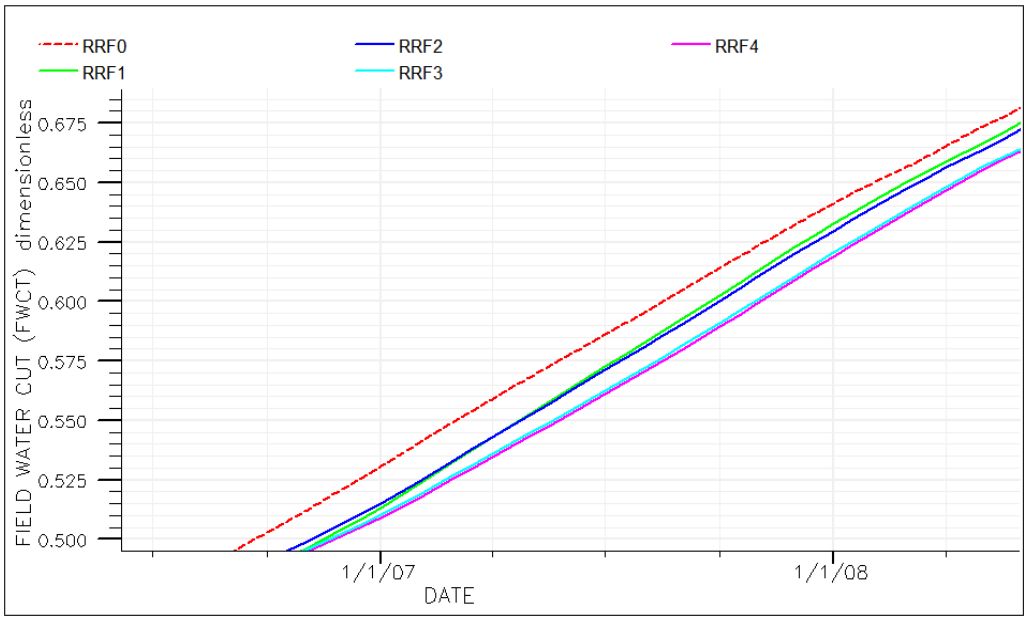

Figure 82: Field water cut for different RRF values (magnified to show grid refinement effect)

5.4 keyword Functionality Results

To study the functionality of these keywords, simulations were run on three cases stated and described in *Table 25* below.

Note: For clarity, the polymer option used for the grid refinement studies done in section 4 was without the PLYATEMP keyword.

Table 25: Cases for keyword functionality test

Case No.	*Options*
K1	Polymer options with PLYATEMP keyword but without PLYTRRF keyword
K2	Polymer options with PLYTRRF keyword but without PLYATEMP keyword
K3	Polymer options with both PLYATEMP and PLYTRRF keywords

The effect of grid refinement on each case was also checked and compared. For Case K1, only two temperatures were used under the PLYATEMP keyword: 69.99ºC and 70ºC. Zero adsorption concentration value were assigned under the 69.99ºC while non-zero adsorption concentration values was assigned to the 70ºC. The idea is that if the PYATEMP keyword function is effective, then no adsorption should be observed below the 70ºC temperature. The results are shown in the figures below.

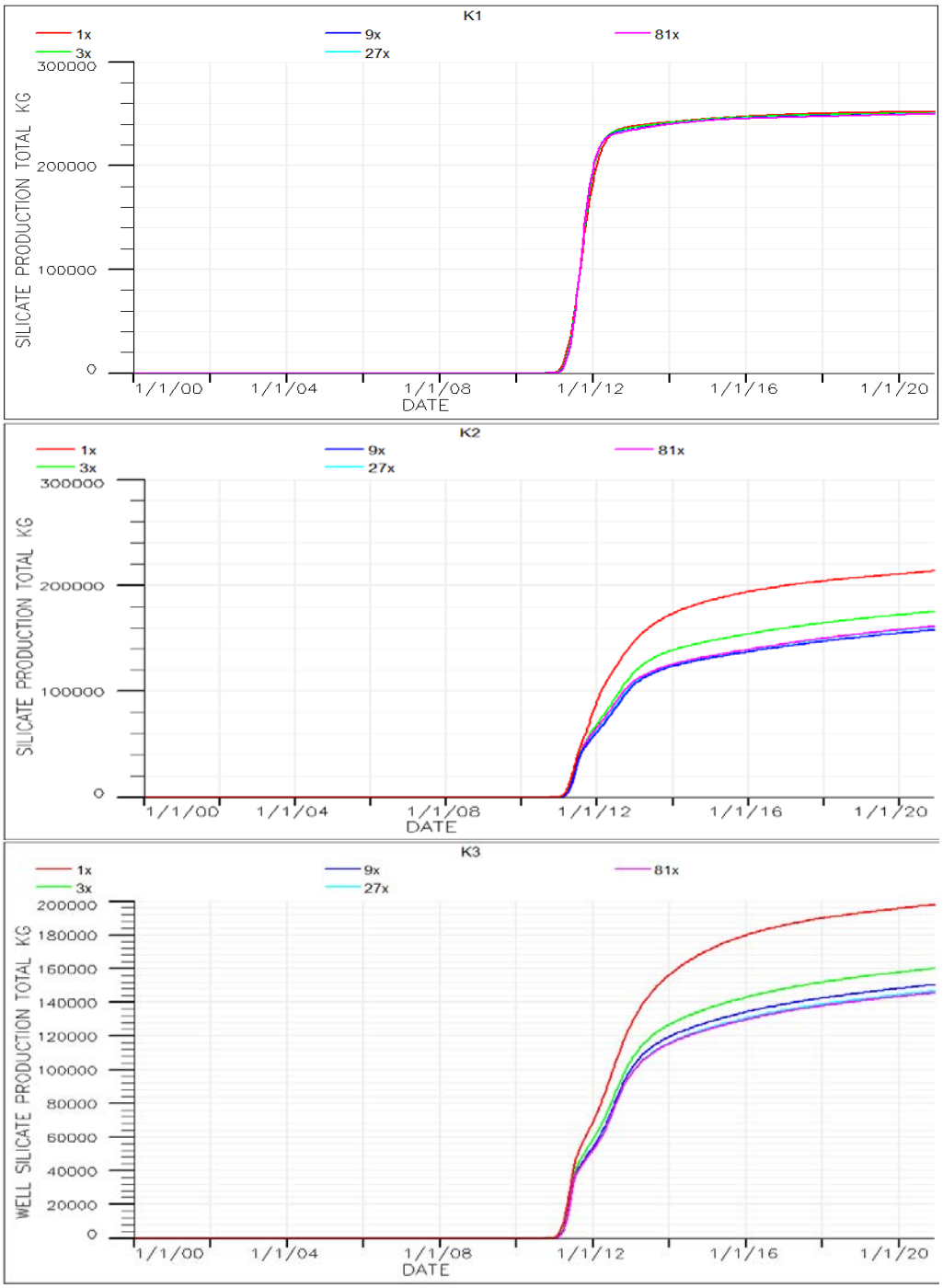

Figure 83: Comparing cumulative polymer production of the three cases

Case K1 result *(Figure 83*) shows higher silicate production values compared to the other two cases. This could be attributed to no gel formation and to lower adsorption since the adsorption was controlled by the silicate concentration and temperature. Adsorption only occurred above 69.99^{o}C in the reservoir as was expected.

Case K2 result (see *Figure 83*) shows that less polymer was produced due to gelling and higher adsorption. In this case, the adsorption was not controlled by temperature but by the silicate concentration only as pre-set in the model.

Case K3 result (see *Figure 83*) shows that when both PLYATEMP and PLYTRRF keywords are used in the polymer option of the model, the polymer production obtained will be lower. This is because temperature is known to favor adsorption.

The visualization for the three cases is presented in *Figure 84*.

Plots of the silicate production rate and the temperature profile are presented in *Figure 85* and *Figure 86* respectively.

From the results and observations, it can be concluded that the PLYATEMP keyword function in ECLIPSE for water diversion processes works as expected. Further studies should be done using this function as adsorption effects are more realistically modeled.

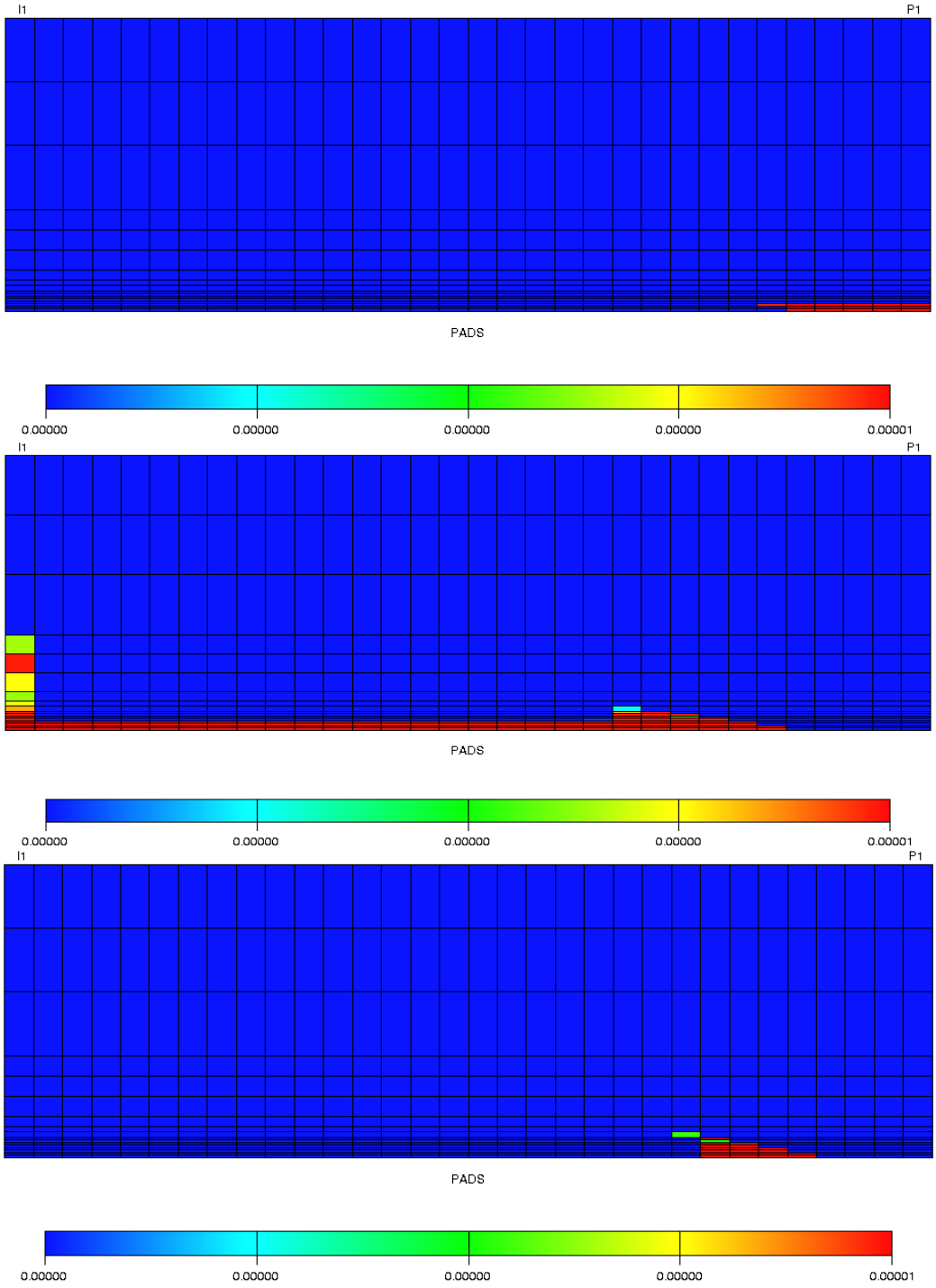

Figure 84: Visualization of adsorption for the three cases of keyword functionality test

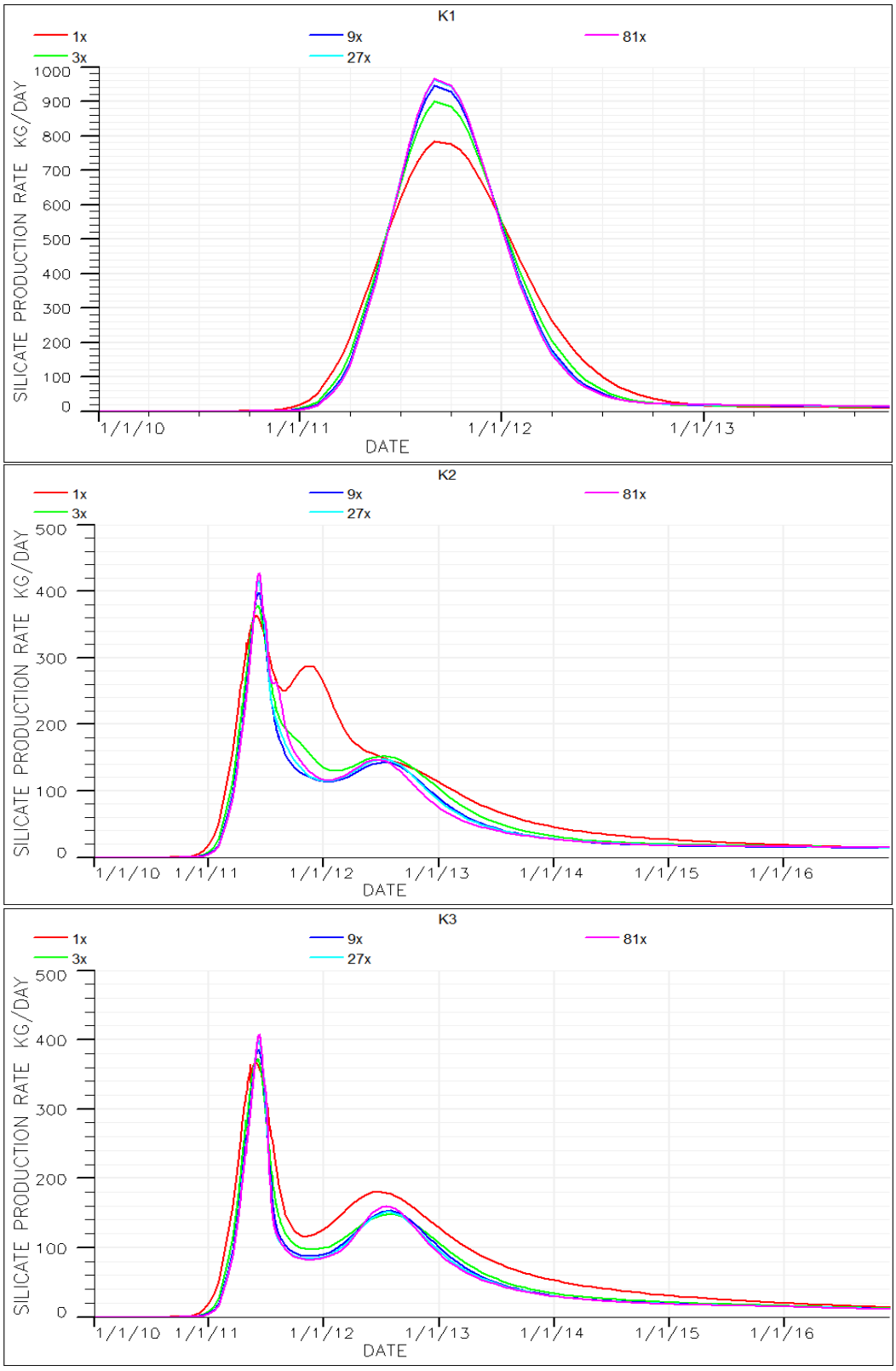

Figure 85: Silicate production rate for the three cases of keyword functionality test with grid refinement

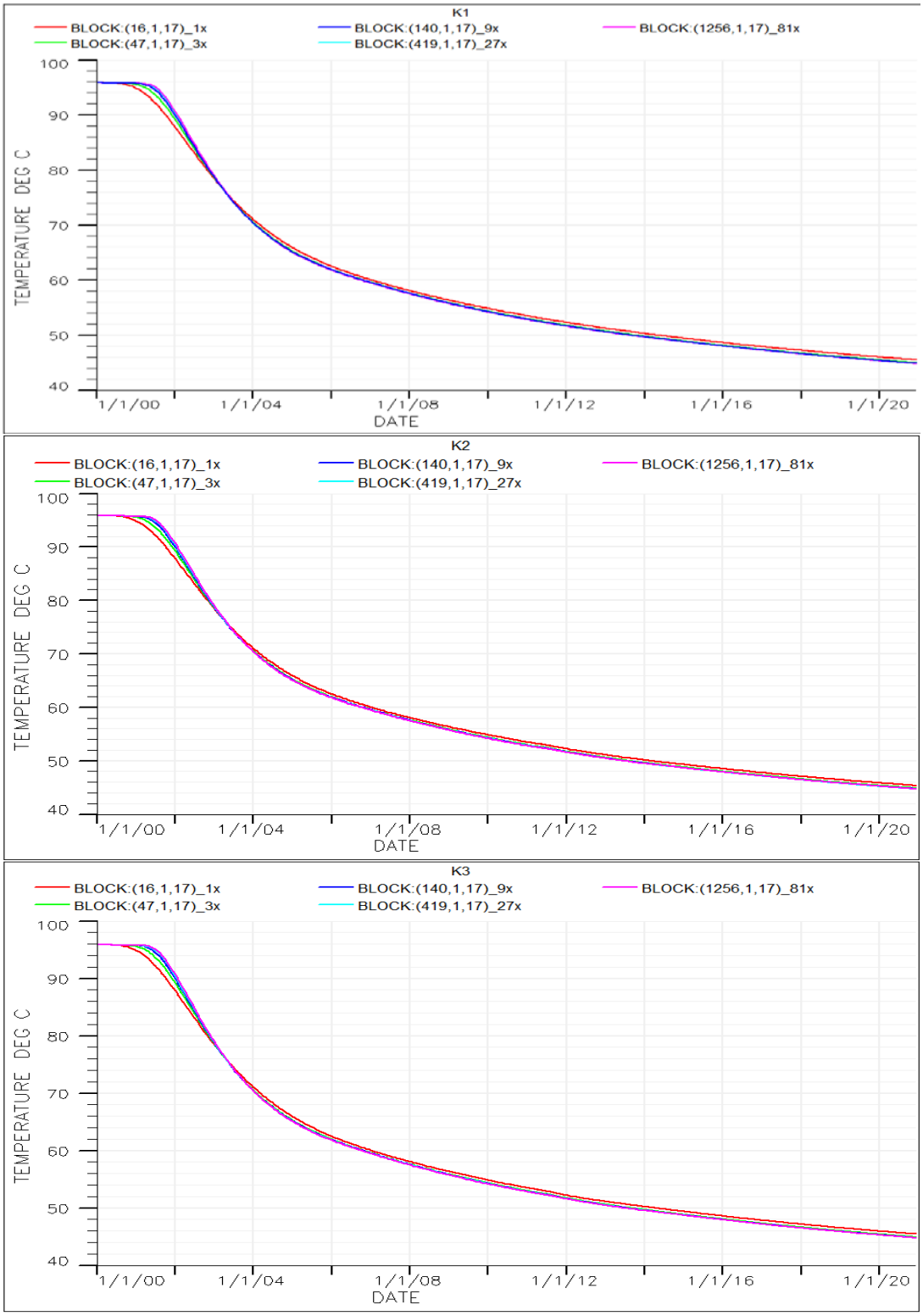

Figure 86: Temperature Profile in a block in the thief zone for the three cases of keyword functionality showing different refinements

6.0 SUMMARY AND CONCLUSION

A summary of the several observations made are:

1. It was proved that the grid size can influence the results obtained to a great extent. The 9x grid refinement was found to give realistic results as there were no significant difference in results obtained between the 9x refinement and higher refinements.
2. Sensitivity on the injection rate using the 2D model showed that the injection rate has no impact on the process. This however, does not agree with literature. It could be that the system here is not in a sensitive range with respect to velocity variations.
3. Results obtained show that if the thief zone is located in an upper layer in the reservoir that gelling could take place faster due to temperature differences.
4. The effect of activation temperature and gel location as observed agrees with literature and shows that these factors can influence the efficiency of the process. Hence, it is important that these factors be adequately considered prior to the implementation of a diversion project.
5. Injection timing was also observed to influence the chemical process efficiency. The time at which a water diversion project is to be implemented should be checked to ascertain whether it is worth going into the project.
6. The incremental oil recovery increased with the silicate slug size, however, a larger slug size could be less efficient compared to a smaller slug size taking into account the economics involved.
7. Permeability contrast between the thief zone and the reservoir was found to influence the incremental recovery obtained from such process. The higher the permeability contrast, the more effective the process will be. A negative effect could be obtained if the process is applied in a reservoir with unsuitable permeability contrast.
8. The PLYATEMP keyword in ECLIPSE for water diversion process was tested and found to work well as expected. It is therefore recommended that further simulation studies on water diversion should take advantage of this function as adsorption effects are more realistically modeled.

Generally, based on the results and discussions, it can be concluded that the polymer option can be used to model water diversion using silicates to a good extent.

REFERENCES

AMINIAN, K. 2009. Water Production Problems and Solutions. *Appalachian Oil and Gas Research Consortium. August,* 9.

BEDAIWI, E., AL-ANAZI, B. D., AL-ANAZI, A. F. & PAIAMAN, A. M. 2009. Polymer Injection for Water Production Control through Permeability Alteration in Fractured Reservoir. *Nafta,* 60**,** 221-231.

BERGEM, J., FULLEYLOVE, R. J., MORGAN, J. C., STEVENS, D. G., DAHL, J. A., EOFF, L. S. & ENKABABIAN, P. G. 1997. Successful Water Shutoff in a High-Temperature, High-Volume Producer - A Case History from the Ula Field, Offshore Norway. Society of Petroleum Engineers.

BURNS, L. D., MCCOOL, C. S., WILLHITE, G. P., BURNS, M., OGLESBY, K. D. & GLASS, J. 2008. New Generation Silicate Gel System for Casing Repairs and Water Shutoff. Society of Petroleum Engineers.

CEES 2013. Soluble Silicates: Chemical, toxicological, ecological and legal aspects of production, transport, handling and application. *Centre Europeen d'Etude des Silicates*.

CHAN, K. S. 1995. Water Control Diagnostic Plots. Society of Petroleum Engineers.

DAHL, J. A., NGUYEN, P. D., DALRYMPLE, E. D. & RAHIMI, A. B. 1992. Current Water-Control Treatment Designs. Society of Petroleum Engineers.

ECLIPSE 2014. ECLIPSE Reservoir Simulator Refernce Manual.

ELFRINK, E. B. 1966. Selective plugging method. Google Patents.

FANCHI, J. R. 1983. Multidimensional Numerical Dispersion.

FERRIS, F. G., STEHMELER, L. G., KANTZAS, A. & MOURITIS, F. M. 1992. Bacteriogenic Mineral Plugging. Petroleum Society of Canada.

GRATTONI, C. A., JING, X. D. & ZIMMERMAN, R. W. 2001. Disproportionate Permeability Reduction When a Silicate Gel is Formed In-Situ to Control Water Production. Society of Petroleum Engineers.

GREEN, D. W. & WILLHITE, G. P. 1998. *Enhanced Oil Recovery*, Henry L. Doherty Memorial Fund of AIME, Society of Petroleum Engineers.

HANSEN, B. 2009. Evaluating tertiary water based EOR methods on the Veslefrikk field, with emphasis on analyzing sodium silicate injection by numerical simulation.

HATZIGNATIOU, D. G., HELLEREN, J. & STAVLAND, A. 2014. Numerical Evaluation of Dynamic Core-Scale Experiments of Silicate Gels for Fluid Diversion and Flow-Zone Isolation.

HERBAS, J., MORENO, R., ROMERO, M. F., COOMBE, D. & SERNA, A. 2004. Gel Performance Simulations and Laboratory/Field Studies to Design Water Conformance Treatments in Eastern Venezuelan HPHT Reservoirs. Society of Petroleum Engineers.

ILER, R. K. 1979. The chemistry of silica. Solubility, polymerization, colloid and surface properties, and biochemistry. . *Acta Polymerica,* 31**,** 406-406.

JURINAK, J. J. & SUMMERS, L. E. 1991. SPE 18505 Supplement: Laboratory Testing of Colloidal Silica Gel for Oilfield Applications. Society of Petroleum Engineers.

KENNEDY, H. T. 1936. Chemical Methods for Shutting Off Water in Oil and Gas Wells.

KOSZTIN, B., PALASTHY, G., UDVARI, F., BENEDEK, L., LAKATOS, I. & LAKATOS-SZABO, J. 2002. Field Evaluation of Iron Hydroxide Gel Treatments. Society of Petroleum Engineers.

KRUMRINE, P. H. & BOYCE, S. D. 1985. Profile Modification and Water Control With Silica Gel-Based Systems. Society of Petroleum Engineers.

LAKATOS, I., LAKATOS-SZABO, J., TISZAI, G., PALASTHY, G., KOSZTIN, B., TRÖMBÖCZKY, S., BODOLA, M. & PATTERMAN-FARKAS, G. 1999. Application of Silicate-Based Well Treatment Techniques at the Hungarian Oil Fields. Society of Petroleum Engineers.

LAKATOS, I. J., LAKATOS-SZABO, J., KOSZTIN, B., AL-SHARJI, H. H., ALI, E., AL-MUJAINI, R. A. R. & AL-ALAWI, N. 2011. Application of Silicate/Polymer Water Shutoff Treatment in Faulted Reservoirs with Extreme High Permeability. Society of Petroleum Engineers.

NASR-EL-DIN, H. & TAYLOR, K. 2005. Evaluation of sodium silicate/urea gels used for water shut-off treatments. *Journal of Petroleum Science and Engineering,* 48**,** 141-160.

NASR-EL-DIN, H. A., RAJU, K. U., HILAB, V. V. & ESMAIL, O. J. 2004. Injection of Incompatible Water as a Means of Water Shut-Off. Society of Petroleum Engineers.

PQCORP. NA. *Soluble silicate for water control & Lost Circulation* [Online]. Available: http://www.pqcorp.com/portals/1/lit/bulletin_35-02.pdf.

RAMSTAD, K. 2013. Water Production and Related Challenges. .

ROLFSVAG, T. A., JAKOBSEN, S. R., LUND, T. A. T. & STROMSVIK, G. 1996. Thin Gel Treatment of an Oil Producer at the Gullfaks Field: Results and Evaluation. Society of Petroleum Engineers.

SECEN, J. 2005. IOR AND EOR - CHANCES FOR INCREASE OF OIL PRODUCTION AND RECOVERIES IN EXISTING, MATURE RESERVOIRS. *Rudarsko-Geolosko-Naftni Zbornik*.

SERIGHT, R. S., LANE, R. H. & SYDANSK, R. D. 2001. A Strategy for Attacking Excess Water Production. Society of Petroleum Engineers.

SHENG, J. 2010. *Modern chemical enhanced oil recovery: theory and practice*, Gulf Professional Publishing.

SKRETTINGLAND, K., DALE, E. I., STENERUD, V. R., LAMBERTSEN, A. M., NORDAAS KULKARNI, K., FEVANG, O. & STAVLAND, A. 2014. Snorre In-depth Water Diversion Using Sodium Silicate - Large Scale Interwell Field Pilot. Society of Petroleum Engineers.

SKRETTINGLAND, K., GISKE, N. H., JOHNSEN, J.-H. & STAVLAND, A. 2012. Snorre In-depth Water Diversion Using Sodium Silicate - Single Well Injection Pilot. Society of Petroleum Engineers.

STAVLAND, A., JONSBRATEN, H. C., VIKANE, O., SKRETTINGLAND, K. & FISCHER, H. 2011b. In-Depth Water Diversion Using Sodium Silicate on Snorre - Factors Controlling In-Depth Placement. Society of Petroleum Engineers.

STAVLAND, A., JONSBRÅTEN, H., VIKANE, O., SKRETTINGLAND, K. & FISCHER, H. 2011a. In-depth water diversion using sodium silicate–Preparation for single well field pilot on Snorre. *IOR 2011.*

SYDANSK, R. D. & ROMERO-ZERON, L. 2011. *Reservoir conformance improvement*, SPE. Society of Petroleum Engineers.

TERRY, R. E. 2000. Enhanced oil recovery. *paper 137048, 503-518.*

TZIMAS, E., GEORGAKAKI, A., CORTES, C. G. & PETEVES, S. 2005. Enhanced oil recovery using carbon dioxide in the European energy system.

VINOT, B., SCHECHTER, R. S. & LAKE, L. W. 1989. Formation of Water-Soluble Silicate Gels by the Hydrolysis of a Diester of Dicarboxylic Acid Solublized as Microemulsions.

APPENDIX

A1 ECLIPSE 2D Coarse Grid Model Data File

```
RUNSPEC----------------------------------------------------

TITLE
 STAIR1

DIMENS
 32 1 17 /

--NOSIM

-- Allow for multregt, etc. Maximum number of regions 20.

GRIDOPTS
 'YES' 0 /

--BLACKOIL

-- Phases
OIL
WATER
GAS

DISGAS

POLYMER

TEMP

VFPPDIMS
 19 10 8 10 0 9 /

METRIC

START
 01 'JAN' 2000 /

EQLDIMS
 1 /

REGDIMS
-- Ntfip
    1 /

TABDIMS
--ntsfun ntpvt nssfun nppvt ntfip nrpvt ntendp
    4     1     55     60   16    60 /

WELLDIMS
-- NWMAXZ NCWMAX NGMAXZ NWGMAX
 30 30 5 10 /

NSTACK
 80 /

UNIFOUT


RPTRUNSP

OPTIONS
 /
```

```
TRACERS
-- NOTR_O NOTR_W NOTR_G NOTR_ENV DIFF?
   0      2      0      0        NODIFF /
-------------------------------------------------------
--
--     Input of grid geometry
--
-------------------------------------------------------

GRID----------------------------------------
-- Generate init file

NEWTRAN

-- Produce Extensive grid files .GRID and .EGRID
GRIDFILE
  2 0 /

-- Optional for post-processing of GRID

GRIDUNIT
METRES /

-- requests output of INIT file
INIT

MESSAGES
  /

NOECHO

-------------------------------------------------------
--
--     Grid and faults
--
-------------------------------------------------------

--
-- Simulation grid, fault traces and transmissibilities and NNC
--
INCLUDE
   'Include/ECLIPSE_G_2D_001.GRDECL' /



-------------------------------------------------------
--
--     Input of grid parameters
--
-------------------------------------------------------

-- Temp
-- Rock thermal conductivity
--     KJ/ (m day C)
EQUALS
 'THCONR' 270.0 /
/

INCLUDE
   'Include/ECLIPSE_PORPERM_001.GRDECL' /

COPY
 'PERMX'  'PERMY' /
 'PERMX'  'PERMZ' /
/

MULTIPLY
 'PERMZ' 0.1 /
```

```
/

NOECHO

PROPS----------------------------------------------
------------------------------------------------------
--
--Input of fluid properties and relative permeability
--
------------------------------------------------------

NOECHO

INCLUDE
   'Include/ecl100_pvt_snorre_8comp_96C_rescaled.inc' /

INCLUDE
   'Include/E100_VISCT_BLACKOIL.INC' /

INCLUDE
   'Include/E100_SPECHEAT_BLACKOIL.INC' /

-- Different section for E100 and E300
INCLUDE
   'Include/E100_SPECROCK.INC' /

INCLUDE
   'Include/ECL_ROCK_COMPRESS.INC' /

-- Rel. perm and cap. Pressure tables --
INCLUDE
   'include/ECL_SF_KROW_H_-_ZERO_CAP_PRES'   /

RPTPROPS
 1 1 1 5*0 0 /

TRACER
-- Name phase
  TR1     WAT /
  TR2     WAT /
/

----------------------------------------
-- Polymer (silicate) section

PLMIXPAR
1.0 / -- Chemical completely mixed with water

PLYMAX
40.0 0.0500 /

PLYVISC
-- cons   water visc factor
  0.0000      1.0
 40.0000      1.00001 /

PLYADS
-- cons    abs.cons
   0.0000   0.00000
   7.01     0.00000000
   8.011    0.0000050
  40.0000   0.0000051 /
   0.0000   0.00000
   7.01     0.00000000
   8.011    0.0000050
  40.0000   0.0000051 /
   0.0000   0.00000
   7.01     0.00000000
```

```
   8.011    0.0000050
  40.0000   0.0000051 /
   0.0000   0.00000
   7.01     0.00000000
   8.011    0.0000050
  40.0000   0.0000051 /

PLYROCK
-- Dead phi; RRF; dens (res.); abs. ind.; max abs.
     0.0    1.0        1880         2       0.0000050 /
     0.0    1.0        1880         2       0.0000050 /
     0.0    1.0        1880         2       0.0000050 /
     0.0    1.0        1880         2       0.0000050 /

PLYTRRF
-- Temp     RRF
   30.0     1.0
   50.0     1.001
   60.0     1.0015
   69.0     1.002
   70.0   10000.0
  100.0   10000.1 /
   30.0     1.0
   50.0     1.001
   60.0     1.0015
   69.0     1.002
   70.0   10000.0
  100.0   10000.1 /
   30.0     1.0
   50.0     1.001
   60.0     1.0015
   69.0     1.002
   70.0   10000.0
  100.0   10000.1 /
   30.0     1.0
   50.0     1.001
   60.0     1.0015
   69.0     1.002
   70.0   10000.0
  100.0   10000.1 /

-- END Polymer (silicate) section
-----------------------------------------------

REGIONS-----------------------------------------

--INCLUDE
--
'/project/arm/Water_Diversion/Sim_test/sim/INCLUDE/GRID/ECL_HOM_ABX_G1.fipnum.inc'
/

INCLUDE
   'Include/ECLIPSE_SATNUM_001.GRDECL' /

SOLUTION----------------------------------------
-----------------------------------------------
-- Equilibrium data: do not include this file in case of RESTART

--Comp PVT
RSVD
  1000.0 96.0
  3000.0 96.0 /

INCLUDE
   'Include/E100_EQUIL.INC' /

RPTRST
 BASIC=2 FREQ=3 /
```

```
INCLUDE
   'Include/ECL_TEMPVD.INC' / (Reservoir temperature vs depth, see Table 7)

-- Make sure the initial restart file is saved.
-- RPTSOL
--     RESTART=2 FIP EQUIL SOIL SWAT /

RPTSOL
 FIP=2 /

--TRACER INITIALIZATION
TVDPFTR1
0      0
10000  0 /

TVDPFTR2
0      0
10000  0 /

SUMMARY----------------------------------------------

INCLUDE
   'Include/ECL_TEMP_REPORT_SMRY.INC' /

INCLUDE
   'Include/ECL_PLY_REPORT_SMRY.INC' /

INCLUDE
   'Include/ECL_GENERAL_REPORT_SMRY.INC' /

INCLUDE
   'Include/ECL_G_2D_BLOCK_REPORT_SMRY_001.INC' /

INCLUDE
   'Include/ECL_G_2D_BLOCK_REPORT_TEMP_001.INC' /

INCLUDE
   'Include/ECL_G_2D_BLOCK_REPORT_TRACER_001.INC' /

INCLUDE
   'Include/ECL_G_2D_BLOCK_REPORT_PLY_001.INC' /

SCHEDULE---------------------------------------------
INCLUDE
   'Include/E100_TUNING.INC' /

RPTSCHED
 'FIP=2' /

INCLUDE
   'Include/ECLIPSE_TEMP30_001_PLY.SCH' /

END
```

A2 Include Files

```
INCLUDE
   'Include/ECLIPSE_PORPERM_001.GRDECL' /
PORO
96*0.05
320*0.2
128*0.25
/

PERMX
96*0
320*300
128*5000
/

============================================
INCLUDE
   'Include/ecl100_pvt_snorre_8comp_96C_rescaled.inc' /

-- Generated with PVTsim version 21.0.0 at 23.05.2014 13:43:48
--#METRIC
--
--
-- Salinity (mg/l)
-- 35000
--
DENSITY
-- OilDens   WaterDens    GasDens
-- Kg/m3       kg/m3       kg/m3
   834.5      1023.8      1.24691 /
--
--
PVTW
--     RefPres        Bw          Cw           Vw         dVw
--       bara       rm3/m3       1/bara        cP        1/bara
        300.0      1.025      0.41720E-04   0.3895       0.0 /
     -- 119.3      1.03329    0.41720E-04   0.32564    0.89743E-04 /
--
--
-- Separator Conditions
-- Tsep(C)    Psep (bara)
-- ---------- ----------
--   15.00        1.01
--
-- Reservoir temperature (C)
-- 95.94
--
-- Experiment type: Constant Mass Expansion
--
--
------------------------------------------------------------
--SOLUTION  PRESSURE  OIL FVF      OIL
-- GOR Rs      Po       Bo      VISCOSITY
-- Sm3/Sm3    bara    rm3/Sm3      cP
------------------------------------------------------------
PVTO
    4.7      10.0    1.06187      1.071
             40.0    1.05759      1.151
             50.0    1.05624      1.178
            100.0    1.05000      1.314
            119.3    1.04779      1.367
            150.0    1.04446      1.452
```

```
          200.0    1.03952      1.592
          250.0    1.03506      1.733
          300.0    1.03101      1.875
          350.0    1.02732      2.018
          400.0    1.02393      2.162
          450.0    1.02081      2.309
          500.0    1.01792      2.458  /
 33.1      40.0    1.16288      0.701
           50.0    1.16083      0.716
          100.0    1.15143      0.793
          119.3    1.14815      0.823
          150.0    1.14326      0.871
          200.0    1.13605      0.950
          250.0    1.12963      1.030
          300.0    1.12387      1.109
          350.0    1.11865      1.188
          400.0    1.11390      1.265
          450.0    1.10955      1.342
          500.0    1.10555      1.418  /
 41.6      50.0    1.19046      0.658
          100.0    1.18010      0.728
          119.3    1.17650      0.755
          150.0    1.17113      0.799
          200.0    1.16326      0.872
          250.0    1.15627      0.944
          300.0    1.15000      1.017
          350.0    1.14435      1.089
          400.0    1.13921      1.160
          450.0    1.13451      1.230
          500.0    1.13019      1.299  /
 80.9     100.0    1.31071      0.526
          119.3    1.30531      0.544
          150.0    1.29734      0.574
          200.0    1.28584      0.623
          250.0    1.27578      0.673
          300.0    1.26688      0.724
          350.0    1.25894      0.774
          400.0    1.25178      0.825
          450.0    1.24529      0.875
          500.0    1.23937      0.924  /
 96.0     119.3    1.35527      0.442
          150.0    1.34608      0.470
          200.0    1.33289      0.515
          250.0    1.32144      0.562
          300.0    1.31136      0.6075
          350.0    1.30240      0.652
          400.0    1.29437      0.698
          450.0    1.28710      0.743
          500.0    1.28049      0.789  /
120.2     150.0    1.42084      0.414
          200.0    1.40692      0.447
          250.0    1.39483      0.480
          300.0    1.38420      0.514
          350.0    1.37475      0.549
          400.0    1.36626      0.583
          450.0    1.35859      0.618
          500.0    1.35161      0.653  /
159.6     200.0    1.51806      0.327
          250.0    1.50501      0.351
          300.0    1.49354      0.376
          350.0    1.48334      0.401
          400.0    1.47418      0.427
          450.0    1.46590      0.452
          500.0    1.45837      0.478  /
198.9     250.0    1.60295      0.258
          300.0    1.59073      0.276
          350.0    1.57986      0.295
          400.0    1.57011      0.313
```

```
            450.0    1.56129      0.332
            500.0    1.55327      0.351  /
  238.3     300.0    1.67552      0.203
            350.0    1.66407      0.217
            400.0    1.65380      0.231
            450.0    1.64452      0.245
            500.0    1.63607      0.258  /
  277.6     350.0    1.73577      0.161
            400.0    1.72506      0.171
            450.0    1.71537      0.181
            500.0    1.70656      0.191  /
  316.9     400.0    1.78370      0.127
            450.0    1.77369      0.134
            500.0    1.76457      0.142  /
/
------------------------------------------------------------
--PRESSURE GAS FVF      GAS
--   Pg       Bg      VISCOSITY
--   bara    rm3/Sm3      cP
------------------------------------------------------------
PVDG
    10.0      0.12713     0.0124
    40.0      0.02986     0.0138
    50.0      0.02358     0.0141
   100.0      0.01130     0.0161
   119.3      0.00939     0.0171
   150.0      0.00742     0.0188
   200.0      0.00568     0.0220
   250.0      0.00474     0.0254
   300.0      0.00418     0.0285
   350.0      0.00380     0.0315
   400.0      0.00353     0.0343
/


 --Warning: Constant reservoir fluid composition assumed above   119.3 bara
 --Tabulated properties corrected to be monotonic with pressure

==========================================
INCLUDE
   'Include/E100_VISCT_BLACKOIL.INC' /

-- Temperature dependency of viscosity
VISCREF
--ref. pressure Rs (only needed when dissolved gas exists)
300 96.0 / --res. pressure and Rs from PVT data

WATVISCT
--Viscosity generated from the PVTsim
--ref.T   Uw
10  1.5135
30  0.9663
50  0.6836
66  0.5509
70  0.5177
90  0.4113
96  0.3895     -- Interpolated linearly
-- 110 0.3386
120 0.2938 /


OILVISCT
--ref.T Uo
10    4.1814
30    2.4421
50    1.6334
```

```
66    1.2072
70    1.1007
90    0.7028
96    0.6075   -- Interpolated linearly
110   0.3851
120   0.2474 / Interpolated from measurements, SAGA PVT Study 1985

=============================================
INCLUDE
   'Include/E100_SPECHEAT_BLACKOIL.INC' /

SPECHEAT
-- Fluid specific heat capacities,
-- T [C]   kJ/(kg*C)   kJ/(kg*C)   kJ/(kg*C)
--         Oil         water       gas
    0      2.1         3.9         2.1
    100    2.1         3.9         2.1
/

=============================================
INCLUDE
   'Include/E100_SPECROCK.INC' /

SPECROCK
-- Rock specific heat,
-- T [C]   Cp [kJ/Rm3 C]
     0     2.35E3
   100     2.35E3
/
     0     2.35E3
   100     2.35E3
/
     0     2.35E3
   100     2.35E3
/
     0     2.35E3
   100     2.35E3
/

=============================================
INCLUDE
   'Include/ECL_ROCK_COMPRESS.INC' /

ROCK
      277.0     4.84E-5 /

=============================================
INCLUDE
   'include/ECL_SF_KROW_H_-_ZERO_CAP_PRES' /

SWOF
-- Table: 1
         0.25              0              1              0
    0.2667422       3.906e-07         0.9152              0
    0.2819575    5.242197e-06       0.8425649             0
    0.3002265       3.164e-05         0.7612              0
    0.3236969       0.0001464         0.6651              0
    0.3391446    0.0003142114        0.606611             0
    0.3671952       0.0009379            0.51             0
    0.3839374          0.0016         0.4579              0
    0.4018531         0.00264         0.4067              0
    0.4208641        0.004228         0.3569              0
    0.4408921        0.006598         0.3091              0
    0.4621719         0.01006         0.2638              0
```

```
    0.4844687         0.01501          0.2214               0
     0.507939         0.02197          0.1824               0
    0.5325047         0.03161          0.1471               0
    0.5581656         0.04477          0.1157               0
        0.585          0.0625         0.08839               0
    0.6117562         0.08503         0.06602               0
    0.6374953          0.1119         0.04868               0
     0.662061          0.1431         0.03541               0
    0.6854531          0.1785         0.02537               0
    0.7078281           0.218         0.01787               0
    0.7290297          0.2614         0.01236               0
    0.7491359          0.3081        0.008373               0
    0.7681469          0.3577        0.005544               0
    0.7859844          0.4096        0.003578               0
    0.8027265          0.4633        0.002242               0
    0.8183734          0.5179        0.001359               0
    0.8463031          0.6274       0.0004414               0
    0.8697735          0.7321       0.0001155               0
    0.8887062            0.826        2.195e-05               0
    0.9038872       0.9071913     2.130945e-06               0
         0.92               1                0               0
    0.9359248               1                0               0
    0.9519436               1                0               0
    0.9679624               1                0               0
    0.9839812               1                0               0
            1               1                0               0
/
--SWOF
-- Table: 2
          0.2               0                1               0
    0.2179916       3.906e-07           0.9152               0
    0.2335451       4.743e-06            0.846               0
    0.2539748       3.164e-05           0.7612               0
    0.2791966       0.0001464           0.6651               0
    0.2950876    0.0003049581        0.6090239               0
    0.3109782    0.0005649915         0.556619               0
    0.3279795      0.00100124        0.5038887               0
    0.3439327          0.0016           0.4579               0
    0.3631854         0.00264           0.4067               0
    0.3836151        0.004228           0.3569               0
    0.4051378        0.006598           0.3091               0
    0.4280056         0.01006           0.2638               0
    0.4519664         0.01501           0.2214               0
    0.4771882         0.02197           0.1824               0
    0.5035871         0.03161           0.1471               0
     0.531163         0.04477           0.1157               0
         0.56          0.0625         0.08839               0
    0.5887529         0.08503         0.06602               0
    0.6164129          0.1119         0.04868               0
    0.6428118          0.1431         0.03541               0
    0.6679496          0.1785         0.02537               0
    0.6919944           0.218         0.01787               0
    0.7147781          0.2614         0.01236               0
    0.7363849          0.3081        0.008373               0
    0.7568146          0.3577        0.005544               0
    0.7759832          0.4096        0.003578               0
    0.7939748          0.4633        0.002242               0
    0.8107894          0.5179        0.001359               0
    0.8264269          0.5729       0.0007921               0
    0.8511747        0.669014    0.0002705328               0
    0.8767865          0.7807        5.291e-05               0
    0.8947781          0.8672        8.021e-06               0
    0.9127697          0.9606            1e-07               0
         0.92               1                0               0
         0.94               1                0               0
         0.96               1                0               0
         0.98               1                0               0
            1               1                0               0
```

```
/
--SWOF
-- Table: 3
        0.175               0               1               0
    0.1936163       3.906e-07          0.9152               0
    0.2097098       4.743e-06           0.846               0
    0.2308489       3.164e-05          0.7612               0
    0.2569465       0.0001464          0.6651               0
    0.2730591    0.0003008377       0.6101115               0
    0.2894463     0.000557336       0.5578134               0
    0.3053141       0.0009379            0.51               0
    0.3239304          0.0016          0.4579               0
    0.3438516         0.00264          0.4067               0
    0.3649907        0.004228          0.3569               0
    0.3872606        0.006598          0.3091               0
    0.4109225         0.01006          0.2638               0
    0.4357152         0.01501          0.2214               0
    0.4618128         0.02197          0.1824               0
    0.4891283         0.03161          0.1471               0
    0.5176617         0.04477          0.1157               0
       0.5475          0.0625         0.08839               0
    0.5772513         0.08503         0.06602               0
    0.6058717          0.1119         0.04868               0
    0.6331872          0.1431         0.03541               0
    0.6591978          0.1785         0.02537               0
    0.6840775           0.218         0.01787               0
    0.7076524          0.2614         0.01236               0
    0.7300093          0.3081        0.008373               0
    0.7511484          0.3577        0.005544               0
    0.7709826          0.4096        0.003578               0
    0.7895989          0.4633        0.002242               0
    0.8069973          0.5179        0.001359               0
    0.8231778          0.5729       0.0007921               0
    0.8465239       0.6600816     0.000301417               0
    0.8641511          0.7321       0.0001155               0
    0.8842322       0.8214894     2.42734e-05               0
    0.9013837          0.9037       2.471e-06               0
    0.9169185       0.9835284    3.765076e-09               0
         0.92               1               0               0
         0.94               1               0               0
         0.96               1               0               0
         0.98               1               0               0
            1               1               0               0
/
--SWOF
-- Table: 4
         0.15               0               1               0
     0.169241       3.906e-07          0.9152               0
    0.1858746       4.743e-06           0.846               0
     0.207723       3.164e-05          0.7612               0
    0.2346964       0.0001464          0.6651               0
    0.2500712       0.0002856          0.6142               0
    0.2667947       0.0005291          0.5623               0
    0.2846871       0.0009379            0.51               0
    0.3039281          0.0016          0.4579               0
    0.3245177         0.00264          0.4067               0
    0.3463662        0.004228          0.3569               0
    0.3693835        0.006598          0.3091               0
    0.3938393         0.01006          0.2638               0
     0.419464         0.01501          0.2214               0
    0.4464374         0.02197          0.1824               0
    0.4746695         0.03161          0.1471               0
    0.5041604         0.04477          0.1157               0
    0.5195802      0.05308287        0.101395               0
        0.535          0.0625         0.08839               0
    0.5503748      0.07312416      0.07662967               0
    0.5657496         0.08503         0.06602               0
    0.5953305          0.1119         0.04868               0
```

```
    0.6235626          0.1431         0.03541              0
    0.6504461          0.1785         0.02537              0
    0.6761607           0.218         0.01787              0
    0.7005266          0.2614         0.01236              0
    0.7236338          0.3081        0.008373              0
    0.7454823          0.3577        0.005544              0
     0.765982          0.4096        0.003578              0
     0.785223          0.4633        0.002242              0
    0.8032053          0.5179        0.001359              0
    0.8199288          0.5729       0.0007921              0
    0.8353036          0.6274       0.0004414              0
    0.8561245       0.7071455    0.0001644183              0
    0.8737856          0.7807       5.291e-05              0
    0.8910722       0.8581345    1.030654e-05              0
    0.9071427           0.935       5.977e-07              0
         0.92               1               0              0
         0.94               1               0              0
         0.96               1               0              0
         0.98               1               0              0
            1               1               0              0
/


SGOF
-- Table: 1
            0               0               1              0
   0.02409922               0               1              0
         0.03               0               1              0
    0.0459961        0.003953          0.9701              0
   0.06362195      0.01203753       0.9373191              0
   0.08450795      0.02484911       0.8986801              0
    0.1003828         0.03648          0.8695              0
    0.1240307      0.05631869       0.8264064              0
    0.1393738      0.07067282       0.7985977              0
    0.1558417      0.08722121       0.7689159              0
    0.1734341       0.1060926        0.737492              0
    0.1920708       0.1275138       0.7043255              0
    0.2119125       0.1514494       0.6695131              0
    0.2326433          0.1782          0.6332              0
    0.2540234          0.2071          0.5963              0
    0.2764179          0.2389           0.558              0
    0.2998269          0.2738          0.5183              0
    0.3244062           0.312          0.4774              0
         0.35          0.3536          0.4353              0
    0.3755938          0.3968          0.3938              0
    0.4000951          0.4398          0.3548              0
    0.4235821          0.4823          0.3181              0
    0.4459766           0.524          0.2837              0
    0.4673567          0.5649          0.2516              0
    0.4875664          0.6046          0.2217              0
    0.5067618           0.643           0.194              0
    0.5249427          0.6801          0.1684              0
    0.5420312          0.7155           0.145              0
    0.5580273          0.7493          0.1235              0
    0.5830406       0.8032751      0.09116465              0
    0.5996172          0.8396         0.07074              0
    0.6220117          0.8896         0.04468              0
    0.6401146          0.9308         0.02528              0
    0.6593099          0.9751        0.007349              0
         0.67               1               0              0
        0.686               1               0              0
        0.702               1               0              0
        0.718               1               0              0
        0.734               1               0              0
         0.75               1               0              0
/
--SGOF
```

```
-- Table: 2
           0              0              1              0
  0.02570584              0              1              0
        0.03              0              1              0
  0.04724579       0.003953         0.9701              0
  0.06786342      0.01285505      0.9345097              0
  0.09014181      0.02572386      0.8963294              0
   0.1058815         0.03648         0.8695              0
   0.1322994      0.05708867      0.8248559              0
   0.1486654      0.07134625      0.7973449              0
   0.1662311      0.08775943      0.7679868              0
   0.1849964       0.1064597      0.7369029              0
   0.2048755       0.1276702       0.704091              0
     0.22604       0.1513517      0.6696503              0
   0.2482327       0.1779034      0.6335904              0
   0.2715252          0.2071         0.5963              0
   0.2956693          0.2389          0.558              0
   0.3209071          0.2738         0.5183              0
   0.3474067           0.312         0.4774              0
       0.375          0.3536         0.4353              0
   0.4025933          0.3968         0.3938              0
   0.4290088          0.4398         0.3548              0
   0.4543307          0.4823         0.3181              0
   0.4784748           0.524         0.2837              0
   0.5015252          0.5649         0.2516              0
   0.5233138          0.6046         0.2217              0
   0.5440088           0.643          0.194              0
   0.5636101          0.6801         0.1684              0
   0.5820337          0.7155          0.145              0
   0.5992794          0.7493         0.1235              0
   0.6153475          0.7814          0.104              0
   0.6371621       0.8253815      0.0785948              0
   0.6567374          0.8657        0.05684              0
   0.6758065       0.9054777     0.03698083              0
   0.6956857       0.9476374     0.01805124              0
   0.7109378        0.980367    0.005512172              0
        0.72               1              0              0
       0.736               1              0              0
       0.752               1              0              0
       0.768               1              0              0
       0.784               1              0              0
         0.8               1              0              0
/
--SGOF
-- Table: 3
           0              0              1              0
  0.02650915              0              1              0
        0.03              0              1              0
  0.04787064       0.003953         0.9701              0
  0.06338759        0.01008         0.9443              0
   0.0808529      0.01897694      0.9152476              0
   0.1062133      0.03480687       0.873468              0
   0.1229273         0.04687         0.8461              0
   0.1384443         0.05907         0.8209              0
   0.1550945         0.07321         0.7939              0
   0.1714258      0.08800067      0.7675711              0
   0.1907775       0.1066242      0.7366393              0
   0.2112779       0.1277402      0.7039861              0
   0.2331038       0.1513081      0.6697116              0
     0.25599       0.1777263      0.6338235              0
   0.2802017       0.2070076      0.5964145              0
    0.305295          0.2389          0.558              0
   0.3314472          0.2738         0.5183              0
    0.358907           0.312         0.4774              0
      0.3875          0.3536         0.4353              0
    0.416093          0.3968         0.3938              0
   0.4434656          0.4398         0.3548              0
    0.469705          0.4823         0.3181              0
```

```
    0.4947238           0.524          0.2837               0
    0.5186095          0.5649          0.2516               0
    0.5411875          0.6046          0.2217               0
    0.5626323           0.643           0.194               0
    0.5829438          0.6801          0.1684               0
    0.6020349          0.7155           0.145               0
    0.6199055          0.7493          0.1235               0
    0.6365557          0.7814           0.104               0
    0.6520727          0.8115         0.08644               0
    0.6715651         0.849939      0.06515567               0
    0.6913881           0.8896         0.04468               0
    0.7077942        0.9229912      0.02879932               0
    0.7259088        0.9601751      0.01293809               0
    0.7414259           0.9925        0.001733               0
        0.745                1               0               0
        0.765                1               0               0
        0.785                1               0               0
        0.805                1               0               0
        0.825                1               0               0
/
--SGOF
-- Table: 4
            0                0               1               0
   0.02731245                0               1               0
         0.03                0               1               0
   0.04597597      0.003169627       0.9741698               0
   0.06218135      0.009059812       0.9480898               0
   0.08330299         0.019341        0.914178               0
    0.1094319       0.03517504       0.8725894               0
    0.1261765          0.04687          0.8461               0
     0.142236          0.05907          0.8209               0
     0.157957       0.07193032       0.7962618               0
    0.1766205       0.08822581       0.7671836               0
    0.1965586        0.1067777       0.7363934               0
    0.2176803        0.1278055       0.7038882               0
    0.2401675        0.1512673       0.6697689               0
    0.2637473        0.1775613       0.6340409               0
    0.2886926        0.2066993       0.5967969               0
    0.3148216        0.2387752       0.5581461               0
    0.3419873           0.2738          0.5183               0
    0.3704072            0.312          0.4774               0
          0.4           0.3536          0.4353               0
    0.4295928           0.3968          0.3938               0
    0.4579225           0.4398          0.3548               0
    0.4850792           0.4823          0.3181               0
    0.5109729            0.524          0.2837               0
    0.5356937           0.5649          0.2516               0
    0.5590612           0.6046          0.2217               0
    0.5812558            0.643           0.194               0
    0.6022775           0.6801          0.1684               0
    0.6220361           0.7155           0.145               0
    0.6405316           0.7493          0.1235               0
     0.657764           0.7814           0.104               0
    0.6738235           0.8115         0.08644               0
    0.6919155        0.8459266      0.06730985               0
    0.7145135           0.8896         0.04468               0
     0.735445           0.9308         0.02528               0
    0.7515045           0.9627         0.01195               0
    0.7665696        0.9930497     0.001581772               0
         0.77                1               0               0
         0.79                1               0               0
         0.81                1               0               0
         0.83                1               0               0
         0.85                1               0               0
/
=========================================
```

```
INCLUDE
   'Include/ECLIPSE_SATNUM_001.GRDECL' /

SATNUM
96*1
320*3
128*4
/
=========================================
INCLUDE
   'Include/E100_EQUIL.INC' /

EQUIL
-- Datum    P     woc     Pc   goc    Pc Rsvd Rvvd
1900.0  270.0  2500   0.0  1900.0  0.0 1 /

=========================================
INCLUDE
   'include/ECL_TEMPVD.INC' /

-- Reservoir temperature - vertical depth
RTEMPVD
1800  90.78
1900  93.36
2300 103.69
2400 106.28
/
=========================================
INCLUDE
   'Include/ECL_TEMP_REPORT_SMRY.INC' /
WTPCHEA
/
WTICHEA
/

INCLUDE
   'Include/ECL_PLY_REPORT_SMRY.INC' /
WCPR
/
WCPC
/
WCPT
/
WCIR
/
WCIC
/
WCIT
/
--=========================================
INCLUDE
   'Include/ECL_GENERAL_REPORT_SMRY.INC' /
FLPR

WLPR
/

ALL

PERFORMA

EXCEL
=========================================
```

```
INCLUDE
   'Include/ECL_G_2D_BLOCK_REPORT_SMRY_001.INC' /

BVOIL
  1   1  17 /
  8   1  17 /
 16   1  17 /
 24   1  17 /
 32   1  17 /
/

BVWAT
  1   1  17 /
  8   1  17 /
 16   1  17 /
 24   1  17 /
 32   1  17 /
/

BDENO
  1   1  17 /
  8   1  17 /
 16   1  17 /
 24   1  17 /
 32   1  17 /
/

BDENW
  1   1  17 /
  8   1  17 /
 16   1  17 /
 24   1  17 /
 32   1  17 /
/

BSWAT
  1   1  17 /
  8   1  17 /
 16   1  17 /
 24   1  17 /
 32   1  17 /
/

BPR
  1   1  17 /
  8   1  17 /
 16   1  17 /
 24   1  17 /
 32   1  17 /
/
==========================================
INCLUDE
   'Include/ECL_G_2D_BLOCK_REPORT_TEMP_001.INC' /

BTCNFHEA
  1   1  17 /
  8   1  17 /
 16   1  17 /
 24   1  17 /
 32   1  17 /
/
==========================================
INCLUDE
   'Include/ECL_G_2D_BLOCK_REPORT_TRACER_001.INC' /
```

```
BTCNFTR1
  1   1  17 /
  8   1  17 /
 16   1  17 /
 24   1  17 /
 32   1  17 /

  1   1  16 /
  8   1  16 /
 16   1  16 /
 24   1  16 /
 32   1  16 /

  1   1  15 /
  8   1  15 /
 16   1  15 /
 24   1  15 /
 32   1  15 /

  1   1  14 /
  8   1  14 /
 16   1  14 /
 24   1  14 /
 32   1  14 /

  1   1  13 /
  8   1  13 /
 16   1  13 /
 24   1  13 /
 32   1  13 /

  1   1  12 /
  8   1  12 /
 16   1  12 /
 24   1  12 /
 32   1  12 /
/

BTCNSTR1
  1   1  17 /
  8   1  17 /
 16   1  17 /
 24   1  17 /
 32   1  17 /

  1   1  16 /
  8   1  16 /
 16   1  16 /
 24   1  16 /
 32   1  16 /

  1   1  15 /
  8   1  15 /
 16   1  15 /
 24   1  15 /
 32   1  15 /

  1   1  14 /
  8   1  14 /
 16   1  14 /
 24   1  14 /
 32   1  14 /

  1   1  13 /
  8   1  13 /
 16   1  13 /
 24   1  13 /
 32   1  13 /
```

```
  1   1  12 /
  8   1  12 /
 16   1  12 /
 24   1  12 /
 32   1  12 /
/

BTIPTTR1
  1   1  17 /
  8   1  17 /
 16   1  17 /
 24   1  17 /
 32   1  17 /

  1   1  16 /
  8   1  16 /
 16   1  16 /
 24   1  16 /
 32   1  16 /

  1   1  15 /
  8   1  15 /
 16   1  15 /
 24   1  15 /
 32   1  15 /

  1   1  14 /
  8   1  14 /
 16   1  14 /
 24   1  14 /
 32   1  14 /

  1   1  13 /
  8   1  13 /
 16   1  13 /
 24   1  13 /
 32   1  13 /

  1   1  12 /
  8   1  12 /
 16   1  12 /
 24   1  12 /
 32   1  12 /
/

BTCNFTR2
  1   1  17 /
  8   1  17 /
 16   1  17 /
 24   1  17 /
 32   1  17 /

  1   1  16 /
  8   1  16 /
 16   1  16 /
 24   1  16 /
 32   1  16 /

  1   1  15 /
  8   1  15 /
 16   1  15 /
 24   1  15 /
 32   1  15 /

  1   1  14 /
  8   1  14 /
 16   1  14 /
```

```
 24   1  14 /
 32   1  14 /

  1   1  13 /
  8   1  13 /
 16   1  13 /
 24   1  13 /
 32   1  13 /

  1   1  12 /
  8   1  12 /
 16   1  12 /
 24   1  12 /
 32   1  12 /
/

BTCNSTR2
  1   1  17 /
  8   1  17 /
 16   1  17 /
 24   1  17 /
 32   1  17 /

  1   1  16 /
  8   1  16 /
 16   1  16 /
 24   1  16 /
 32   1  16 /

  1   1  15 /
  8   1  15 /
 16   1  15 /
 24   1  15 /
 32   1  15 /

  1   1  14 /
  8   1  14 /
 16   1  14 /
 24   1  14 /
 32   1  14 /

  1   1  13 /
  8   1  13 /
 16   1  13 /
 24   1  13 /
 32   1  13 /

  1   1  12 /
  8   1  12 /
 16   1  12 /
 24   1  12 /
 32   1  12 /
/

BTIPTTR2
  1   1  17 /
  8   1  17 /
 16   1  17 /
 24   1  17 /
 32   1  17 /

  1   1  16 /
  8   1  16 /
 16   1  16 /
 24   1  16 /
 32   1  16 /

  1   1  15 /
```

```
  8   1  15 /
 16   1  15 /
 24   1  15 /
 32   1  15 /

  1   1  14 /
  8   1  14 /
 16   1  14 /
 24   1  14 /
 32   1  14 /

  1   1  13 /
  8   1  13 /
 16   1  13 /
 24   1  13 /
 32   1  13 /

  1   1  12 /
  8   1  12 /
 16   1  12 /
 24   1  12 /
 32   1  12 /
/

-- Tracer Data INJ
FTPRTR1
FTPTTR1
FTPCTR1
FTIRTR1
FTITTR1
FTICTR1

WTPRTR1
/
WTPTTR1
/
WTPCTR1
/
WTIRTR1
/
WTITTR1
/
WTICTR1
/

FTPRTR2
FTPTTR2
FTPCTR2
FTIRTR2
FTITTR2
FTICTR2

WTPRTR2
/
WTPTTR2
/
WTPCTR2
/
WTIRTR2
/
WTITTR2
/
WTICTR2
/
==========================================
```

```
INCLUDE
   'Include/ECL_G_2D_BLOCK_REPORT_PLY_001.INC' /

BCCN
  1   1  17 /
  8   1  17 /
 16   1  17 /
 24   1  17 /
 32   1  17 /
/


BRK
  1   1  17 /
  8   1  17 /
 16   1  17 /
 24   1  17 /
 32   1  17 /
/

BCAD
  1   1  17 /
  8   1  17 /
 16   1  17 /
 24   1  17 /
 32   1  17 /
/
============================================
INCLUDE
   'Include/E100_TUNING.INC' /

TUNING
0.5 30.0 1* 0.0001 4*/
9* /
2* 80 3*/

============================================
INCLUDE
   'Include/ECLIPSE_TEMP30_001_PLY.SCH' /
WELSPECS
 'P1' GROUP 32 1    1885.0 'OIL'   7*/
 'I1' GROUP 1  1    1885.0 'WATER' 7*/
/

COMPDAT
 'P1' 2* 4 17 3*   0.2 /
 'I1' 2* 4 17 3*   0.2 /
/

WCONPROD
        'P1' OPEN LRAT 3* 125 1* 120 /
/

WCONINJE
        'I1' WATER OPEN BHP 12000 1* 370 /
/

SKIP300
--E100
WTEMP
    'I1'     30.000 /
/
ENDSKIP
```

```
RPTRST
 BASIC=3 FREQ=3 /


DATES
1 'FEB' 2000 /
/

WTRACER
  'I1' TR1   1.0 /
/

DATES
2 'FEB' 2000 /
/

WTRACER
  'I1' TR1   0.0 /
/

DATES
1 'MAR' 2000 /
/

DATES
1 'APR' 2000 /
/

DATES
1 'MAY' 2000 /
/

DATES
1 'JUN' 2000 /
/

DATES
1 'JLY' 2000 /
/

DATES
1 'AUG' 2000 /
/

DATES
1 'SEP' 2000 /
/

DATES
1 'OCT' 2000 /
/

DATES
1 'NOV' 2000 /
/

DATES
1 'DEC' 2000 /
/


DATES
1 'JAN' 2001 /
/

DATES
1 'FEB' 2001 /
/
```

```
DATES
1 'MAR' 2001 /
/

DATES
1 'APR' 2001 /
/

DATES
1 'MAY' 2001 /
/

DATES
1 'JUN' 2001 /
/

DATES
1 'JLY' 2001 /
/

DATES
1 'AUG' 2001 /
/

DATES
1 'SEP' 2001 /
/

DATES
1 'OCT' 2001 /
/

DATES
1 'NOV' 2001 /
/

DATES
1 'DEC' 2001 /
/

DATES
1 'JAN' 2002 /
/

DATES
1 'FEB' 2002 /
/

DATES
1 'MAR' 2002 /
/

DATES
1 'APR' 2002 /
/

DATES
1 'MAY' 2002 /
/

DATES
1 'JUN' 2002 /
/

DATES
1 'JLY' 2002 /
/
```

```
DATES
1 'AUG' 2002 /
/

DATES
1 'SEP' 2002 /
/

DATES
1 'OCT' 2002 /
/

DATES
1 'NOV' 2002 /
/

DATES
1 'DEC' 2002 /
/

DATES
1 'JAN' 2003 /
/

DATES
1 'FEB' 2003 /
/

DATES
1 'MAR' 2003 /
/

DATES
1 'APR' 2003 /
/

DATES
1 'MAY' 2003 /
/

DATES
1 'JUN' 2003 /
/

DATES
1 'JLY' 2003 /
/

DATES
1 'AUG' 2003 /
/

DATES
1 'SEP' 2003 /
/

DATES
1 'OCT' 2003 /
/

DATES
1 'NOV' 2003 /
/

DATES
1 'DEC' 2003 /
/
```

```
DATES
1 'JAN' 2004 /
/

DATES
1 'FEB' 2004 /
/

DATES
1 'MAR' 2004 /
/

DATES
1 'APR' 2004 /
/

DATES
1 'MAY' 2004 /
/

DATES
1 'JUN' 2004 /
/

DATES
1 'JLY' 2004 /
/

DATES
1 'AUG' 2004 /
/

DATES
1 'SEP' 2004 /
/

DATES
1 'OCT' 2004 /
/

DATES
1 'NOV' 2004 /
/

DATES
1 'DEC' 2004 /
/

DATES
1 'JAN' 2005 /
/

DATES
1 'FEB' 2005 /
/

DATES
1 'MAR' 2005 /
/

DATES
1 'APR' 2005 /
/

DATES
1 'MAY' 2005 /
```

```
/

DATES
1 'JUN' 2005 /
/

DATES
2 'JUN' 2005 /
/


DATES
1 'JLY' 2005 /
/

DATES
1 'AUG' 2005 /
/

DATES
1 'SEP' 2005 /
/

DATES
1 'OCT' 2005 /
/

DATES
1 'NOV' 2005 /
/

DATES
1 'DEC' 2005 /
/

DATES
1 'JAN' 2006 /
/

DATES
1 'FEB' 2006 /
/

DATES
1 'MAR' 2006 /
/

DATES
1 'APR' 2006 /
/

DATES
1 'MAY' 2006 /
/

DATES
1 'JUN' 2006 /
/

DATES
1 'JLY' 2006 /
/


DATES
1 'AUG' 2006 /
/
```

```
DATES
1 'SEP' 2006 /
/

DATES
1 'OCT' 2006 /
/

DATES
1 'NOV' 2006 /
/

DATES
1 'DEC' 2006 /
/

DATES
1 'JAN' 2007 /
/

DATES
1 'FEB' 2007 /
/

DATES
1 'MAR' 2007 /
/

DATES
1 'APR' 2007 /
/

DATES
1 'MAY' 2007 /
/

DATES
1 'JUN' 2007 /
/

DATES
1 'JLY' 2007 /
/

DATES
1 'AUG' 2007 /
/

DATES
1 'SEP' 2007 /
/

DATES
1 'OCT' 2007 /
/

DATES
1 'NOV' 2007 /
/

DATES
1 'DEC' 2007 /
/

DATES
1 'JAN' 2008 /
/
```

```
DATES
1 'FEB' 2008 /
/

DATES
1 'MAR' 2008 /
/

DATES
1 'APR' 2008 /
/

DATES
1 'MAY' 2008 /
/

DATES
1 'JUN' 2008 /
/

DATES
1 'JLY' 2008 /
/

DATES
1 'AUG' 2008 /
/

DATES
1 'SEP' 2008 /
/

DATES
1 'OCT' 2008 /
/

DATES
1 'NOV' 2008 /
/

DATES
1 'DEC' 2008 /
/


DATES
1 'JAN' 2009 /
/

DATES
1 'FEB' 2009 /
/

DATES
1 'MAR' 2009 /
/

DATES
1 'APR' 2009 /
/

DATES
1 'MAY' 2009 /
/

DATES
1 'JUN' 2009 /
/
```

```
DATES
1 'JLY' 2009 /
/

DATES
1 'AUG' 2009 /
/

DATES
1 'SEP' 2009 /
/

DATES
1 'OCT' 2009 /
/

DATES
1 'NOV' 2009 /
/

DATES
1 'DEC' 2009 /
/

DATES
1 'JAN' 2010 /
/

DATES
1 'FEB' 2010 /
/

DATES
1 'MAR' 2010 /
/

DATES
1 'APR' 2010 /
/

DATES
1 'MAY' 2010 /
/

DATES
1 'JUN' 2010 /
/

DATES
1 'JLY' 2010 /
/

WPOLYMER
    'I1’ 40.0 0.0   /
/

DATES
 7 'JUL' 2010 /
/

DATES
 14 'JUL' 2010 /
/

DATES
 21 'JUL' 2010 /
/
```

```
DATES
 28 'JUL' 2010 /
/

DATES
 1 'AUG' 2010 /
/

DATES
 7 'AUG' 2010 /
/

DATES
 14 'AUG' 2010 /
/
DATES
 21 'AUG' 2010 /
/

DATES
 28 'AUG' 2010 /
/

DATES
 1 'SEP' 2010 /
/

WPOLYMER
    'I1' 0.0 0.0   /
/

DATES
1 'OCT' 2010 /
/

DATES
1 'NOV' 2010 /
/

DATES
1 'DEC' 2010 /
/

DATES
1 'JAN' 2011 /
/

DATES
1 'FEB' 2011 /
/

DATES
1 'MAR' 2011 /
/

DATES
1 'APR' 2011 /
/

DATES
1 'MAY' 2011 /
/

DATES
1 'JUN' 2011 /
/
```

```
WTRACER
  'I1' TR2   1.0 /
/

DATES
2 'JUN' 2011 /
/

WTRACER
  'I1' TR2   0.0 /
/


DATES
1 'JLY' 2011 /
/

DATES
1 'AUG' 2011 /
/

DATES
1 'SEP' 2011 /
/

DATES
1 'OCT' 2011 /
/

DATES
1 'NOV' 2011 /
/

DATES
1 'DEC' 2011 /
/

DATES
1 'JAN' 2012 /
/

DATES
1 'FEB' 2012 /
/

DATES
1 'MAR' 2012 /
/

DATES
1 'APR' 2012 /
/

DATES
1 'MAY' 2012 /
/

DATES
1 'JUN' 2012 /
/

DATES
1 'JLY' 2012 /
/

DATES
1 'AUG' 2012 /
/
```

```
DATES
1 'SEP' 2012 /
/

DATES
1 'OCT' 2012 /
/

DATES
1 'NOV' 2012 /
/

DATES
1 'DEC' 2012 /
/

DATES
1 'JAN' 2013 /
/

DATES
1 'FEB' 2013 /
/

DATES
1 'MAR' 2013 /
/

DATES
1 'APR' 2013 /
/

DATES
1 'MAY' 2013 /
/

DATES
1 'JUN' 2013 /
/

DATES
1 'JLY' 2013 /
/

DATES
1 'AUG' 2013 /
/

DATES
1 'SEP' 2013 /
/

DATES
1 'OCT' 2013 /
/

DATES
1 'NOV' 2013 /
/

DATES
1 'DEC' 2013 /
/

DATES
1 'JAN' 2014 /
/
```

```
DATES
1 'FEB' 2014 /
/

DATES
1 'MAR' 2014 /
/

DATES
1 'APR' 2014 /
/

DATES
1 'MAY' 2014 /
/

DATES
1 'JUN' 2014 /
/

DATES
1 'JLY' 2014 /
/

DATES
1 'AUG' 2014 /
/

DATES
1 'SEP' 2014 /
/

DATES
1 'OCT' 2014 /
/

DATES
1 'NOV' 2014 /
/

DATES
1 'DEC' 2014 /
/


DATES
1 'JAN' 2015 /
/

DATES
1 'FEB' 2015 /
/

DATES
1 'MAR' 2015 /
/

DATES
1 'APR' 2015 /
/

DATES
1 'MAY' 2015 /
/

DATES
1 'JUN' 2015 /
```

```
/

DATES
1 'JLY' 2015 /
/

DATES
1 'AUG' 2015 /
/

DATES
1 'SEP' 2015 /
/

DATES
1 'OCT' 2015 /
/

DATES
1 'NOV' 2015 /
/

DATES
1 'DEC' 2015 /
/

DATES
1 'JAN' 2016 /
/

DATES
1 'FEB' 2016 /
/

DATES
1 'MAR' 2016 /
/

DATES
1 'APR' 2016 /
/

DATES
1 'MAY' 2016 /
/

DATES
1 'JUN' 2016 /
/

DATES
1 'JLY' 2016 /
/

DATES
1 'AUG' 2016 /
/

DATES
1 'SEP' 2016 /
/

DATES
1 'OCT' 2016 /
/

DATES
1 'NOV' 2016 /
```

```
/

DATES
1 'DEC' 2016 /
/

DATES
1 'JAN' 2017 /
/

DATES
1 'FEB' 2017 /
/

DATES
1 'MAR' 2017 /
/

DATES
1 'APR' 2017 /
/

DATES
1 'MAY' 2017 /
/

DATES
1 'JUN' 2017 /
/

DATES
1 'JLY' 2017 /
/

DATES
1 'AUG' 2017 /
/

DATES
1 'SEP' 2017 /
/

DATES
1 'OCT' 2017 /
/

DATES
1 'NOV' 2017 /
/

DATES
1 'DEC' 2017 /
/

DATES
1 'JAN' 2018 /
/

DATES
1 'FEB' 2018 /
/

DATES
1 'MAR' 2018 /
/

DATES
1 'APR' 2018 /
```

```
/

DATES
1 'MAY' 2018 /
/

DATES
1 'JUN' 2018 /
/

DATES
1 'JLY' 2018 /
/

DATES
1 'AUG' 2018 /
/

DATES
1 'SEP' 2018 /
/

DATES
1 'OCT' 2018 /
/

DATES
1 'NOV' 2018 /
/

DATES
1 'DEC' 2018 /
/


DATES
1 'JAN' 2019 /
/

DATES
1 'FEB' 2019 /
/

DATES
1 'MAR' 2019 /
/

DATES
1 'APR' 2019 /
/

DATES
1 'MAY' 2019 /
/

DATES
1 'JUN' 2019 /
/

DATES
1 'JLY' 2019 /
/

DATES
1 'AUG' 2019 /
/

DATES
```

```
1 'SEP' 2019 /
/

DATES
1 'OCT' 2019 /
/

DATES
1 'NOV' 2019 /
/

DATES
1 'DEC' 2019 /
/

DATES
1 'JAN' 2020 /
/

DATES
1 'FEB' 2020 /
/

DATES
1 'MAR' 2020 /
/

DATES
1 'APR' 2020 /
/

DATES
1 'MAY' 2020 /
/

DATES
1 'JUN' 2020 /
/

DATES
1 'JLY' 2020 /
/

DATES
1 'AUG' 2020 /
/

DATES
1 'SEP' 2020 /
/

DATES
1 'OCT' 2020 /
/

DATES
1 'NOV' 2020 /
/

DATES
1 'DEC' 2020 /
/


END
```

A3 ECLIPSE 3D Grid Model Data File with Polymer Options

```
---------------------------------------------------------------------------

-- Syntetisk modell for uttesting av grid metoder. Pillar grid
-------------------------------------
RUNSPEC

TITLE
 STAIR1

DIMENS
 48 48 18 /

--NOSIM

--
-- Allow for multregt, etc. Maximum number of regions 20.
--
GRIDOPTS
 'YES' 0 /

--BLACKOIL

-- Phases
OIL
WATER
GAS

DISGAS

POLYMER

TEMP

VFPPDIMS
 19  10  8  10  0  9 /

METRIC

START
 01 'JAN' 2000 /

EQLDIMS
 1 /

REGDIMS
-- Ntfip
    1 /

TABDIMS
--ntsfun ntpvt nssfun nppvt ntfip nrpvt ntendp
    4     1     55     60   16    60 /

WELLDIMS
-- NWMAXZ NCWMAX NGMAXZ NWGMAX
 10 10 5 10 /

NSTACK
 80 /

UNIFOUT


RPTRUNSP

OPTIONS
```

```
 /

-- Changing this for making the simulation go through. Should not do this.
MESSAGES
 8* 1000000 10000 1 /

------------------------------------------------------------
--
--     Input of grid geometry
--
------------------------------------------------------------
GRID
-- Generate init file

NEWTRAN

-- Produce Extensive grid files .GRID and .EGRID
GRIDFILE
  2  0 /

-- Optional for post-processing of GRID

GRIDUNIT
METRES /

-- requests output of INIT file
INIT

MESSAGES
 /

NOECHO

------------------------------------------------------------
--
--     Grid and faults
--
------------------------------------------------------------

--
-- Simulation grid, fault traces and transmissibilities and NNC
--
INCLUDE
   'Include/ECL_HOM_ABX_G1.coord.inc' /

INCLUDE
   'Include/ECL_HOM_ABX_G1.zcorn.inc' /

INCLUDE
   'Include/ECL_HOM_ABX_G1.actnum_overunder.inc' /

------------------------------------------------------------
--
--     Input of grid parameters
--
------------------------------------------------------------

-- Temp
-- Rock thermal conductivity
--     kJ/ (m day C)
EQUALS
 'THCONR' 270.0 /
/

INCLUDE
   'Include/ECL_THIEFZONE_ABX_G1.poro.inc' /

INCLUDE
```

```
   'Include/ECL_THIEFZONE_ABX_G1.permx.inc' /


COPY
 'PERMX'  'PERMY' /
 'PERMX'  'PERMZ' /
/

MULTIPLY
 'PERMZ' 0.1 /
/

NOECHO

-----------------------------------------------------------------------------
EDIT
-----------------------------------------------------------------------------


-----------------------------------------------------------------------------
PROPS
-----------------------------------------------------------------------------
--
--Input of fluid properties and relative permeability
--
-------------------------------------------------------

NOECHO

INCLUDE
   'Include/ecl100_pvt_snorre_8comp_96C_rescaled.inc' /

INCLUDE
   'Include/E100_VISCT_BLACKOIL.INC' /

INCLUDE
   'Include/E100_SPECHEAT_BLACKOIL.INC' /

-- Different section for E100 and E300
INCLUDE
   'Include/E100_SPECROCK.INC' /

INCLUDE
   'Include/ECL_ROCK_COMPRESS.INC' /

-- Rel. perm and cap. Pressure tables --
INCLUDE
   'include/ECL_SF_KROW_H_-_ZERO_CAP_PRES'   /

RPTPROPS
 1 1 1 5*0 0 /

----------------------------------------
-- Polymer (silicate) section

PLMIXPAR
1.0 / -- Chemical completely mixed with water

PLYMAX
40.0 0.0500 /

PLYVISC
-- cons   water visc factor
  0.0000      1.0
 40.0000      1.00001 /

PLYADS
-- cons    abs.cons
```

```
   0.0000   0.00000
   7.01     0.00000000
   8.011    0.0000050
  40.0000   0.0000051 /
   0.0000   0.00000
   7.01     0.00000000
   8.011    0.0000050
  40.0000   0.0000051 /
   0.0000   0.00000
   7.01     0.00000000
   8.011    0.0000050
  40.0000   0.0000051 /
   0.0000   0.00000
   7.01     0.00000000
   8.011    0.0000050
  40.0000   0.0000051 /


PLYROCK
-- Dead phi ; RRF ; dens (res.) ; abs. ind. ; max abs.
     0.0    1.0        1880         2       0.0000050 /
     0.0    1.0        1880         2       0.0000050 /
     0.0    1.0        1880         2       0.0000050 /
     0.0    1.0        1880         2       0.0000050 /

PLYTRRF
-- Temp     RRF
   30.0     1.0
   50.0     1.001
   60.0     1.0015
   69.0     1.002
   70.0   10000.0
  100.0   10000.1 /
   30.0     1.0
   50.0     1.001
   60.0     1.0015
   69.0     1.002
   70.0   10000.0
  100.0   10000.1 /
   30.0     1.0
   50.0     1.001
   60.0     1.0015
   69.0     1.002
   70.0   10000.0
  100.0   10000.1 /
   30.0     1.0
   50.0     1.001
   60.0     1.0015
   69.0     1.002
   70.0   10000.0
  100.0   10000.1 /

-- END Polymer (silicate) section
-----------------------------------------------


-------------------------------------------------------------------------------
REGIONS
-------------------------------------------------------------------------------

INCLUDE
   'Include/ECL_HOM_ABX_G1.fipnum.inc' /

INCLUDE
   'Include/ECL_THIEFZONE_ABX_G1.satnum.inc' /

-------------------------------------------------------------------------------
SOLUTION
```

```
-------------------------------------------------------------------------------
-- Equilibrium data: do not include this file in case of RESTART
--

--Comp PVT
RSVD
  1000.0 96.0
  3000.0 96.0 /

INCLUDE
   'Include/E100_EQUIL.INC' /

RPTRST
 BASIC=2 FREQ=3 /

INCLUDE
   'Include/ECL_TEMPVD.INC' /

-- Make sure the initial restart file is saved.
-- RPTSOL
--     RESTART=2 FIP EQUIL SOIL SWAT /

RPTSOL
 FIP=2 /

-------------------------------------------------------------------------------
SUMMARY
-------------------------------------------------------------------------------

INCLUDE
   'Include/ECL_TEMP_REPORT_SMRY.INC' /

INCLUDE
   'Include/ECL_PLY_REPORT_SMRY.INC' /

INCLUDE
   'Include/ECL_GENERAL_REPORT_SMRY.INC' /

INCLUDE
   'Include/ECL_THIEFZONE_ABX_G1_BLOCK_REPORT_SMRY.INC' /

INCLUDE
   'Include/ECL_THIEFZONE_ABX_G1_BLOCK_REPORT_TEMP_SMRY.INC' /

INCLUDE
   'Include/ECL_THIEFZONE_ABX_G1_BLOCK_REPORT_PLY_SMRY.INC' /

-------------------------------------------------------------------------------
SCHEDULE
-------------------------------------------------------------------------------

INCLUDE
   'Include/E100_TUNING.INC' /

RPTSCHED
 'FIP=2' /

INCLUDE
   'Include/ECL_THIEFZONE_ABX_G1_30_PLY.INC' /

END
```

A4 3D Well Specifications and Schedule

```
INCLUDE
        'include/ECL_THIEFZONE_ABX_G1_30_PLY.INC' /


WELSPECS
 'P1' GROUP  18  8    1* 'OIL'   7*/
 'P2' GROUP  40 22    1* 'OIL'   7*/
 'I3' GROUP  15 39    1* 'WATER' 7*/
/

COMPDAT
 'P1'  2* 5  14  3*   0.2  /
 'P2'  2* 5  14  3*   0.2  /
 'I3'  2* 5  14  3*   0.2  /
/

WCONPROD
        'P1'  OPEN  LRAT 3* 3000 1* 50 /
        'P2'  OPEN  LRAT 3* 3000 1* 50 /
/

WCONINJE
        'I3'  WATER OPEN  BHP  7000 1*  1000 /
/

SKIP300
--E100
WTEMP
    'I3'     30.000 /
/
ENDSKIP

SKIP100
--E300
WINJTEMP
         'I3' 1* 30 370 1* /
/
ENDSKIP


RPTRST
 BASIC=3 FREQ=3 /


DATES
1 'FEB' 2000 /
/

DATES
1 'MAR' 2000 /
/

DATES
1 'APR' 2000 /
/

DATES
1 'MAY' 2000 /
/

DATES
1 'JUN' 2000 /
/

DATES
```

```
1 'JLY' 2000 /
/

DATES
1 'AUG' 2000 /
/

DATES
1 'SEP' 2000 /
/

DATES
1 'OCT' 2000 /
/

DATES
1 'NOV' 2000 /
/

DATES
1 'DEC' 2000 /
/


DATES
1 'JAN' 2001 /
/

DATES
1 'FEB' 2001 /
/

DATES
1 'MAR' 2001 /
/

DATES
1 'APR' 2001 /
/

DATES
1 'MAY' 2001 /
/

DATES
1 'JUN' 2001 /
/

DATES
1 'JLY' 2001 /
/

DATES
1 'AUG' 2001 /
/

DATES
1 'SEP' 2001 /
/

DATES
1 'OCT' 2001 /
/

DATES
1 'NOV' 2001 /
/
```

```
DATES
1 'DEC' 2001 /
/


DATES
1 'JAN' 2002 /
/

DATES
1 'FEB' 2002 /
/

DATES
1 'MAR' 2002 /
/

DATES
1 'APR' 2002 /
/

DATES
1 'MAY' 2002 /
/

DATES
1 'JUN' 2002 /
/

DATES
1 'JLY' 2002 /
/

DATES
1 'AUG' 2002 /
/

DATES
1 'SEP' 2002 /
/

DATES
1 'OCT' 2002 /
/

DATES
1 'NOV' 2002 /
/

DATES
1 'DEC' 2002 /
/


DATES
1 'JAN' 2003 /
/

DATES
1 'FEB' 2003 /
/

DATES
1 'MAR' 2003 /
/

DATES
1 'APR' 2003 /
```

```
/

DATES
1 'MAY' 2003 /
/

DATES
1 'JUN' 2003 /
/

DATES
1 'JLY' 2003 /
/

DATES
 1 'AUG' 2003 /
/

DATES
 1 'SEP' 2003 /
/

DATES
1 'OCT' 2003 /
/

DATES
1 'NOV' 2003 /
/

DATES
1 'DEC' 2003 /
/


DATES
1 'JAN' 2004 /
/

DATES
1 'FEB' 2004 /
/

DATES
1 'MAR' 2004 /
/

DATES
1 'APR' 2004 /
/

DATES
1 'MAY' 2004 /
/

DATES
1 'JUN' 2004 /
/

DATES
1 'JLY' 2004 /
/

DATES
1 'AUG' 2004 /
/

DATES
```

```
1 'SEP' 2004 /
/

DATES
1 'OCT' 2004 /
/

DATES
1 'NOV' 2004 /
/

DATES
1 'DEC' 2004 /
/


DATES
1 'JAN' 2005 /
/

DATES
1 'FEB' 2005 /
/

DATES
1 'MAR' 2005 /
/

DATES
1 'APR' 2005 /
/

DATES
1 'MAY' 2005 /
/

DATES
1 'JUN' 2005 /
/

DATES
1 'JLY' 2005 /
/

WPOLYMER
    'I3'  40.0  0.0   /
/

DATES
 7 'JUL' 2005 /
/

DATES
 14 'JUL' 2005 /
/

DATES
 21 'JUL' 2005 /
/

DATES
 28 'JUL' 2005 /
/

DATES
 1 'AUG' 2005 /
/
```

```
DATES
 7 'AUG' 2005 /
/

DATES
 14 'AUG' 2005 /
/

DATES
 21 'AUG' 2005 /
/

DATES
 28 'AUG' 2005 /
/

DATES
 1 'SEP' 2005 /
/

WPOLYMER
    'I3'  0.0  0.0   /
/

DATES
1 'OCT' 2005 /
/

DATES
1 'NOV' 2005 /
/

DATES
1 'DEC' 2005 /
/


DATES
1 'JAN' 2006 /
/

DATES
1 'FEB' 2006 /
/

DATES
1 'MAR' 2006 /
/

DATES
1 'APR' 2006 /
/

DATES
1 'MAY' 2006 /
/

DATES
1 'JUN' 2006 /
/

DATES
1 'JLY' 2006 /
/

DATES
1 'AUG' 2006 /
/
```

```
DATES
1 'SEP' 2006 /
/

DATES
1 'OCT' 2006 /
/

DATES
1 'NOV' 2006 /
/

DATES
1 'DEC' 2006 /
/


DATES
1 'JAN' 2007 /
/

DATES
1 'FEB' 2007 /
/

DATES
1 'MAR' 2007 /
/

DATES
1 'APR' 2007 /
/

DATES
1 'MAY' 2007 /
/

DATES
1 'JUN' 2007 /
/

DATES
1 'JLY' 2007 /
/

DATES
1 'AUG' 2007 /
/

DATES
1 'SEP' 2007 /
/

DATES
1 'OCT' 2007 /
/

DATES
1 'NOV' 2007 /
/

DATES
1 'DEC' 2007 /
/


DATES
```

```
1 'JAN' 2008 /
/

DATES
1 'FEB' 2008 /
/

DATES
1 'MAR' 2008 /
/

DATES
1 'APR' 2008 /
/

DATES
1 'MAY' 2008 /
/

DATES
1 'JUN' 2008 /
/

DATES
1 'JLY' 2008 /
/

DATES
1 'AUG' 2008 /
/

DATES
1 'SEP' 2008 /
/

DATES
1 'OCT' 2008 /
/

DATES
1 'NOV' 2008 /
/

DATES
1 'DEC' 2008 /
/


DATES
1 'JAN' 2009 /
/

DATES
1 'FEB' 2009 /
/

DATES
1 'MAR' 2009 /
/

DATES
1 'APR' 2009 /
/

DATES
1 'MAY' 2009 /
/
```

```
DATES
1 'JUN' 2009 /
/

DATES
1 'JLY' 2009 /
/

DATES
1 'AUG' 2009 /
/

DATES
1 'SEP' 2009 /
/

DATES
1 'OCT' 2009 /
/

DATES
1 'NOV' 2009 /
/

DATES
1 'DEC' 2009 /
/


DATES
1 'JAN' 2010 /
/

DATES
1 'FEB' 2010 /
/

DATES
1 'MAR' 2010 /
/

DATES
1 'APR' 2010 /
/

DATES
1 'MAY' 2010 /
/

DATES
1 'JUN' 2010 /
/

DATES
1 'JLY' 2010 /
/

DATES
 1 'AUG' 2010 /
/

DATES
 7 'AUG' 2010 /
/

DATES
 14 'AUG' 2010 /
/
```

```
DATES
 21 'AUG' 2010 /
/

DATES
 28 'AUG' 2010 /
/

DATES
 1 'SEP' 2010 /
/

DATES
1 'OCT' 2010 /
/

DATES
1 'NOV' 2010 /
/

DATES
1 'DEC' 2010 /
/


DATES
1 'JAN' 2011 /
/

DATES
1 'FEB' 2011 /
/

DATES
1 'MAR' 2011 /
/

DATES
1 'APR' 2011 /
/

DATES
1 'MAY' 2011 /
/

DATES
1 'JUN' 2011 /
/

DATES
1 'JLY' 2011 /
/

DATES
1 'AUG' 2011 /
/

DATES
1 'SEP' 2011 /
/

DATES
1 'OCT' 2011 /
/

DATES
1 'NOV' 2011 /
```

```
/

DATES
1 'DEC' 2011 /
/


DATES
1 'JAN' 2012 /
/

DATES
1 'FEB' 2012 /
/

DATES
1 'MAR' 2012 /
/

DATES
1 'APR' 2012 /
/

DATES
1 'MAY' 2012 /
/

DATES
1 'JUN' 2012 /
/

DATES
1 'JLY' 2012 /
/

DATES
1 'AUG' 2012 /
/

DATES
1 'SEP' 2012 /
/

DATES
1 'OCT' 2012 /
/

DATES
1 'NOV' 2012 /
/

DATES
1 'DEC' 2012 /
/


DATES
1 'JAN' 2013 /
/

DATES
1 'FEB' 2013 /
/

DATES
1 'MAR' 2013 /
/
```

```
DATES
1 'APR' 2013 /
/

DATES
1 'MAY' 2013 /
/

DATES
1 'JUN' 2013 /
/

DATES
1 'JLY' 2013 /
/

DATES
1 'AUG' 2013 /
/

DATES
1 'SEP' 2013 /
/

DATES
1 'OCT' 2013 /
/

DATES
1 'NOV' 2013 /
/

DATES
1 'DEC' 2013 /
/


DATES
1 'JAN' 2014 /
/

DATES
1 'FEB' 2014 /
/

DATES
1 'MAR' 2014 /
/

DATES
1 'APR' 2014 /
/

DATES
1 'MAY' 2014 /
/

DATES
1 'JUN' 2014 /
/

DATES
1 'JLY' 2014 /
/

DATES
1 'AUG' 2014 /
/
```

```
DATES
1 'SEP' 2014 /
/

DATES
1 'OCT' 2014 /
/

DATES
1 'NOV' 2014 /
/

DATES
1 'DEC' 2014 /
/


DATES
1 'JAN' 2015 /
/

DATES
1 'FEB' 2015 /
/

DATES
1 'MAR' 2015 /
/

DATES
1 'APR' 2015 /
/

DATES
1 'MAY' 2015 /
/

DATES
1 'JUN' 2015 /
/

DATES
1 'JLY' 2015 /
/

DATES
1 'AUG' 2015 /
/

DATES
1 'SEP' 2015 /
/

DATES
1 'OCT' 2015 /
/

DATES
1 'NOV' 2015 /
/

DATES
1 'DEC' 2015 /
/
```

```
DATES
1 'JAN' 2016 /
/

DATES
1 'FEB' 2016 /
/

DATES
1 'MAR' 2016 /
/

DATES
1 'APR' 2016 /
/

DATES
1 'MAY' 2016 /
/

DATES
1 'JUN' 2016 /
/

DATES
1 'JLY' 2016 /
/

DATES
1 'AUG' 2016 /
/

DATES
1 'SEP' 2016 /
/

DATES
1 'OCT' 2016 /
/

DATES
1 'NOV' 2016 /
/

DATES
1 'DEC' 2016 /
/



DATES
1 'JAN' 2017 /
/

DATES
1 'FEB' 2017 /
/

DATES
1 'MAR' 2017 /
/

DATES
1 'APR' 2017 /
/
```

```
DATES
1 'MAY' 2017 /
/

DATES
1 'JUN' 2017 /
/

DATES
1 'JLY' 2017 /
/

DATES
1 'AUG' 2017 /
/

DATES
1 'SEP' 2017 /
/

DATES
1 'OCT' 2017 /
/

DATES
1 'NOV' 2017 /
/

DATES
1 'DEC' 2017 /
/



DATES
1 'JAN' 2018 /
/

DATES
1 'FEB' 2018 /
/

DATES
1 'MAR' 2018 /
/

DATES
1 'APR' 2018 /
/

DATES
1 'MAY' 2018 /
/

DATES
1 'JUN' 2018 /
/

DATES
1 'JLY' 2018 /
/

DATES
1 'AUG' 2018 /
/

DATES
```

```
1 'SEP' 2018 /
/

DATES
1 'OCT' 2018 /
/

DATES
1 'NOV' 2018 /
/

DATES
1 'DEC' 2018 /
/



DATES
1 'JAN' 2019 /
/

DATES
1 'FEB' 2019 /
/

DATES
1 'MAR' 2019 /
/

DATES
1 'APR' 2019 /
/

DATES
1 'MAY' 2019 /
/

DATES
1 'JUN' 2019 /
/

DATES
1 'JLY' 2019 /
/

DATES
1 'AUG' 2019 /
/

DATES
1 'SEP' 2019 /
/

DATES
1 'OCT' 2019 /
/

DATES
1 'NOV' 2019 /
/

DATES
1 'DEC' 2019 /
/
```

```
DATES
1 'JAN' 2020 /
/

DATES
1 'FEB' 2020 /
/

DATES
1 'MAR' 2020 /
/

DATES
1 'APR' 2020 /
/

DATES
1 'MAY' 2020 /
/

DATES
1 'JUN' 2020 /
/

DATES
1 'JLY' 2020 /
/

DATES
1 'AUG' 2020 /
/

DATES
1 'SEP' 2020 /
/

DATES
1 'OCT' 2020 /
/

DATES
1 'NOV' 2020 /
/

DATES
1 'DEC' 2020 /
/


END
```